Mechanical regulation of bone development

Esther Tanck

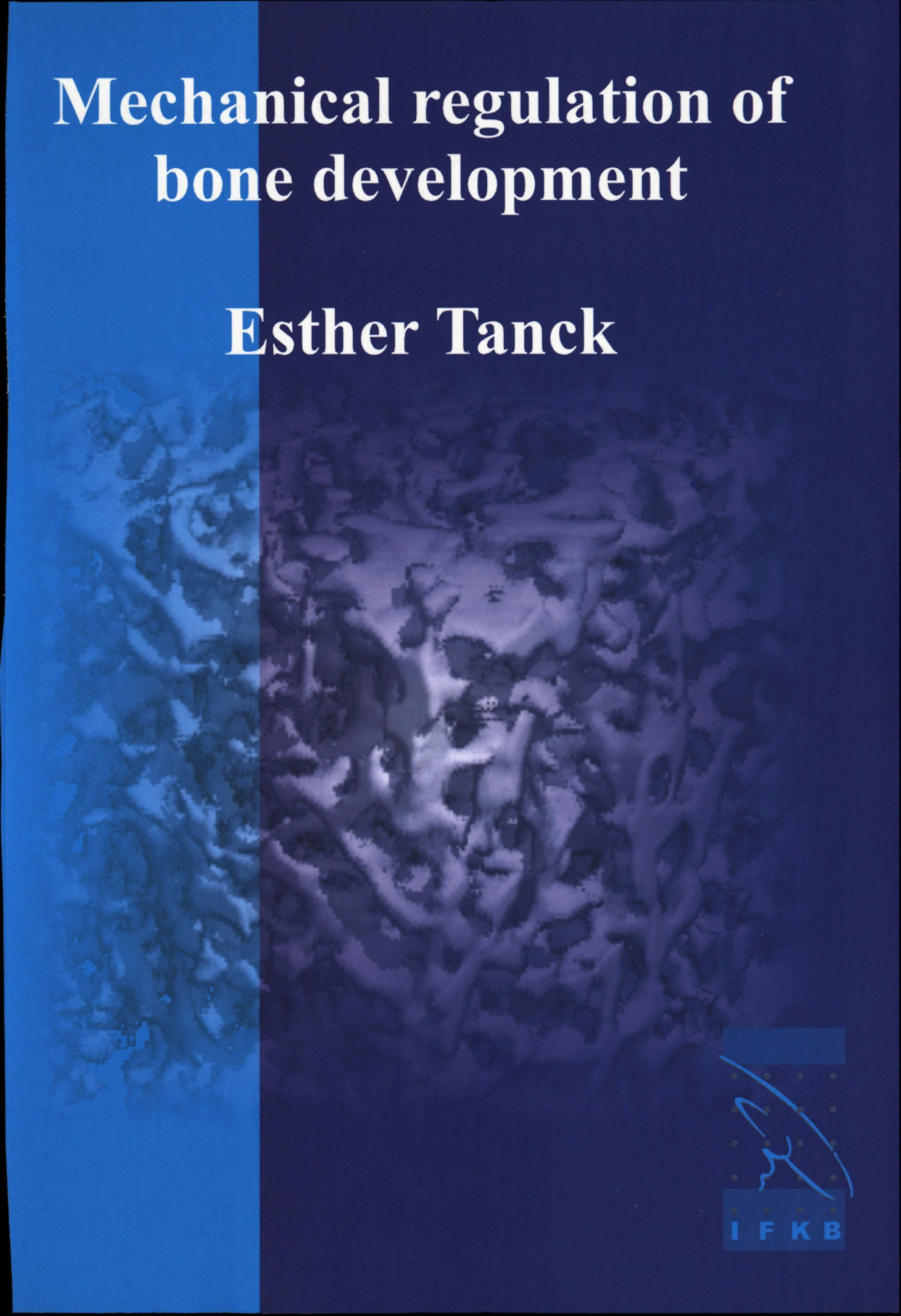

Mechanical regulation of bone development

E. J. M. TANCK

ISBN 90-9014803-5

Printing: PrintPartners Ipskamp B.V.

Research fund was provided by:
Dutch organization of Research (NWO)

This thesis was financially supported by:
"Anna-Fonds" te Leiden
Institute for Fundamental and Clinical Human Movement Sciences
Ortomed B V.
Waldemar Link GmBH & Co
Curasan Benelux B.V
Stryker Howmedica B.V.
PricewaterhouseCoopers N.V.
Oudshoorn Chirurgische Techniek B.V.
Scanco Medical A.G.
Basko Healthcare
SOMAS Orthopaedie B.V
Bauerfeind Benelux B.V
NTOC medische techniek
Smith & Nephew Nederland B V

Mechanical regulation of bone development

een wetenschappelijke proeve op het gebied van de
Medische Wetenschappen

Proefschrift

ter verkrijging van de graad van doctor
aan de Katholieke Universiteit Nijmegen,
volgens besluit van het College van Decanen in het
openbaar te verdedigen op maandag 11 juni 2001
des namiddags om 3.30 uur precies
door

ESTHER JOHANNA MARIA TANCK

geboren op 18 november 1971
te Zevenaar

promotores:

Prof. Dr. Ir. R. Huiskes (TUE)

Prof. Dr. E.H. Burger (VU)

co-promotor:

Dr. Ir. L. Blankevoort (UVA)

Manuscriptcommissie

Prof. Dr. C.C.A.M. Gielen (voorzitter)

Prof. Dr. Ir. F.P.T. Baaijens (TUE)

Prof. Dr. T.M.G.J. van Eijden (UVA)

CONTENTS

Voor Albert en mijn ouders

1

INTRODUCTION

Bones provide mechanical strength to the body; they protect organs like the hart, the lungs, and the brains against trauma; they produce blood cells from bone marrow; and they serve as a calcium reservoir. From a mechanical viewpoint, two types of bone are present in the skeleton, cortical bone, which is dense and compact, and trabecular bone, which is porous, owing to its structure of rods and plates. The latter is found predominantly in vertebral bodies and in the distal ends of long bones. However, at the cellular level there is no principal difference and both types are remodeled in a similar fashion, via Basic Multicellular Units (BMU) that form osteons in compact bone and hemi-osteons in trabecular bone (Jee, 2001). During the development from embryonic to adult bone many processes have to be completed. If, for any reason, one of these processes is disturbed, compromised bone development and function may result. Proper understanding of the regulatory mechanisms in bone development is important for prevention and treatment of musculoskeletal congenital deformities and osteoporosis, but also for bone regeneration during fracture healing and implant fixation, and for tissue engineering.

During embryonic development of long bones, cartilaginous tissue develops into bone tissue (Figure 1). This endochondral ossification process passes the subsequent stages of cartilage cell (chondrocyte) proliferation, chondrocyte hypertrophy (Figure 1B) -which is primarily achieved by accumulation of water (Buckwalter et al., 1986; Pauwels, 1980)- and mineralization of the cartilage matrix (Figure 1C). The mineralization process starts in the primary ossification center, in the middle of the rudiment, extends towards the periphery and subsequently towards the distal ends of the bone. Matrix vesicles play an important role in the initiation of mineral deposition (Kirsch et al., 1997), but the actual mineralization process is a physical one, occurring in the extracellular matrix by deposition of a calcium phosphate. Pauwels (1980) proposed that cell hypertrophy increases the pressure on the extracellular matrix. Whether the mineralization process is regulated or affected by this pressure is unknown. Mineralization proceeds very fast. In embryonic metatarsals of the mouse, for example, about one-fourth of the metatarsal is mineralized within one day (Figure 2) (Burger et al., 1992; Haaijman et al., 1997; Van Loon et al., 1995). Mineralization always occurs around hypertrophic chondrocytes. Shortly after the matrix is mineralized these cells die by apoptosis (Bronckers et al., 1996). Blood vessels penetrate the tissue (Figure 1D), the mineralized cartilage is resorbed by osteoclasts, and bone tissue is formed by osteoblasts on remnants of mineralized cartilage. At the distal ends of the bone, the secondary ossification centers develop, in

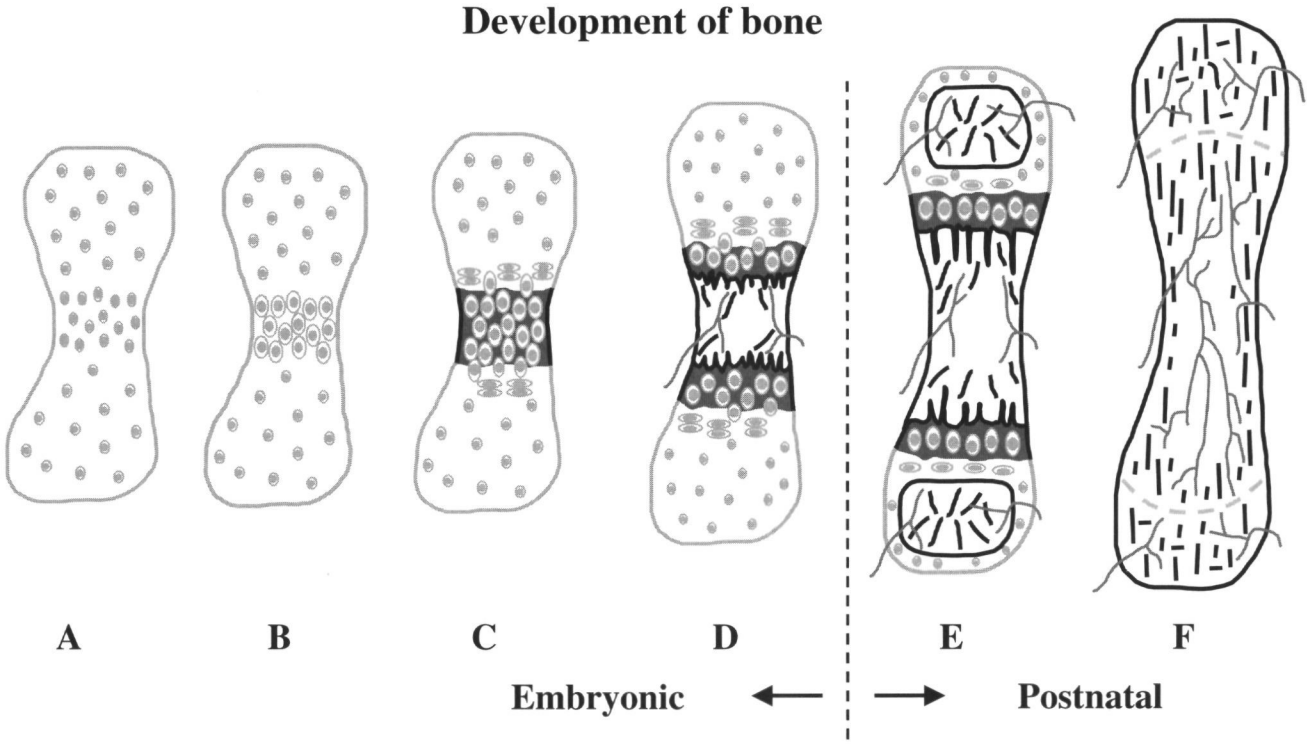

Figure 1: Schematic illustration of the development of long bones from embryonic to mature bone. The figures are not to scale. **A)** Cartilaginous rudiment; **B)** Chondrocytes in the center swell; **C)** Cartilage mineralization occurs around hypertrophic chondrocytes, proliferating flattened cells develop; **D)** Blood vessels penetrate the tissue, mineralized cartilage is resorbed, bone formation takes place, and longitudinal growth commences; **E)** Secondary ossification centers develop and growth-plates remain; **F)** Growth plates are closed and mature bone is present.

which the same cascade of processes takes place (Figure 1E). These centers create the trabecular bone of the epiphyses. Between the primary and secondary ossification centers, cartilaginous growth plates remain in which the endochondral ossification process continues (Figure 1D, 1E). In this way, the length of bones increases. During growth to maturity, cell proliferation, matrix production, and cell swelling determine the longitudinal growth rate (Hunziker and Schenk, 1989). In addition to longitudinal growth, the growth plate continuously produces new bone trabeculae in the metaphysis, oriented in the direction of the marrow cavity. Eventually, these trabeculae are remodeled to optimally withstand the forces on the bone (Wolff's Law). At maturity, the longitudinal growth stops because chondrocyte proliferation stops, and the growth plates are closed (Figure 1F). All cartilage is then replaced by bone tissue, except at the joint surfaces where a layer of articular cartilage remains present.

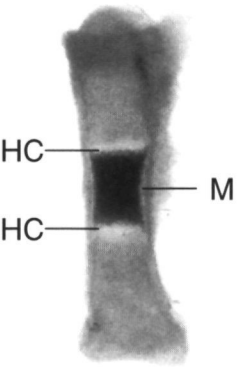

Figure 2: Embryonic metatarsal at 17 days of gestational age. It contains a center of mineralized cartilage (M) and areas of hypertrophic chondrocytes (HC).

All these processes are regulated by genetic, biological, and biomechanical factors (Carter et al., 1991). The leading question for this thesis was, if and how these processes are governed or influenced by mechanical loading. Several studies have shown that mechanical stimulation influences chondrocyte metabolism (Gray et al., 1989; Guilak et al., 1994; Lee and Bader, 1997; Sah et al., 1989; Wright et al., 1996). Evidence was found for the presence of stretch-activated membrane ion channels in articular chondrocytes, so that deformations may affect cell activity (Wright et al., 1996). Guilak et al. (1994) showed that cell deformation changes the Ca^{2+} concentration in the cytoplasm. Static compression of articular cartilage generally leads to dose-dependent reductions in cell activity, while the response to dynamic loading is not consistent (Gray et al., 1989). Dynamic strains applied to articular chondrocytes embedded in agarose increased chondrocyte proliferation (Lee and Bader, 1997). Furthermore, it was shown that chondrocytes *in vitro* can alter their activity by changes in osmotic pressure (Urban, 1994; Urban and Hall, 1994), fluid flow (Kim et al., 1994, 1995), hydrostatic pressure (Urban, 1994; Urban and Hall,

1994; Lammi et al., 1994; Parkkinen et al., 1994, 1995), electrical potential gradients (Kim et al., 1995; Frank and Grodzinsky, 1987), and pH (Gray et al., 1988). These studies were mainly performed on articular cartilage and articular chondrocytes. The cartilage that is present during endochondral ossification differs from articular cartilage in cell expression: hypertrophic chondrocytes mainly produce type-X collagen, whereas articular chondrocytes produce type-II collagen. In addition, in contrast to articular chondrocytes, hypertrophic chondrocytes accumulate large amounts of intracellular calcium (Iannotti et al., 1989). It is, therefore, important to study the influence of mechanical stimulation to the endochondral ossification process as well.

Klein-Nulend et al. (1986) performed *in vitro* culture experiments on 16-day-old embryonic mouse metatarsals to study the influence of mechanical loads on the cartilage mineralization process. The organs were loaded for a period of five days with a cyclic hydrostatic pressure (13 kPa, 0.3 Hz). The results showed that the loaded metatarsals had a mineralized diaphyseal part two to three times longer than that of the unloaded controls (Klein-Nulend et al., 1986). Others showed that cultures of the metatarsals under microgravity conditions, i.e. during spaceflight, reduced the mineralization process compared with controls (Van Loon et al., 1995). Furthermore, it was observed that the mineralization process in the metatarsals starts at 16 days of gestational age, just when the first muscle contractions in the feet occur (Burger et al., 1991; Platzer et al., 1978). These studies suggest that the mineralization process is stimulated by external mechanical loads. How the external loads are transferred to the cell level, and to which mechanical stimulus the cells could react is unknown.

Local stress stimuli in the tissues can be calculated from the external loads using Finite Element Analysis (FEA). With this method, a geometry is divided into a finite number of elements for each of which the mechanical stress and strain situation is calculated by the computer. Besides the geometry of the tissue, mechanical tissue properties and loading conditions are input of the model. Based on FEA, Carter et al. (1987, 1988) and Wong and Carter (1990a, 1990b) have proposed that cyclic shear stresses accelerate the endochondral ossification process, while dynamic hydrostatic pressure inhibits the process. They assumed linear-elastic material properties for the cartilaginous tissue. However, cartilage consists of a solid phase, mainly collagen and proteoglycans, and a fluid phase of interstitial water. Depending on the type of loading, biphasic tissues display non-linear behavior with time dependent deformation (Mow et al., 1980; Spilker et al., 1988). These viscoelastic effects can be

studied using biphasic FEA models (Mow et al, 1980) or poroelastic FEA models (Biot, 1941), which consist of solid and fluid components With such models, not only deformation, but also pressure gradients and interstitial fluid flow can be studied Using models like this, Prendergast et al (1997) studied the tissue differentiation between metal implants and bone, in dogs The tissue changed in time, from fibrous, to fibrocartilage, to bone In their model, a combination of low fluid flow and low tissue strain would stimulate fibrocartilage to develop in bone Cartilage mineralization was, however, not modeled

Mineralized cartilage is first replaced by woven bone, which is soon thereafter replaced by lamellar bone Once the trabecular architecture is formed, it is continuously remodeled According to Frost (1988), growth and development of the trabecular structure is defined as 'modeling', whereas the stage of dynamic morphological equilibrium of the trabecular architecture (metabolic homeostasis), is defined as 'remodeling' The dynamic capacity of bone metabolism has several advantages, like the competence to repair itself, but also the ability to adapt to environmental changes If the mechanical load increases by, for instance, increased physical activity, then bone mass will increase as well (Bailey et al , 1999) If, on the other hand, the load is decreased by bed rest or immobilization, this will lead to decreased bone mass (Leblanc et al , 1995) Not only bone mass, but also bone architecture adapts to external loads In the adult stage, the trabeculae are aligned to the principal stress directions, as Wolff described it (1892) In this way, trabecular bone is believed to be adapted to the typical external loads of daily living in both density and architecture A computer model that could explain remodeling at the cellular level, in terms of bone alignment, was recently published (Smit and Burger, 2000), while computer simulations of trabecular bone remodeling could explain the emergence and maintenance of trabecular architecture (Huiskes et al , 2000)

Little quantitative data is available on the development of architecture and mechanical adaptation in juvenile trabecular bone Korstjens et al (1995) analyzed the two-dimensional trabecular patterns of the distal radius in children, aged 4-14 years, using radiographs and digital imaging They found that the refined trabecular patterns of young children had coarsened in the older ones Nafei et al (2000a, 2000b) analyzed trabecular bone in epiphyseal proximal tibiae of immature and mature sheep Using mechanical tests and serial sectioning, they found that architectural and mechanical properties changed significantly with skeletal maturity A study in rats showed that the highest bone formation rates were present directly

after birth (Sontag, 1992). From there on, the formation rates decreased continuously with increasing age in both epiphysis and metaphysis, whereby formation rates were higher than resorption rates during the first 150 days of age (Sontag, 1992). The recent development of micro-computer tomography (μCT) has made it possible to analyze the three-dimensional (3D) architecture of trabecular bone accurately (Feldkamp et al., 1989). To date, this technique has been used to study adult cancellous bone and to investigate the effects of aging (Ciarelli et al., 2000; Ding and Hvid, 2000; Hildebrand et al., 1999; Rüegsegger et al., 1996).

In recapitulation, the development from embryonic towards mature bone passes many stages. If one of the stages is disturbed by biological, genetic, or biomechanical factors, then this may lead to disturbed bone development and function. The research described in this thesis was focused on mechanical factors. The purpose was to investigate the influence of mechanical loading on different stages in the development from embryonic bone to mature bone. The particular stages that we studied were cartilage mineralization and trabecular bone development. Proper understanding of normal bone development is important for prevention and treatment of musculoskeletal developmental deformities and osteoporosis, and also for bone regeneration during fracture healing and implant fixation, and for the principles of tissue engineering.

Structure of the thesis

We hypothesize that cartilage mineralization is affected by mechanical forces. But mineralization, in its turn, affects the mechanical signals felt by the cells, because the matrix becomes stiffer. The question posed in chapter two, is 'what is the change in stiffness during bone development?' To answer this question, four-point-bending experiments on unmineralized (cartilaginous) and mineralized embryonic mouse ribs were performed, and the change in stiffness was calculated. This information may be important for the understanding of cell behavior and cell regulatory processes. The stiffness values can also serve as input parameters for FE analysis on embryonic bones.

It has been shown that cartilage mineralization does occur in the absence of external forces, i.e. *in vitro* during weightlessness (Van Loon et al., 1995). This suggests that mineralization would not be stimulated by mechanics. However, the tissue (and the cells) could also be stimulated by other mechanical effects than those of external loads. It can be hypothesized that internal mechanical stimulation due to chondrocyte

hypertrophy (Pauwels, 1980) initiates or stimulates the mineralization process. In chapter three this hypothesis is discussed.

The question in chapter four was 'which factor could have stimulated the cartilage mineralization process in the *in vitro* culture experiments of Klein-Nulend et al. (1986), in which embryonic mouse metatarsals were loaded with an intermittent hydrostatic pressure?' In chapter five, the questions were 'is the mineralization geometry in embryonic bones affected by muscular load?' And, if so, 'which mechanical factor could be responsible for that?' In both chapters we used poroelastic FE analysis to study how external loads are transferred to the cells and to which mechanical stimulus they could react.

The question in chapter six was 'how do trabecular bone density and architecture change during growth?' As an increase in density due to increased loading would only have to involve bone formation, but the adaptation of architecture must involve both formation and resorption, we hypothesize that there is a time lag between these processes. In a computer simulation of bone-cell based modeling and remodeling (Huiskes et al., 2000), it was found that adaptation of density due to increased loading would occur much faster than trabecular adaptation due to changes in loading orientation. We investigated this hypothesis in the project described in chapter six by checking whether this time lag actually occurs in growing bone.

In chapter seven, we questioned 'does the trabecular architecture of the epiphysis reflect a more mature state than the architecture of the metaphysis during growth?' Trabeculae in the metaphysis are rapidly renewed due to the rapid growth of the growth plate, whereas trabeculae in the center of the epiphysis are formed from the secondary ossification center early in the development. Hence, in the developmental stage, trabeculae in the epiphysis are older than those in the metaphysis.

Chapter eight is the general discussion of this thesis. The process of bone development and its relation to mechanical forces were discussed in general.

REFERENCES

Bailey DA, Mckay HA, Mirwald RL, Crocker PRE, Faulkner RA: A six-year longitudinal study of the relationship of physical activity to bone mineral accrual in growing children: the university of saskatchewan bone mineral accrual study. J Bone Miner Res 14:1672-1679, 1999.

Biot MA: General theory of three-dimensional consolidation. J Appl Phys 12:155-164, 1941.

Bronckers AL, Goei W, Luo G, Karsenty G, D'Souza RN, Lyaruu DM, Burger EH: DNA

fragmentation during bone formation in neonatal rodents assessed by transferase-mediated end labeling J Bone Miner Res 11 1281-1291, 1996

Buckwalter JA, Mower D, Ungar R, Schaeffer J, Ginsberg B Morphometric analysis of chondrocyte hypertrophy J Bone Joint Surg [Am] 68 243-255, 1986

Burger EH, Klein-Nulend J, Veldhuijzen JP Modulation of osteogenesis in fetal bone rudiments by mechanical stress in vitro J Biomech 24 101-109, 1991

Burger EH, Klein-Nulend J, Veldhuijzen JP Mechanical stress and osteogenesis in vitro J Bone Miner Res 7 S397-S401, 1992

Carter DR, Orr TE, Fyhrie DP, Schurman DJ Influences of mechanical stress on prenatal and postnatal skeletal development Clin Orthop 219 237-250, 1987

Carter DR, Wong M The role of mechanical loading histories in the development of diarthrodial joints J Orthop Res 6 804-816, 1988

Carter DR, Wong M, Orr TE Musculoskeletal ontogeny, phylogeny, and functional adaptation J Biomech 24 3-16, 1991

Ciarelli TE, Fyhrie DP, Schaffler MB, Goldstein SA Variations in three-dimensional cancellous bone architecture of the proximal femur in female hip fractures and in controls J Bone Miner Res 15 32-40, 2000

Ding M, Hvid I Quantification of age-related changes in the structure model type and trabecular thickness of human tibial cancellous bone Bone 26 291-295, 2000

Feldkamp LA, Goldstein SA, Parfitt AM, Jesion G, Kleerekoper M The direct examination of three-dimensional bone architecture in vitro by computed tomography J Bone Miner Res 4 3-11, 1989

Frank EH, Grodzinsky AJ Cartilage mechanics-I Electrokinetic transduction and the effects of electrolyte pH and ionic strength J Biomech 20 615-627, 1987

Frost HM Vital biomechanics proposed general concepts for skeletal adaptations to mechanical usage Calcif Tissue Int 42 145-156, 1988

Gray ML, Pizzanelli AM, Grodzinsky AJ, Lee RC Mechanical and physicochemical determinants of the chondrocyte biosynthetic response J Orthop Res 6 777-792, 1988

Gray ML, Pizzanelli AM, Lee RC, Grodzinsky AJ, Swann DA Kinetics of the chondrocyte biosynthetic response to compressive load and release Biochim Biophys Acta 991 415-425, 1989

Guilak F, Donahue HJ, Zell RA, Grande D, McLeod KJ, Rubin CT Deformation-induced calcium signaling in articular chondrocytes In Cell mechanics and cellular engineering Eds VC Mow, F Guilak, R Transon-Tay, and RM Hochmuth, pp 380-397, Springer-Verlag, New York, 1994

Haaijman A, D'Souza RN, Bronckers ALJJ, Goei SW, Burger EH OP-1 (BMP-7) affects mRNA expression of type I, II, X collagen, and matrix Gla protein in ossifying long bones in vitro J Bone Miner Res 12 1815-1823, 1997

Hildebrand T, Laib A, Muller R, Dequeker J, Ruegsegger P Direct three-dimensional morphometric analysis of human cancellous bone microstructural data from spine, femur, iliac crest, and calcaneus J Bone Miner Res 14 1167-1174, 1999

Huiskes R, Ruimerman R, van Lenthe GH, Janssen JD Effects of mechanical forces on maintenance and adaptation of form in trabecular bone Nature 405 704-706, 2000

Hunziker EB, Schenk RK Physiological mechanisms adopted by chondrocytes in regulating

longitudinal bone growth in rats J Physiol 414 55-71, 1989

Iannotti JP, Brighton CT, Stambough JE Subcellular regulation of the ionized calcium pool in isolated growth-plate chondrocytes Clin Orthop 242 285-293, 1989

Jee WSS Integrated bone tissue physiology In Bone mechanics handbook Ed SC Cowin, CRC press, Ft Lauderdale, 2001 (in press)

Kim Y-J, Sah RLY, Grodzinsky AJ, Plaas AHK, Sandy JD Mechanical regulation of cartilage biosynthetic behavior Physical stimuli Arch Biochem Biophys 311 1-12, 1994

Kim Y-J, Bonassar LJ, Grodzinsky AJ The role of cartilage streaming potential, fluid flow and pressure in the stimulation of chondrocyte biosynthesis during dynamic compression J Biomech, 28 1055-1066, 1995

Kirsch T, Nah HD, Shapiro IM, Pacifici M Regulated production of mineralization-competent matrix vesicles in hypertrophic chondrocytes J Cell Biol 137 1149-1160, 1997

Klein-Nulend J, Veldhuijzen JP, Burger EH Increased calcification of growth plate cartilage as a result of compressive force in vitro Arth Rheum 29 1002-1009, 1986

Korstjens CM, Geraets WGM, Van Ginkel FC, Prahl-Andersen B, van der Stelt PF, Burger EH Longitudinal analysis of radiographic trabecular pattern by image processing Bone 17 527-532, 1995

Lammi MJ, Inkinen R, Parkkinen JJ, Hakkinen T, Jortikka M, Nelimarkka LO, Jarvelainen HT, Tammi MI Expression of reduced amounts of structurally altered aggrecan in articular cartilage chondrocytes exposed to high hydrostatic pressure J Biochem 304 723-730, 1994

Leblanc A, Schneider V, Spector E, Evans H, Rowe R, Lane H, Demers L, Lipton A Calcium absorption, endogenous excretion, and endocrine changes during and after long-term bed rest Bone 16 S301-S304, 1995

Lee DA, Bader DL Compressive strains at physiological frequencies influence the metabolism of chondrocytes seeded in agarose J Orthop Res 15 181-188, 1997

Mow VC, Kuei SC, Lai WM, Armstrong CG Biphasic creep and stress relaxation of articular cartilage in compression Theory and experiments J Biomech Eng 102 73-84, 1980

Nafei A, Danielsen CC, Linde F, Hvid I Properties of growing trabecular ovine bone Part I mechanical and physical properties J Bone Joint Surg [Br] 82B 910-920, 2000a

Nafei A, Kabel J, Odgaard A, Linde F, Hvid I Properties of growing trabecular ovine bone Part II architectural and mechanical properties J Bone Joint Surg [Br] 82B 921-927, 2000b

Parkkinen JJ, Lammi MJ, Tammi MI, Helminen HJ Proteoglycan synthesis and cytoskeleton in hydrostatically loaded chondrocytes In Cell mechanics and cellular engineering Eds VC Mow, F Guilak, R Transon-Tay, and RM Hochmuth, pp 420-444, Springer-Verlag, New York, 1994

Parkkinen JJ, Lammi MJ, Inkinen R, Jortikka M, Tammi M, Virtanen I, Helminen HJ Influence of short-term hydrostatic pressure on organization of stress fibers in cultured chondrocytes J Orthop Res 13, 495-502, 1995

Pauwels F Biomechanics of fracture healing In Biomechanics of the locomotor apparatus Translated from the 1965 German edition by P Manquet and R Furlong, pp 106-120, Springer, Berlin, 1980

Platzer AC The ultrastructure of normal myogenesis in the limb of the mouse Anat Rec 190 639-658, 1978

Prendergast PJ, Huiskes R, Søballe K Biophysical stimuli on cells during tissue differentiation at

implant interfaces J Biomech, 30 539-548, 1997

Ruegsegger P, Koller B, Muller R A microtomographic system for the nondestructive evaluation of bone architecture Calcif Tissue Int 58 24-29, 1996

Sah RLY, Kim Y-J, Doong J-Y H, Grodzinsky AJ, Plaas AHK, Sandy JD Biosynthetic response of cartilage explants to dynamic compression J Orthop Res 7 619-636, 1989

Smit TH, Burger EH Is BMU-coupling a strain-regulated phenomenon? A finite element analysis J Bone Miner Res 15 301-307, 2000

Sontag W Age-dependent morphometric alterations in the distal femora of male and female rats Bone 13 297-310, 1992

Spilker RL, Suh J K Mow VC A finite element formulation of the nonlinear biphasic model for articular cartilage and hydrated soft tissue including strain-dependent permeability In Computational Methods in Bioengineering Eds RL Spilker and BR Simon, pp 81-92, BED-9, ASME, New York, 1988

Urban JPG The chondrocyte A cell under pressure Br J Rheum 33 901-908, 1994

Urban JPG, Hall AC The effects of hydrostatic and osmotic pressures on chondrocyte metabolism In Cell mechanics and cellular engineering Eds VC Mow, F Guilak, R Transon-Tay, RM Hochmuth, pp 398-419, Springer-Verlag, New York, 1994

Van Loon JWA, Bervoets DJ, Burger EH, Dieudonné SC, Hagen JW, Semeins CM, Zandieh Doulabi B, Veldhuijzen JP Decreased mineralization and increased calcium release in isolated fetal mouse long bones under near weightlessness J Bone Miner Res 10 550-557, 1995

Wolff J Das Gesetz der Transformation der Knochen, Hirchwild, Berlin, 1892, translated as The Law of Bone Remodeling by P Maquet and R Furlong, Springer-Verlag, Berlin, 1986

Wong M, Carter DR A theoretical model of endochondral ossification and bone architectural construction in long bone ontogeny Anat Embryol 181 523-532, 1990a

Wong M, Carter DR Theoretical stress analysis of organ culture osteogenesis Bone 11 127-131, 1990b

Wright M, Jobanputra P, Bavington C, Salter DM, Nuki G Effects of intermittent pressure-induced strain on the electrophysiology of cultured human chondrocytes Evidence for the presence of stretch-activated membrane ion channels Clin Sci 90 61-71, 1996

2

THE MECHANICAL CONSEQUENCES OF MINERALIZATION IN EMBRYONIC BONE

To be submitted for publication

ABSTRACT

The purpose of this study was to examine the effect of mineralization on the mechanical properties of embryonic bone rudiments. For this purpose, four-point-bending experiments were performed on unmineralized and mineralized embryonic mouse ribs at 16 and 17 days of gestational age. Young's modulus was calculated using force-displacement data from the experiment in combination with Finite Element Analysis. For the unmineralized specimens, a calculated average for the Young's modulus of 1.11 (± 0.62) MPa was established after correction for 'sticking' and aspect ratio. For the mineralized specimens, the value was 117 (± 62) MPa after corrections. Young's modulus for embryonic bone rudiments during endochondral ossification increases therefore by two orders of magnitude within one day. Hence, the chondrocytes in the calcifying cartilage experience a significant change in their mechanical environments; they are effectively stress shielded, with severely reduced deformability as a result. Since the transition is so suddenly and gigantic, it can be seen as a process of 'catastrophic' proportion for the cells. The subsequent resorption of calcified cartilage and the expansion of the marrow cavity could be consequential to the stress shielding.

INTRODUCTION

In embryonic development of long bones, a cartilaginous anlage develops into bone tissue. The process of endochondral ossification includes the stages of chondrocyte proliferation, chondrocyte hypertrophy, and mineralization of the cartilage matrix. The mineralization process starts in the center of the cartilaginous rudiment, in the area of hypertrophic chondrocytes. It extends towards the periphery and subsequently towards the distal ends of the bone. Cartilage mineralization proceeds very fast. In embryonic metatarsals of the mouse, for example, one-fourth of the metatarsal length mineralizes within one day (Burger et al., 1992; Haaijman et al., 1997; Tanck et al., 2000; Van Loon et al., 1995). Shortly after the mineralization process takes place, most hypertrophic chondrocytes go into apoptosis (Bronckers et al., 1996). Blood vessels penetrate the tissue, the mineralized cartilage is resorbed by osteoclasts, and bone tissue is formed on remnants of mineralized cartilage. These processes continue

in growth plates after establishment of secondary ossification centers, and also occur during fracture healing.

Little is known about the changes in mechanical properties of the tissue during endochondral ossification. Mechanical tests on growth-plate cartilage were performed by Bachrach (1995) and Cohen et al. (1992). They showed that Young's modulus of hypertrophic cartilage for compression was about 0.44 MPa. In the study of Wong and Carter (1990), elastic moduli of 6 MPa for uncalcified tissue and 300 MPa for calcified tissue were assumed for Finite Element Analysis (FEA) of embryonic bones. These values were estimated from articular cartilage and bone, but not based on experiments with embryonic bone. In a study by Mente and Lewis (1994), properties of calcified cartilage were determined in bovine patellae and femurs with three-point-bending tests of pure subchondral bone specimens, and composites of calcified cartilage and subchondral bone. They found that the bending stiffness of calcified cartilage was about 320 MPa. It is, however, questionable whether the value for calcified articular cartilage is similar to that of calcified cartilage during embryonic bone development. Many studies have been performed to determine compressive properties of articular cartilage in confined compression and indentation tests (Armstrong et al., 1982; Eisenberg and Grodzinsky, 1985; Mow et al., 1980, 1991). No such data on embryonic cartilage or embryonic calcified cartilage is available, although this information is important for the understanding of cell behavior and regulatory processes during bone development, which are eventually of importance for treatment or prevention of musculoskeletal diseases. Recent studies emphasize the regulating role of mechanical stimuli on skeletal cells (Klein-Nulend et al., 1995; Prendergast et al., 1997; Huiskes et al., 1997). The magnitude of these stimuli is largely determined by the mechanical properties of the extracellular matrix. In addition, mechanical function seems important not only for maintenance, but also during development of the embryonic skeleton. To better understand the role of tissue mechanics during bone development, data on the mechanical properties of embryonic cartilage and bone is needed. The purpose of this study was to examine the mechanical properties of unmineralized and mineralized cartilage in developing embryonic bones. For this purpose, four-point-bending experiments were performed on embryonic mouse ribs.

MATERIAL AND METHODS

Embryos of gestational age 16 or 17 days were harvested from three pregnant Sprague Dawly mice (Harlan, USA). Under microscopic control, ribs were removed from the embryos, cleaned of adhering soft tissue and transversely cut in pieces consisting entirely of either unmineralized tissue (cartilage) or mineralized tissue (calcified cartilage plus thin bone collar). Only pieces with a length of at least 1.5 mm and a reasonably small longitudinal curvature, i.e. $1/r < 0.2$ mm^{-1}, were selected for mechanical testing. The diameter of each specimen was measured using a microscopic ruler.

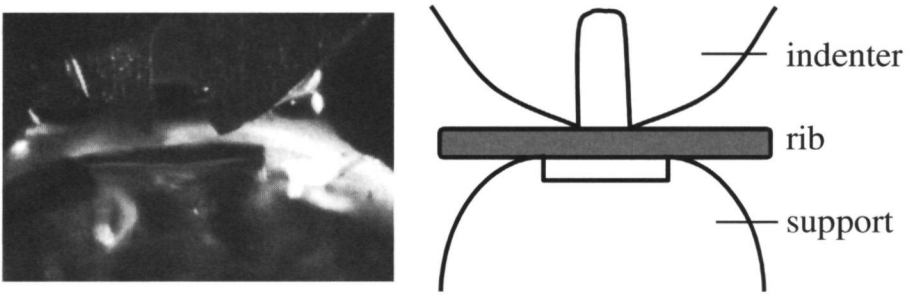

Figure 1: Photograph and a drawing of the four-point-bending experiment.

Mechanical testing was performed by four-point-bending experiments, using a servo-controlled micro-mechanical system (Figure 1) (Kuhn et al., 1989). Each bone was tested at an actuator-displacement rate of 100 µm/s. Care was taken to prevent loss of water from the tissue by application of phosphate-buffered saline. For each specimen, force and displacement values were registered. Young's modulus was calculated assuming a linear-elastic beam theory for a solid circular cross-section, according to Gere and Timoshenko (1991):

$$E = \frac{F \cdot a}{12 \cdot \delta \cdot \pi \cdot r^4} \cdot \left(3 \cdot l^2 - 4 \cdot a^2\right)$$

for which F is the applied force, l is the length between the contact points (1248 µm), a is the length between contact point and force point (392 µm), δ is the deflection at the center of the beam, and r is the radius of the beam (Figure 2).

To calculate the Young's modulus from the beam theory, it is required that the contact between specimen and support or indenter is frictionless. However, preliminary video analysis of the experiments showed that most bones were 'sticking' to the support points. Another complication was that the diameters of the specimens differ, resulting in different aspect ratios (length/diameter). This variation may have influence on the calculated Young's modulus. For compensation of these errors, a correction factor was determined from Finite Element Analysis (FEA). For this, a 3D linear-elastic FEA model from one of the specimens was constructed, with 786 elements (Figure 2) (Marc Analysis Research Corporation, Palo Alto, CA, USA). One of the bending experiments was simulated and different boundary conditions were applied, i.e. frictionless and fixed contact between specimen and support or indenter points. Also the effect of diameter size of the specimen was analyzed in this parametric FE study.

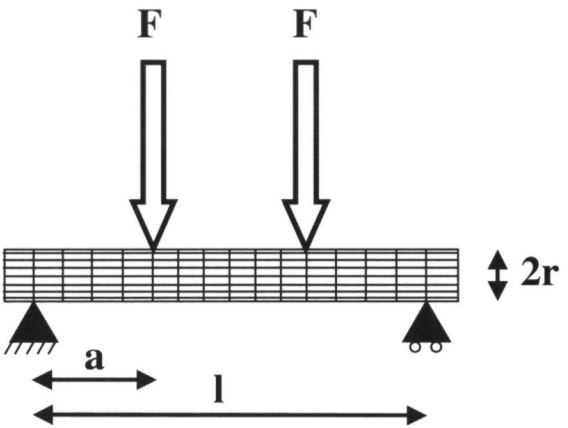

Figure 2: Finite Element model of an embryonic rib. Four-point-bending is applied to the model. *F* is the applied force and *r* is the radius of the specimen. The length between the contact points, *l*, is 1248 μm and the length between contact point and force point, *a*, is 392 μm.

To test the importance of hydration for the mechanical behavior of the ribs one unmineralized cartilaginous specimen was tested, left to dry for approximately 30 minutes, tested, rehydrated by immersion in phosphate-buffered saline, and tested again.

RESULTS

Of the 10 unmineralized specimen, 8 tests were successfully performed, and of the 9 mineralized ones, all tests were successful. The average diameter of the ribs was 271 (± 69) μm, with a range between 186 and 389 μm. The average aspect ratio was 4.9 (± 1.2), with a range between 3.2 and 6.7.

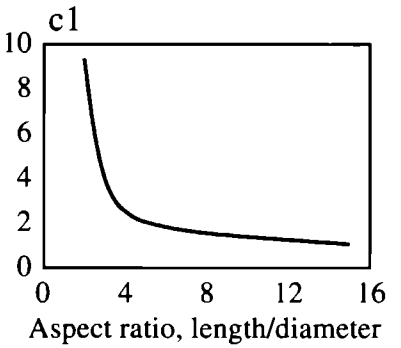

Figure 3: Correction factor c1 as a function of the aspect ratio of length and diameter.

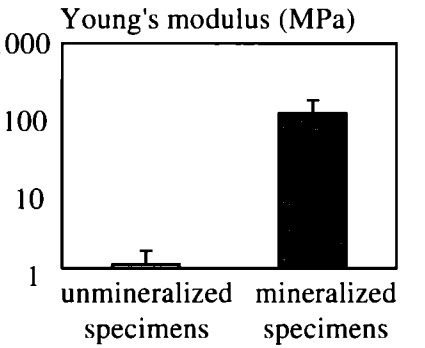

Figure 4: Young's moduli for unmineralized and mineralized cartilage of embryonic mouse ribs. Note that the scaling is logarithmic.

The correction factor for 'sticking' was 0.296, while the correction factor for aspect ratio (c1) decreased with increasing ratio (Figure 3). The corrected value for Young's modulus (E) was then defined as E = 0.296*c1*E(beam theory). From the unmineralized specimen, an average Young's modulus of 1.76 (± 1.08) MPa was determined with classical beam theory. After correction, a value of 1.11 (± 0.62) MPa was established (Figure 4). For the mineralized specimens, the calculated values for the Young's modulus were 250 (± 145) MPa, and 117 (± 62) MPa, for calculations using the classical beam theory and after corrections, respectively (Figure 4). Hence, the mineralized specimens were two orders of magnitude stiffer than the unmineralized specimens.

In the particular case that the cartilaginous specimen was tested, dried out, tested, rehydrated and tested again, the diameter of the specimen was about similar before and after dehydration-rehydration, i.e. 330 μm versus 336 μm, respectively. The

average Young's moduli, calculated from the beam theory, before dehydration was 2.94 MPa, versus 3.26 MPa after dehydration and rehydration. During dehydration of the tissue, the diameter of the rib reduced to 116 μm. Stiffness was then mainly determined by the collagen of the perichondrium that behaved like a piece of string, hence could not be determined with a bending test. A simple analytic tension model estimated a modulus of 220 MPa.

DISCUSSION

This study showed that the mineralized part, consisting of calcified cartilage is two orders of magnitude stiffer than the unmineralized cartilaginous ends of embryonic mouse ribs. The mineralization process in metatarsals of embryonic mice starts just when the first muscle contractions in the feet occur (Burger et al., 1991). This suggests that the mineralization process is stimulated by mechanical loads. Within a short period of time the chondrocytes in the tissue experience a dramatic change in mechanical environment, severely limiting cell deformations, which must have consequences for cell processes. In addition, the mineralized matrix may be less permeable for nutrients, which may kill the hypertrophic chondrocytes. Many authors suggested that the majority of hypertrophic chondrocytes would undergo apoptosis (Bronckers et al., 1996; Gerstenfeld and Shapiro, 1996; Szuwart et al., 1998).

The increase in stiffness results in stress shielding of the tissue. Bones are primarily loaded in compression and bending. These external loads must be transmitted through the different zones of development. Assuming continuity in external loads, the deformation of the mineralized area is less than in the unmineralized area, so that stress shielding of the mineralized area occurs. The subsequent resorption of the calcified cartilage could be consequential to this stress shielding. A second area in which resorption of mineralized tissue occurs is at the metaphyseal/bone-marrow border (Nordahl et al., 1998). Here, stress shielding may also play a role, since at this level most of the load is probably carried by the diaphyseal cortex, leaving the trabecular bone relatively unloaded.

We applied corrections for fixed boundary conditions and different aspect ratios of the specimen because these affected the Young's modulus significantly. Factors like ellipticity of the cross-section and the straightness of the bones were not taken into account. A pilot study showed that these had minor effects on the Young's modulus

for the bones that were tested (Huiskes et al., 1995). Other factors, like the visco-elastic behavior of the tissue, non-linear deformation of the material, and non-homogeneous material distribution, were not taken into account.

As a curiosity, we tested the importance of hydration for the mechanical behavior of the ribs in one case. During dehydration of the tissue, the proteoglycans loose their function to retain water, which explains the loss in diameter of the rib. When the tissue was rehydrated, the proteoglycans were able to fulfill their mechanical function again. The specimen swelled, probably until it was restricted by the collagenous perichondrium and behaved again like a stiff rod. This suggests that under hydrated conditions proteoglycans determine the mechanical behavior of the cartilaginous pre-mineralized bone rudiment.

The Young's modulus for embryonic cartilaginous tissue in this study was of the same order of magnitude as that for articular cartilage (Mow et al., 1980). The Young's modulus for mineralized tissue in embryonic ribs is lower than for calcified cartilage in articular joints, i.e. 117 MPa versus 320 MPa (Mente and Lewis, 1994). It is about one order of magnitude lower than the stiffness of subchondral bone (Mente and Lewis, 1994; Brown et al., 1984; Choi et al., 1990).

In conclusion, the Young's modulus for embryonic tissue during endochondral ossification increases with two orders of magnitude within one day, which is mechanically speaking a process of 'catastrophic' proportions.

ACKNOWLEDGEMENTS

CC van Donkelaar, KJ Jepsen, H Weinans, SA Goldstein

REFERENCES

Armstrong CG, Mow VC Variations in the intrinsic mechanical properties of human articular cartilage with age, degeneration, and water content J Bone Joint Surg [Am] 64A·88-94, 1982

Bachrach NM Growth plate chondrocyte deformation in situ and a biphasic inclusion model for cells within hydrated soft tissues PhD thesis, Columbia University, 1995

Bronckers AL, Goei W, Luo G, Karsenty G, D'Souza RN, Lyaruu DM, Burger EH. DNA fragmentation during bone formation in neonatal rodents assessed by transferase-mediated end labeling. J Bone Miner Res 11 1281-1291, 1996

Brown TD, Vrahas MS The apparent elastic modulus of the juxtaarticular subchondral bone of the femoral head J Orthop Res 2 32 38, 1984

Burger EH, Klein-Nulend J, Veldhuijzen JP Modulation of osteogenesis in fetal bone rudiments by mechanical stress in vitro J Biomech 24 101-109, 1991

Burger EH, Klein-Nulend J, Veldhuijzen JP Mechanical stress and osteogenesis in vitro J Bone Miner Res 7 S397-S401, 1992

Choi K, Kuhn JL, Ciarelli MJ, Goldstein SA The elastic moduli of human subchondral, trabecular, and cortical bone tissue and the size dependency of cortical bone modulus J Biomech 23 1103-1113 1990

Cohen B, Chorney GS, Phillips DP, Dick HM, Mow VC Inhomogeneous and anisotropic mechanical properties of bovine growth plate and chondroepiphysis Trans Orthop Res Soc 17 153, 1992

Eisenberg SR, Grodzinsky AJ Swelling articular cartilage and other connective tissues electromechanochemical forces J Orthop Res 3 148-159, 1985

Gere JM, Timoshenko SP In Mechanics of materials, 3rd ed, pp 761, 775, Chapman and Hall, London, UK, 1991

Gerstenfeld LC, Shapiro FD Expression of bone-specific genes by hypertrophic chondrocytes implications of the complex functions of the hypertrophic chondrocyte during endochondral bone development J Cell Biochem 62 1-9, 1996

Haaijman A, D'Souza RN, Bronckers ALJJ, Goei SW, Burger EH OP-1 (BMP-7) affects mRNA expression of type I, II, X collagen, and matrix Gla protein in ossifying long bones in vitro J Bone Miner Res 12 1815-1823, 1997

Huiskes R, van Donkelaar CC, Jepsen KJ, Weinans H, Goldstein SA, Burger EH The mechanical consequences of mineralization in fetal bone Trans Orthop Res Soc 20 450, 1995

Huiskes R, van Driel WD, Prendergast PJ, Søballe K A biomechanical regulatory model for periprosthetic fibrous-tissue differentiation J Mat Sci Mat Med 8 785-788, 1997

Klein Nulend J, van der Plas A, Semeins CM, Ajubi NE, Frangos JA, Nijweide PJ, Burger EH Sensitivity of osteocytes to biomechanical stress in vitro FASEB J 9 441-445, 1995

Kuhn JL, Goldstein SA, Choi K, London M, Feldkamp LA, Matthews LS Comparison of the trabecular and cortical tissue moduli from human iliac crests J Orthop Res 7 876-884, 1989

Mente PL, Lewis JL Elastic modulus of calcified cartilage is an order of magnitude less than that of subchondral bone J Orthop Res 12 637-647, 1994

Mow VC, Kuei SC, Lai WM, Armstrong CG Biphasic creep and stress relaxation of articular cartilage in compression Theory and experiments J Biomech Eng 102 73-84, 1980

Mow VC, Zhu W, Ratcliffe A Structure and function of articular cartilage and meniscus In Basic Orthopaedic Biomechanics Eds VC Mow and WC Hayes, pp 143-198, Raven press, Ltd, New York, 1991

Nordahl J, Andersson G, Reinholt FP Chondroclasts and osteoclasts in bones of young rats comparison of ultrastructural and functional features Calcif Tissue Int 63 401-408, 1998

Prendergast PJ, Huiskes R, Søballe K Biophysical stimuli on cells during tissue differentiation at implant interfaces J Biomech, 30 539-548, 1997

Szuwart T, Kierdorf H, Kierdorf U, Clemen G Ultrastructural aspects of cartilage formation, mineralization, and degeneration during primary antler growth in fallow deer (dama dama) Ann

Anat 180:501-510, 1998.

Tanck E, Blankevoort L, Haaijman A, Burger EH, Huiskes R: The influence of muscular activity on local mineralization patterns in metatarsals of the embryonic mouse. J Orthop Res 18:613-619, 2000.

Van Loon JWA, Bervoets DJ, Burger EH, Dieudonné SC, Hagen JW, Semeins CM, Zandieh Doulabi B, Veldhuijzen JP: Decreased mineralization and increased calcium release in isolated fetal mouse long bones under near weightlessness. J Bone Miner Res 10:550-557, 1995.

Wong M, Carter DR: Theoretical stress analysis of organ culture osteogenesis. Bone 11:127-131, 1990.

3

PROPOSAL FOR THE EFFECT OF CHONDROCYTE VOLUME ON THE MINERALIZATION RATE

E Tanck, ME van Dijk, RJ Errington, L Blankevoort, EH Burger, R Huiskes

Journal of Musculoskeletal Research Vol 5
No 1 (in press), 2001

ABSTRACT

Mineralization of the cartilage matrix in embryonic long bones and growth plates is preceded by hypertrophy of chondrocytes. We hypothesize that the swollen hypertrophic cells exert pressure on the matrix, and that this pressure plays a role in the cartilage mineralization process. For this study we asked the following questions. First, does the ratio of cell volume to matrix volume (CV/MV) increase from the proliferation to the hypertrophic zone in embryonic long bones? Second, is there a correlation between cell-volume increase and the mineralization rate in embryonic and postnatal long bones? The CV/MV ratios in the proliferation and hypertrophic zones in embryonic mouse metatarsals at 17 days of gestational age were determined using morphometric analyses. Confocal laser scanning microscopy was used to determine chondrocyte volumes. Cell volumes in the proliferation and hypertrophic zones of embryonic mouse metatarsals at 17 days of gestational age were compared to the ones in metatarsal growth plates of 9-day-old mice. The mineralization rate was determined using photographs at 24-hour intervals. The CV/MV increased significantly from the proliferation to the hypertrophic zone, from 1.30 (± 0.15) (mean ± standard deviation) to 1.80 (± 0.18). The relative increase in cell volume from the proliferation to the hypertrophic zone was 1.6 for embryonic cells, i.e. from 370 (± 101) to 610 (± 107) μm^3, and 2.8 for postnatal cells, i.e. from 280 (± 41) to 786 (± 155) μm^3 ($p<0.05$). The mineralization rate was 295 (± 47) and 382 (± 149) μm/24 hour for embryonic and postnatal metatarsals respectively ($p<0.05$). The finding that chondrocyte volume increase is accompanied by a higher mineralization rate supports the hypothesis that cell hypertrophy plays an important role during the mineralization process.

INTRODUCTION

Cartilage mineralization is essential in embryonic bone development, bone growth, and fracture healing. Conversely, mineralization is undesirable in articular cartilage after transplantations, or during cartilage regeneration. However, the mineralization process is still poorly understood. Matrix vesicles play an important role in the initiation of mineral deposition (Kirsch et al., 1997), but the actual mineralization

process is a physical one, occurring in the extracellular matrix. Mineralization of cartilage is preceded by hypertrophy of chondrocytes, which is primarily achieved by accumulation of water (Buckwalter et al., 1986; Pauwels, 1980). Hypertrophy, in its turn, is preceded by cell proliferation. The cellular processes involved in the mineralization process are regulated by a combination of genetic, biological, and biomechanical factors (Carter et al., 1991).

Cell proliferation, matrix production, and cell hypertrophy determine the longitudinal growth rate in long bones. In postnatal mammals the rate of longitudinal bone growth is correlated with the volume of hypertrophic chondrocytes (Breur et al., 1991; Kuhn et al., 1996). This correlation was shown in different bones, different species, and for different ages (Kuhn et al., 1996). In avian growth plates, there was also a positive linear correlation, although it was somewhat weaker (Barreto and Wilsman, 1994). These studies suggest that hypertrophic cell-volume increases are one of the important factors in the determination of growth rate.

Several studies showed the modulation of cartilage mineralization by mechanical stimulation (Burger et al., 1991; Carter et al., 1987, 1991; Copray et al., 1985a, 1985b, 1985c; Klein-Nulend et al., 1986; Tanck et al., 2000). For example, the mineralization rate of embryonic mouse metatarsals increased during culture as result of intermittent hydrostatic pressure (Klein-Nulend et al., 1986). Furthermore, muscle forces were suggested to stimulate the mineralization process by causing distortional strains at the unmineralized/mineralized cartilage interface in embryonic long bones (Carter et al., 1991; Tanck et al., 2000). However, the mineralization process also occurs *in vitro* without external muscular forces, or in space during weightlessness (Burger et al., 1991; Van Loon et al., 1995). This may have genetic causes, but it is also possible that the process can be explained by mechanics; internal mechanical stimulation may initiate and stimulate the mineralization process. In this study, we addressed the latter possibility.

Pauwels (1980) proposed that cell hypertrophy increases the pressure on the extracellular matrix. If the matrix is indeed pressurized by hypertrophic chondrocytes, then the cell volume must increase relative to the volume of the matrix during hypertrophy. Indeed, this has been shown in the proximal tibial growth plate of rats and mice (Buckwalter et al., 1986; Cruz-Orive and Hunziker 1986; Hunziker et al., 1987). For the present study, it was hypothesized that hypertrophic chondrocytes pressurize the matrix, stress the collagen network, and stimulate the mineralization process. The rate of mineralization is assumed to be proportional to the pressure or

stress on the matrix. Hence, the level of hypertrophy should then correlate with the mineralization rate.

The following questions were addressed in this study. Does the ratio of cell volume to matrix volume (CV/MV) increase during hypertrophy, i.e. from the proliferation zone to the hypertrophic zone, in embryonic metatarsals of the mouse? Is a difference in chondrocyte hypertrophy accompanied by a difference in mineralization rate in embryonic and postnatal metatarsals of the mouse? To answer these questions, CV/MV was determined using morphometric analysis, cell volumes were measured using confocal laser scanning microscopy (CLSM), and the mineralization rate was measured using photographs with a 24-hour interval.

METHODS

Metatarsal source

Embryonic mouse metatarsals were dissected from 17-day pregnant Swiss albino mice (Harlan Inc., Zeist, The Netherlands). The embryonic metatarsals were obtained from a total of 25 embryos, from 8 different nests. At 17 days of gestational age (E17), the metatarsals contain a mineralized center with proximally and distally zones of hypertrophic, proliferating, and resting chondrocytes. Postnatal mouse metatarsals were dissected at eight and nine days after birth (see '***Mineralization rate***'). At nine days after birth, the development of the secondary ossification center in the distal epiphysis has just started. The postnatal metatarsals were obtained from one nest by randomly dividing the total of 14 mice into two equal groups. In each mouse, the three middle metatarsals of one foot were dissected for the measurements. Institutional approval was obtained for all experiments.

CV/MV ratio, morphometric approach

To determine if the ratio cell volume to matrix volume (CV/MV) increases from the proliferation zone to the hypertrophic zone in embryonic metatarsals of the mouse, five mineralized metatarsals were fixed and embedded according to the protocol of Cruz-Orive and Hunziker (1986). Prefixation was performed for 2.5 hours in a solution containing 2% (v/v) glutaraldehyde, 0.05 M sodium cacodylate buffer (pH=7.4), and 0.7% (w/v) ruthenium hexamine trichloride (RHT). Thereafter, the rudiments were washed in 0.05 M sodium cacodylate buffer (pH=7.4) and postfixed

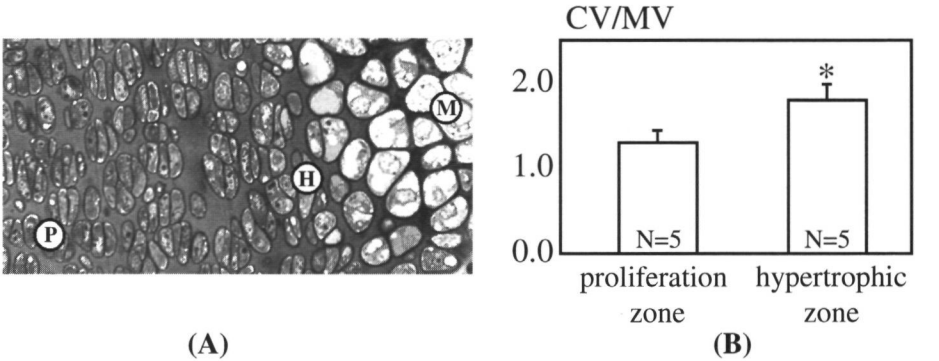

Figure 1: **(A)** Histological view of an embryonic (E17) mouse metatarsal in which the proliferation zone (P), hypertrophic zone (H) and mineralized zone (M) are visible. This photo was used for morphometric analyses. **(B)** Results of the CV/MV measurements of the proliferation and hypertrophic zones. *$p<0.05$. Error bars represent the standard deviation.

for 2.5 hours in an immersion containing 0.1 M sodium cacodylate, 1% (w/v) OsO_4, and 0.7% (w/v) RHT. Subsequently they were washed in 0.1 M sodium cacodylate (pH=7.4). The tissue was dehydrated in ethanol, from 50% to 100%, followed by infiltration and embedding with propylene oxide and Epon 812.

One-µm slices were collected from the specimens, which were positioned in a microtome (Reichert ultracut E) with their longitudinal axis parallel to a diamond knife. The orientation of the metatarsals about the longitudinal axis was at random to satisfy the random positioning rule (Gundersen et al., 1988). The sections were mounted on glass slides and stained with toluidine blue for light microscopic examination (Figure 1A).

The CV/MV was determined by point-counting (Cruz-Orive and Hunziker, 1986), i.e. determination of the fraction of points in cells to the fraction of points in the matrix, in the centers of the proliferation and hypertrophic zones at both proximal and distal sides of the mineralized region. The equivalent zones, proximally and distally from the mineralized area, were assumed to be similar and were taken together. To analyze if this assumption was justified, a Student's t-test for paired analysis was performed to compare proximal with distal data. Transitional zones were not included. From each metatarsal, six sections were measured using a light microscope with a drawing arm, and a point grid for anisotropic measurements (Cruz-Orive and Hunziker, 1986). Pointcounting was performed at 1000x magnification. At this magnification, the proliferation and hypertrophic zones were each covered by at least 60 grid points.

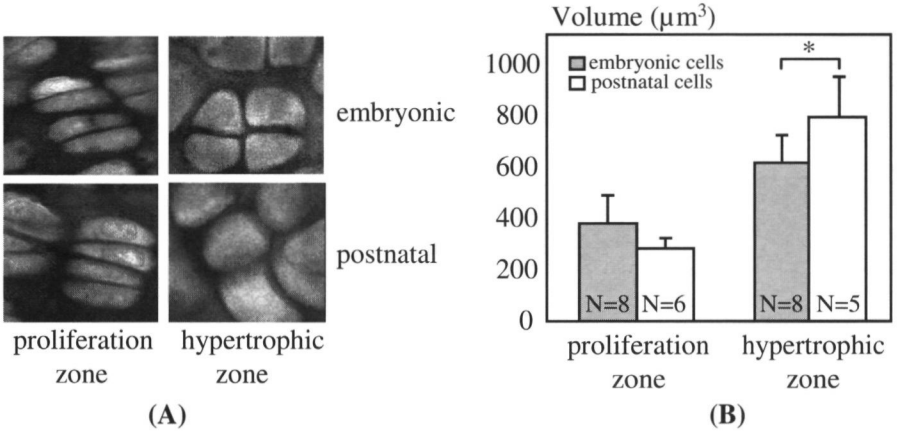

Figure 2: **(A)** Chondrocytes in the proliferation zone and hypertrophic zone for embryonic (E17) and postnatal (d9) mouse metatarsals, which are fixed, as seen using confocal laser scanning microscopy. **(B)** Cell volumes in the proliferation zone and hypertrophic zone of embryonic and postnatal metatarsals, which are fixed. 'N' is the number of metatarsals. *$p<0.05$. Error bars represent the standard deviation.

Differences in CV/MV between the proliferation and hypertrophic zone were analyzed using a paired t-test.

Cell volume using CLSM

Cell volumes in the proliferation and hypertrophic zones in embryonic mouse metatarsals (E17) were determined and compared to cell volumes in the distal growth plates of 9-day-old metatarsals (d9). The metatarsals were fixed in 4% paraformaldehyde for at least 48 hour and subsequently bathed with 50 μMol Fluorescein Isothiocyanate (FITC), which labels all proteins throughout the tissue. The rudiments were then placed in a chamber with buffer, which was mounted on a Bio-Rad MRC-1000 confocal laser scanning microscope (CLSM) (Biorad Microscience, UK) attached to a Nikon inverted microscope. Data collection was carried out using an objective x40, 1.25 NA water-immersion lens. Three-dimensional optical sections with increments of 0.5 μm were acquired through the tissue in the middle of the proliferation and the hypertrophic zone at the same tissue depth, longitudinal to the bone. For each zone, between 5 and 8 bones were used. Although FITC labels everything throughout the tissue, the cells were much brighter and therefore could be segmented from the background (Figure 2A). As fixation presumably leads to cell shrinkage, cells in living metatarsals were measured to

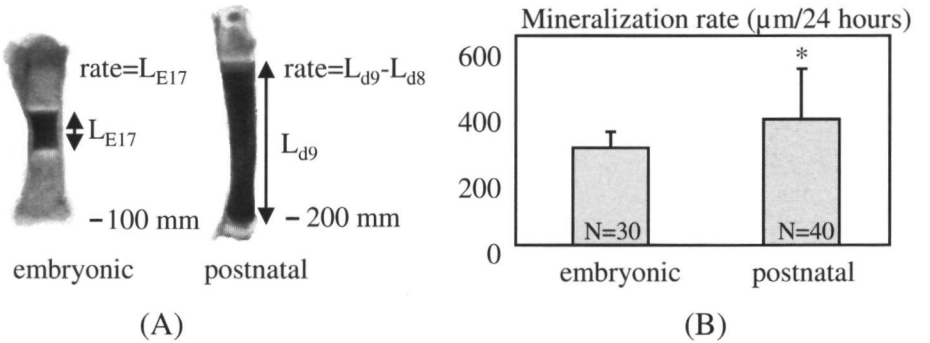

Figure 3: **(A)** Measurement of the 24-hour mineralization rate. For the embryonic metatarsals, the length of the mineralized zone was measured at 17 days of gestational age (E17). For the postnatal metatarsals, the length of the mineralized zone at 8 or 9 days after birth was measured; the mineralization rate is the difference between the average length at day 9 and 8. Note that the embryonic metatarsal is scaled twice as large compared to the postnatal metatarsal. **(B)** Mineralization rate in embryonic and postnatal metatarsals. 'N' is the number of metatarsals used in the analysis. *$p<0.05$. Error bars represent the standard deviation.

verify the results of the measurements in fixed tissue. For this purpose, cells were positively labeled for 15 minutes with 4.5 µM 5-chloromethylfluorescein diacetate (CMFDA). To measure the cell volumes in the proliferation and hypertrophic zones, five and four bones were used, respectively. Further procedures were similar to the cell measurements of fixed tissue.

Cell volumes were determined according to a previously described method (Errington et al., 1997). Briefly, cell boundaries were objectively defined using a 50% threshold between dye intensity in the cell and in the matrix. Volumes were calculated by adding cell areas in each optical section. Appropriate corrections were implemented according to the protocol described by Errington and White (1999). Differences in cell volumes were analyzed using Student's t-test.

Mineralization rate

To determine the 24-hour mineralization rate for the embryonic and postnatal mouse metatarsals, isolated metatarsals were placed on a dish and photographed under an inverted microscope. The length of the ossification zone, which appeared dark as a result of matrix mineralization (Haaijman et al., 1997; Klein-Nulend et al., 1986; Van Loon et al., 1995; Van't Veen et al., 1995), was measured (Figure 3A). For embryonic metatarsals (N=30, from two pregnant mice), the length of the calcified zone at 17

days of gestational age was assumed to be the 24-hour mineralization increase, as the mineralization process starts at 16 days of gestational age (Burger et al., 1991; Tanck et al., 2000). For postnatal metatarsals, the lengths of the mineralized zones were measured at 8 days (N=19) and 9 days after birth (N=21); the average 24-hour mineralization rate was the difference between these two lengths (Figure 3A). Differences in mineralization rate were analyzed using Student's t-test.

RESULTS

The cell volume over matrix volume (CV/MV) in embryonic metatarsals of the mouse increased significantly during hypertrophy, from 1.30 (± 0.15) in the proliferation zone to 1.80 (± 0.18) in the hypertrophic zone ($p<0.05$) (Figure 1B). There were no statistical differences in CV/MV between similar zones proximal and distal from the mineralized area.

The average volume for hypertrophic chondrocytes in fixed embryonic metatarsals was 610 (± 107) μm^3 and in 9-day old metatarsals 786 (± 155) μm^3 (Figure 2B). This difference was statistically significant ($p<0.05$), whereas the average volume in the proliferation zone was not significantly different between embryonic and postnatal metatarsals (Figure 2B). From the proliferation zone to the hypertrophic zone, the cells in embryonic and postnatal metatarsals increased their volumes on average with factors 1.6 and 2.8, respectively ($p<0.05$). Cell volumes of the living tissue were about 12% higher, but not significantly different, compared to the volumes in fixed tissue (data not shown).

The mineralization rate for embryonic metatarsals was 295 (± 47) µm/24 hours and for postnatal metatarsals 382 (± 149) µm/24 hours (Figure 3B). This difference was statistically significant ($p<0.05$).

DISCUSSION

This study showed that during embryonic development of mouse metatarsals, the ratio of cell volume to matrix volume significantly increased from the proliferation zone to the hypertrophic zone, i.e. chondrocytes increased their relative cell volume.

Earlier studies reported similar results for postnatal growth plates of rats and mice (Buckwalter et al., 1986; Cruz-Orive and Hunziker, 1986; Hunziker et al., 1987). Our results support the hypothesis that cell hypertrophy pressurizes the extracellular matrix (Pauwels, 1980). The amount of pressure to the extracellular matrix, and the stress in the collagen network are unknown. It will depend on the material properties of matrix and cells, matrix production, cell growth, and transport of fluid and matrix components between cells and matrix. To determine the stress, further analysis is required using, for example, mechanical models in which the effects of the different parameters can be studied.

The present study showed that a relatively high hypertrophic cell volume was accompanied by a relatively high mineralization rate, in embryonic and postnatal metatarsals of the mouse (Figure 2B, 3B). In postnatal metatarsals, the average increase in cell volume from the proliferation zone to the hypertrophic zone was higher than in embryonic metatarsals. This increase was accompanied by a higher mineralization rate (Figure 3B). Based on these results and based on results from earlier studies (Barreto and Wilsman, 1994; Breur et al., 1991; Kuhn et al., 1996), it may be concluded that the correlation between mineralization rate and volume of hypertrophic chondrocytes is not only valid in a situation of longitudinal bone growth, but also for early (embryonic) bone development. The results support the hypothesis that chondrocyte hypertrophy influences the mineralization process. Not only the hypertrophic cell volume increases during bone development at young age, the mechanical load increases as well due to increased muscular force. This increased mechanical load may enhance the mineralization process as well.

The average cell volumes and the average increase in cell volume from the proliferation zone to the hypertrophic zone in the present study, were on the same order of magnitude compared to the study of Bachrach (1995), performed on distal ulnae of immature calves (hypertrophic: 896 μm^3, proliferating: 626 μm^3, cell volume increase: factor 1.43). However, the cell volume increase in other growth plates is often higher than in this study, for example a tenfold volume increase has been reported in the proximal tibial growth plate of rats (Hunziker and Schenk, 1989). This may be due to differences in age, species, growth plate location, measuring technique, and the presence of different loading conditions.

The pattern of cartilage mineralization in embryonic mouse bone is slightly different from postnatal mineralization. In embryonic bones, the mineralization is randomly distributed around the hypertrophic cells, i.e. not oriented yet (Haaijman et al., 1999),

whereas mineralization in postnatal growth plates is primarily oriented in the longitudinal growth direction (Hunziker, 1988). Our hypothesis predicts that in the postnatal growth plate cell hypertrophy stresses the collagen network mainly in the axial direction, while in embryonic bone, where the hypertrophic cells are not yet oriented, the stresses on the matrix are not oriented either. The two different mineralization patterns observed in embryonic versus postnatal bone concur with this hypothesis.

There are advantages and shortcomings in using CLSM as a technique to determine actual cell volumes in fixed metatarsals. The metatarsals can be scanned without extensive tissue preparations like embedding, cutting, and staining. Fixation presumably results in cell shrinkage, which may have different effects in the proliferation and hypertrophic zones. These effects were, however, small considering the present results, which showed that cell volumes in fixed embryonic metatarsals were not significantly different from cell volumes in fresh, living metatarsals. In addition, it is more convenient to work with fixed tissue than with living tissue. In living metatarsals, it is difficult to label the cells. Although it was possible to label living cells in articular cartilage without serious problems (Errington et al., 1997), in embryonic cartilage it was more difficult; the fluorescent dye in embryonic tissue deteriorated more quickly compared to articular cartilage, presumably due to the presence of more enzymes.

In conclusion, the hypothesis that the mineralization process is governed by cell pressure on the matrix, which additionally causes stress in the collagen network, is supported by the present study. Manipulation of the mineralization process could then potentially be obtained through manipulation of hypertrophic cell volumes. For example, if mineralization is undesirable, then attempts should be made to decrease cell volumes, or to prevent increases in cell volumes; parathyroid hormone related protein (PTHrP) is one of the molecules that is known to block hypertrophic cell differentiation, resulting in decreased mineralization (Vortkamp et al., 1996). Further studies must test the hypothesis in more detail, such as studying the effects of enhancing or inhibiting volume increases on cartilage mineralization, using osmotic perturbations or drugs.

ACKNOWLEDGEMENTS

CM Semeins and P Buma for help in preparing the histological slices

REFERENCES

Bachrach NM Growth plate chondrocyte deformation in situ In Growth plate chondrocyte deformation in situ and a biphasic inclusion model for cells within hydrated soft tissues PhD thesis, pp 64-97, Columbia University, 1995

Barreto C, Wilsman NJ Hypertrophic chondrocyte volume and growth rates in avian growth plates Res Vet Sci 56 53-61, 1994

Breur GJ, VanEnkevort BA, Farnum CE, Wilsman NJ Linear relationship between the volume of hypertrophic chondrocytes and the rate of longitudinal bone growth in growth plates J Orthop Res 9 348-359, 1991

Buckwalter JA, Mower D, Ungar R, Schaeffer J, Ginsberg B Morphometric analysis of chondrocyte hypertrophy J Bone Joint Surg [Am] 68 243-255, 1986

Burger EH, Klein-Nulend J, Veldhuijzen JP Modulation of osteogenesis in fetal bone rudiments by mechanical stress in vitro J Biomech 24 101-109, 1991

Carter DR, Orr TE, Fyhrie DP, Schurman DJ Influences of mechanical stress on prenatal and postnatal skeletal development Clin Orthop 219 237-250, 1987

Carter DR, Wong M, Orr TE Musculoskeletal ontogeny, phylogeny, and functional adaptation J Biomech 24 3-16, 1991

Copray JCVM, Jansen HWB, Duterloo HS Effects of compressive forces on proliferation and matrix synthesis in mandibular condylar cartilage of the rat in vitro Arch Oral Biol 30 299-304, 1985

Copray JCVM, Jansen HWB, Duterloo HS An in-vitro system for studying the effect of variable compressive forces on the mandibular condylar cartilage of the rat Arch Oral Biol 30 305-311, 1985

Copray JCVM, Jansen HWB, Duterloo HS Effect of compressive forces on phosphatase activity in mandibular condylar cartilage of the rat in vitro J Anat 140 479-489, 1985

Cruz-Orive LM, Hunziker EB Stereology for anisotropic cells application to growth cartilage J Microsc 143(Pt 1) 47-80, 1986

Errington RJ, Fricker MD, Wood JL, Hall AC, White NS Four-dimensional imaging of living chondrocytes in cartilage using confocal microscopy a pragmatic approach Am J Physiol Cell Physiol 41 C1040-C1051, 1997

Errington RJ, White NS Measuring dynamic cell volume in situ by confocal microscopy Methods Mol Biol 122 315-340, 1999

Gundersen HJG, Bendtsen TF, Korbo L, Marcussen N, Møller A, Nielsen K, Nyengaard JR, Pakkenberg B, Sørensen FB, Vesterby A, West MJ Some new, simple and efficient stereological methods and their use in pathological research and diagnosis APMIS 96 379-394,

1988

Haaijman A, D'Souza RN, Bronckers ALJJ, Goei SW, Burger EH OP-1 (BMP-7) affects mRNA expression of type I, II, X collagen, and matrix Gla protein in ossifying long bones in vitro J Bone Miner Res 12 1815-1823, 1997

Haaijman A, Karperien M, Lanske B, Hendriks J, Lowik CWGM, Bronkers ALJJ, Burger EH Inhibition of terminal chondrocyte differentiation by bone morphogenetic protein 7 (OP-1) in vitro depends on the periarticular region but is independent of parathyroid hormone-related peptide Bone 25.397-404, 1999

Hunziker EB Growth plate structure and function Pathol Immunopath Res 7 9-13, 1988

Hunziker EB, Schenk RK Physiological mechanisms adopted by chondrocytes in regulating longitudinal bone growth in rats J Physiol 414 55-71, 1989

Hunziker EB, Schenk RK, Cruz-Orive LM Quantitation of chondrocyte performance in growth-plate cartilage during longitudinal bone growth J Bone and Joint Surg [Am] 69 162-173, 1987

Kirsch T, Nah HD, Shapiro IM, Pacifici M Regulated production of mineralization-competent matrix vesicles in hypertrophic chondrocytes J Cell Biol 137 1149-1160, 1997

Klein-Nulend J, Veldhuijzen JP, Burger EH Increased calcification of growth plate cartilage as a result of compressive force in vitro Arth Rheum 29 1002-1009, 1986

Kuhn JL, DeLacey JH, Leenellett EE Relationship between bone growth rate and hypertrophic chondrocyte volume in New Zealand white rabbits of varying ages J Orthop Res 14 706-711, 1996

Pauwels F Biomechanics of fracture healing In Biomechanics of the locomotor apparatus Translated from the 1965 German edition by Manquet P and Furlong R, pp 106-120, Berlin, Springer, 1980

Tanck E, Blankevoort L, Haaijman A, Burger EH, Huiskes R The influence of muscular activity on local mineralization patterns in metatarsals of the embryonic mouse J Orthop Res 18 613-619, 2000

Van Loon JWA, Bervoets DJ, Burger EH, Dieudonné SC, Hagen JW, Semeins CS, Doulabi BZ, Veldhuijzen JP Decreased mineralization and increased calcium release in isolated fetal mouse long bones under near weightlessness J Bone Miner Res 10 550-557, 1995

Van't Veen SJGA, Hagen JW, van Ginkel FC, Prahl-Andersen B, Burger EH Intermittent compression stimulates cartilage mineralization Bone 17 461-465, 1995

Vortkamp A, Lee K, Lanske B, Segre GV, Kronenberg HM, Tabin CJ· Regulation of rate of cartilage differentiation by Indian hedgehog and PTH-related protein Science 273 613-622, 1996

4

WHY DOES INTERMITTENT HYDROSTATIC PRESSURE ENHANCE THE MINERALIZATION PROCESS IN FETAL CARTILAGE?

E Tanck, WD van Driel, JW Hagen, EH Burger, L Blankevoort, R Huiskes

Journal of Biomechanics,32: 153-161, 1999

LETTER TO THE EDITOR

DR Carter, GS Beaupré

Journal of Biomechanics, 32. 1255-1256, 1999

AUTHORS RESPONSE

E Tanck, WD van Driel, JW Hagen, EH Burger, L Blankevoort, R Huiskes

Journal of Biomechanics, 32: 1257, 1999

ABSTRACT

The purpose of this study was to determine which factor is the most likely one to have stimulated the mineralization process in the *in vitro* experiments of Klein-Nulend et al. (*Arth. Rheum.*, 29, 1002-1009, 1986), in which fetal cartilaginous metatarsals were externally loaded with an intermittent hydrostatic pressure, by compressing the gas phase above the culture medium. Analytical calculations excluded the possibility that the tissue was stimulated by changes in dissolved gas concentration, pH or temperature of the culture medium through compression of the gas phase. The organ culture experiments were also mechanically analyzed using a poroelastic finite element model of a partly mineralized metatarsal with compressible solid and fluid constituents. The results showed that distortional strains occurred in the region were mineralization proceeded. The value of this strain was, however, very sensitive to the value of the intrinsic compressibility modulus of the solid matrix (K_s). For realistic values of K_s the distortional strain was probably too small (about 2 μstrain) to have stimulated the mineralization. If the distortional strain was not the factor to have enhanced the mineralization process, then the only candidate variable left is the hydrostatic pressure itself. We hypothesize that the pressure may have created the physical environment enhancing the mineralization process. When hydrostatic pressure is applied, the balance of the chemical potential of water across cell membranes may be disturbed, and restored again by diffusion of ions until equilibrium is reached again. The diffusion of ions may have contributed to the mineralization process.

INTRODUCTION

The process of endochondral ossification in the fetal skeleton commences in the diaphysis where the primary ossification center is formed by hypertrophied chondrocytes. In a short period of time, a calcium phosphate is deposited in the matrix around these hypertrophied cells. Hence, the chondrocytes hypertrophe before the matrix mineralizes. The processes of hypertrophy and mineralization progress towards the distal ends of the fetal bone, where the epiphyses are formed. Finally the mineral is resorbed by osteoclasts and replaced by bone tissue. *In vivo*, the mineralization process in fetal mouse metatarsals starts at 16 days of gestational age.

It was observed that this process coincides with the first muscle contractions of the feet (Burger et al , 1991) The deposition of calcium phosphate might, therefore, be stimulated by mechanical loads

To study the influence of mechanical loads on the mineralization process, Klein-Nulend et al (1986) performed *in vitro* culture experiments on 16-day-old fetal mouse metatarsals The organs were loaded for a period of five days with a cyclic hydrostatic pressure (13 kPa, 0 3 Hz) The pressure was applied through compression of the gas phase (5% CO_2 in air) above the culture medium (Klein-Nulend et al , 1986) The results showed that loaded metatarsals had a mineralized diaphyseal part which was two to three times longer than that of the unloaded controls (Klein-Nulend et al , 1986) Hence, it was concluded that the mineralization process in fetal cartilage is stimulated by mechanical load However, it is also possible that physical changes of the culture medium affected the results of the experiments

It is known that the physical conditions of the culture medium may be important for the mineralization process of the fetal metatarsal For instance, whether the metatarsal mineralizes or not depends amongst others on the pH and the temperature of the medium It has already been shown that chondrocytes *in vitro* can alter their activity by changes in their biophysical environment, such as osmotic pressure (Urban, 1994, Urban and Hall, 1994), fluid flow (Kim et al , 1994, 1995), hydrostatic pressure (Urban, 1994, Urban and Hall, 1994, Lammi et al , 1994, Parkkinen et al , 1994, 1995), electrical potential gradients (Kim et al , 1995, Frank and Grodzinsky, 1987), and pH (Gray et al , 1988) As the hydrostatic pressure in the *in vitro* culture experiments was applied through a gas phase, it was suggested that it is possible that the mineralization process was stimulated by changes in dissolved gas concentration or pH, rather than by the pressure itself (Urban, 1994)

Wong and Carter (1990) performed a Finite Element (FE) stress analysis of the organ culture experiments of Klein-Nulend et al (1986) They suggested, based on their results, that the mineralization process might have been stimulated by shear stresses at the cartilage/mineralized cartilage interface, as local effects of the external hydrostatic pressure In this FE analysis, however, they considered the tissue as a linear-elastic material In fact, cartilage consists of a solid phase, mainly collagen and proteoglycans, and a fluid phase of interstitial water Biphasic tissues like this are known to display strong non-linear, time dependent deformational behavior when loaded (Mow et al , 1980, Spilker et al , 1988) Hence, it is questionable whether the stress patterns determined in a linear-elastic FE analysis are realistic In addition, not

only deformation, but also pressure gradients and interstitial fluid flow play roles that might affect the mineralization process.

The following questions were addressed in this study: (1) Is it likely that the mineralization process in the *in vitro* organ culture experiments of Klein-Nulend et al. (1986) was stimulated by one of the physical changes in the culture medium, e.g. dissolved gas concentration, pH, or temperature? (2) Is it likely that the mineralization process was stimulated by one of the mechanical factors in the tissue, e.g. internal strain, stress, fluid pressure and fluid flow, as local effects of the external hydrostatic pressure? To answer these questions, we analyzed the physical changes of the culture medium under the experimental loading conditions. In addition, a poroelastic FE analysis was performed to determine the distribution of mechanical variables at the mineralization front. Information about the mineralization process may be important for the prevention and treatment of musculoskeletal developmental deformities.

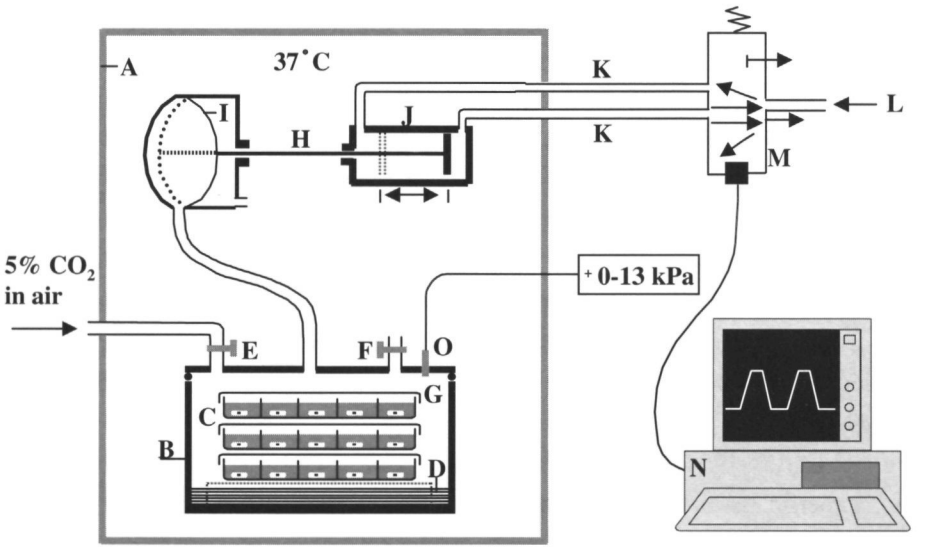

Figure 1: Schematic drawing of the intermittent hydrostatic compression (IHC) apparatus. IHC was generated by intermittently compressing the gas phase (one second of loading, followed by two seconds of unloading) of a closed culture chamber with 98% humidity, which contained the culture dishes and was placed in a 37°C incubator. The maximum pressure was 13 kPa. **(A)** 37°C incubator; **(B)** culture chamber; **(C)** culture dishes containing organ cultures and fluid culture medium; **(D)** H_2O; **(E)** tap inlet; **(F)** tap outlet; **(G)** gas phase of 5% CO_2 in air; **(H)** piston-rod; **(I)** membrane; **(J)** compressed air cylinder; **(K)** inlet; **(L)** pressure supply; **(M)** electronic valve; **(N)** pulse generator; **(O)** pressure transducer.

METHODS

Physical analysis of the culture medium

As the hydrostatic pressure in the organ culture experiments was applied through the gas phase (Figure 1), the volume in the culture system decreased during compression, leading to an increase in partial CO_2 and O_2 pressures, which resulted in their increased absorptions in the culture medium. The compression period is one second, which is followed by two seconds of relaxation in which the volume in the culture system returns to normal again. When the gas is compressed from pressure p_1 to p_2, the partial CO_2 and O_2 pressures will increase with a factor p_2/p_1, as will the quantities of CO_2 and O_2 absorbed in the liquid. In the experiment, the total pressure changed between 100 kPa and 113 kPa. Since the medium was buffered by bicarbonates, a change in the CO_2 concentration led to a change in the pH of the medium due to a shift in the chemical equilibrium

$$CO_2 + H_2O \rightleftarrows HCO_3^- + H^+. \tag{1}$$

To calculate the change in pH during compression, the following equation was solved

$$pH = -\log [H^+] = -\log \left(K_a \cdot \frac{[CO_2]}{[HCO_3^-]} \right), \tag{2}$$

where K_a is the equilibrium constant, which can be calculated under control conditions with the equation

$$K_a = \frac{[HCO_3^-][H^+]}{[CO_2]}, \tag{3}$$

where the concentration of HCO_3^- is known from the added amount of $NaHCO_3$ in the medium as 2.2 g/l (i.e. $[HCO_3^-]$=0.0262 mol/l), and the concentration H^+ is known from the pH value of 7.4 (i.e. $[H^+]=10^{-7.4}$). The concentration of CO_2 is unknown and can be calculated from *Henry's law* (Perry, 1950) with the assumption that the quantity of CO_2 absorbed in the medium is similar to that in water, such that

$$p = H\,x, \tag{4}$$

in which p is the partial CO_2 pressure, H is the constant of Henry's law, and x is the mole fraction of the gas solved in the total liquid. The concentration of O_2 is calculated in the same way. The partial pressures p under control conditions are 5.07×10^3 Pa (=5%) for CO_2 and 2.13×10^4 Pa (=21%) for O_2, whereas the values of H at 37 °C are calculated from the values at 35 °C and 40 °C, assuming a linear scale between 35 °C and 40 °C, giving 2.22×10^8 Pa for CO_2 and 5.25×10^9 Pa for O_2 (Perry, 1950). The mole fraction (x) is calculated from Eq. (4). The quantity of CO_2 ($m_{CO_2}/44$) or O_2 ($m_{O_2}/32$) in moles, dissolved in a defined mass of water (m_{H_2O}) of 37 °C can now be calculated under control conditions and during compression from

$$x = \frac{\frac{m_{CO_2}}{44}}{\left(\frac{m_{CO_2}}{44} + \frac{m_{H_2O}}{18}\right)} \quad \text{or} \quad x = \frac{\frac{m_{O_2}}{32}}{\left(\frac{m_{O_2}}{32} + \frac{m_{H_2O}}{18}\right)}. \tag{5}$$

However, the calculated quantities of CO_2 and O_2 will certainly not be reached within one second of compression as the diffusion process of these molecules in the liquid proceeds very slowly. Hence, the changes calculated in dissolved gas concentrations and the pH are only valid for that part of the culture medium in which the gas is diffused. The mean distance traveled by the gas particles ($< x >$) during compression should, therefore, be calculated by (Atkins, 1990)

$$< x >= \sqrt{\frac{2kT}{3\pi^2 \eta a}}\cdot\sqrt{t} \tag{6}$$

in which k is the Boltzmann constant (1.3807×10^{-23} J/K), T the temperature of the gas (K), η the viscosity of the solvent (for culture medium: $\eta = 1.027\times10^{-3}$ Pa.s, experimentally determined by CM Semeins, ACTA, Amsterdam), a the radius of the gas particles (for CO_2: 1.615×10^{-10} m; for O_2: 1.460×10^{-10} m) (Weast, 1970), and t the time (s). The gas temperature T varies during the dynamic experiment. Since the compression of the gas phase is an adiabatic process, e.g. there is no heat flow in or out of the system, the laws for adiabatic processes must be applied in order to

calculate the increase in gas temperature during compression, hence (Griffiths and Thomas, 1962; Marion, 1979)

$$p.V^{\gamma} = \text{constant} \tag{7}$$

Using the universal gas law (Marion, 1979) this results in

$$T^{\gamma}.\, p^{1-\gamma} = \text{constant} \tag{8}$$

in which p is the pressure (Pa), V is the volume (m^3), γ is the specific heat ratio, and T is the temperature (K). For air the value of γ is about 1.4 (Washburn, 1928). During the adiabatic compression of gas from pressure p_1 to p_2, the temperature raises from T_1 to T_2 ($\Delta T = T_2 - T_1$). With the use of Eq. (8) temperature T_2 can be calculated as

$$T_2 = T_1 . \left(\frac{p1}{p2}\right)^{\frac{1-\gamma}{\gamma}}. \tag{9}$$

Adiabatic expansion of the gas from p_2 to p_1, i.e. during the relaxation period, causes an equal decrease in temperature. As the mean temperature of the system is 37 °C (i.e. 310 K) the temperature will fluctuate between 37 °C-½ΔT and 37 °C+½ΔT. Finally, the mean diffusion distance of the gasses for the most unfavorable situation, which is at a gas temperature of 37 °C+½ΔT, can be calculated. The consequences of this variation must be analyzed, in the perspective that the height of the culture medium in the culture well is 1700 µm and that the thickness of a fetal metatarsal is about 300-400 µm.

Finite element analysis

To simulate the *in vitro* culture experiments of Klein-Nulend et al. (1986), a FE model of a fetal mouse metatarsal was developed using a poroelastic description of the tissue. An axialsymmetric model was used which consisted of 175 eight-noded elements with quadratically interpolated displacements and pressures (Figure 2). Because the project was aimed at the process of enhanced mineralization through the loading experiment, the model contained mineralized cartilage in the central part and unmineralized cartilage in the diaphysial part of the metatarsal (Figure 2). The

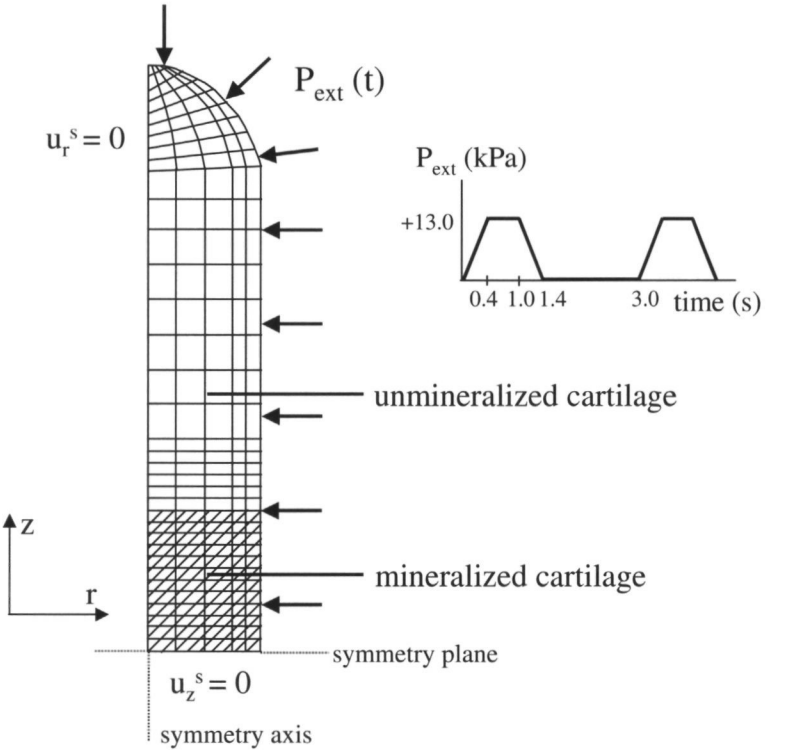

Figure 2: Axialsymmetric FE model of a fetal mouse metatarsal. The model contains mineralized cartilage in the central part and unmineralized cartilage in the remainder part of the metatarsal. The surface was assumed to be permeable to fluid. The model was loaded with a cyclic hydrostatic pressure of 13 kPa at 0.3 Hz. This load was applied to the boundary elements of the FE mesh.

surface of the metatarsal was assumed to be permeable to fluid. As in the culture experiments, the model was loaded with a cyclic hydrostatic pressure of 13 kPa at 0.3 Hz (Figure 2). The model was generated using the preprocessor MENTAT (MARC, Palo Alto, California, USA), and the analysis was performed using the code DIANA (TNO, Delft, The Netherlands). This code is based on the poroelastic theory of Biot (1941), which has the possibility to incorporate compressible solid and fluid constituents. Prendergast et al. (1996) showed that this theory is compatible with the biphasic theory (Mow et al., 1980) for linear-elastic solid matrices saturated by a Newtonian fluid assuming intrinsic incompressible constituents.

According to the poroelastic theory, soft tissues such as articular cartilage, can be modeled as a mixture of fluid and solid components. For an extensive description of

this theory the reader is referred to the literature (Bowen, 1992; De Boer, 1996; Simon, 1992). Here, the basic principles will be recapitulated. Both fluid and solid constituents with volume fractions ϕ_f, respectively ϕ_s are present at each material point in the mixture. Because of this continuity, the sum of the volume fractions has to equal one. The solid constituent is assumed to be isotropic, linear elastic, and porous, and the fluid is assumed to be Newtonian. There are two possible ways in which the volume of the tissue can change. The first is expelled fluid from the tissue. This produces a relative fluid velocity according to Darcy's law

$$(v_s - v_f) = k \nabla(p) \tag{10}$$

in which $(v_s - v_f)$ is the relative fluid velocity (m/s), k is the permeability (m^4/N.s), and p is the fluid pressure (Pa). The second way in which the volume of the tissue can change is by compression of the solid and fluid phases themselves. For this to occur the constituents must be intrinsically compressible. It should be noted that at this point, that the poroelastic model (Biot, 1941) differs from the biphasic model of Mow et al. (1980) as the latter one does not incorporate compressibility of the individual constituents. The extent of compressibility is expressed by the compressibility modulus (K, in Pa), according to

$$K = -\frac{\Delta p}{\Delta V / V_0}, \tag{11}$$

where Δp is the change in hydrostatic pressure (Pa), ΔV is the volume change (m^3) and V_0 is the unstretched volume of the tissue (m^3) (Carew et al., 1968). The compressibility was implemented in the FE model by adding two parameters: the intrinsic compressibility modulus of the solid phase (K_s, in Pa) and the intrinsic compressibility modulus of the fluid phase (K_f, in Pa) (Biot, 1941).

Table 1 presents the material properties of the fetal cartilage, which were implemented in the FE model. The tissue properties of fetal cartilage are unknown but are probably close to the properties of growth plate cartilage, as the process of development (i.e. cell proliferation, cell hypertrophy, and mineralization around hypertrophied chondrocytes) is similar. The Young's modulus (E) and permeability (k) for the unmineralized cartilage were obtained from average values of literature data on hypertrophied cartilage (Bachrach, 1995; Cohen et al., 1992), whereas the

Table 1. Material properties of the unmineralized and mineralized cartilage. The Young's modulus (E) and the Poisson's ratio (ν) refer to the drained solid matrix, whereas the compressibility moduli (K_f and K_s) refer to the intrinsic properties of the fluid and solid constituents.

	unmineralized cartilage	mineralized cartilage
E (MPa)	0.44	117
k (m^4/N.s)	6.7×10^{-15}	6.7×10^{-16}
ν	0.25	0.30
n	0.31	0.25
K_f (MPa)	2200	2200
K_s (MPa)	1-10000	10000

average Poisson's ratio (ν) of articular cartilage was used (Mow et al., 1991). For the porosity value (n), or fluid volume fraction, only the free movable water of the tissue was considered. We assumed that the water in the chondrocytes is fixed and moves with the solid matrix. Hence the porosity was calculated by quantifying the fraction of matrix in the fetal tissue (0.54, using image analysis) (data not shown), times the fraction of water in the matrix (0.75) (Mow et al., 1991, 1984), times the fraction of free water in the matrix (0.77) (Torzilli, 1988). This resulted in a porosity estimate of 0.31. In mineralized cartilage, the matrix contains calcium phosphate, which increases its Young's modulus (117 MPa) (Huiskes et al., 1995), while reducing permeability and porosity. The permeability and porosity values were estimated, as no proper literature data was available. The Poisson's ratio of bone was used (Table 1). The value of K_f is known to be 2200 MPa (Tamura et al., 1993) (Table 1). However, little is known about the values of K_s of fetal cartilage. Therefore, K_s of the unmineralized cartilage was varied between 1 MPa (highly compressible) and 10000 MPa (virtually incompressible), and that of the mineralized cartilage was held constant at an average value of cortical bone of 10000 MPa (S Tepic, personal communication, 1996).

As in the organ culture experiments (Klein-Nulend et al., 1986) the dynamic hydrostatic pressure was applied to the FE model. The distributions of shear stresses, shear strains, fluid velocity and fluid pressure were determined for the whole range of K_s values, in order to analyze which of the factors is the most likely one to have stimulated the mineralization process in the *in vitro* experiments.

RESULTS

Physical analysis of the culture medium

During the dynamic hydrostatic pressure experiments, the physical changes in dissolved gas concentration, pH, and temperature in the culture medium were small and only present in the top layer of the culture medium; hence not at the bottom where the metatarsals were lying (Table 2). One second compression of the gas phase from p_1=100 kPa to p_2=113 kPa increased the concentration of O_2 and CO_2 in the culture medium from 0.225 to 0.254 mmol/l, and from 1.271 to 1.436 mmol/l, respectively (Table 2). In addition, the pH value was decreased from 7.400 to 7.347 (Table 2). The temperature of the gas phase was increased with 5.5 K, which led to mean diffusion distances in the culture medium of 44.3 μm and 42.1 μm for O_2 and CO_2, respectively (Table 2). The temperature variation in the culture medium was negligible compared to the temperature variation in the gas phase because of the poor heat transmission from gas to liquid (data not shown). During the two seconds of relaxation, i.e. from p_2=113 kPa to p_1=100 kPa, the dissolved gas concentration and pH return to their original values.

Table 2. Changes in gas temperature, dissolved gas concentrations and pH in the culture medium after compression of the gas phase from p_1=100 kPa through p_2=113 kPa, and the mean distance traveled in 1 second, $\langle x \rangle_{1s}$, by O_2 and CO_2.

gas pressure (kPa)	T (K)	$[O_2]$ (mol/l)	$[CO_2]$ (mol/l)	pH	$\langle x \rangle_{1s}$ O_2 (μm)	$\langle x \rangle_{1s}$ CO_2 (μm)
100	310.2	0.225×10^{-3}	1.27×10^{-3}	7.400	43.92	41.76
113	315.7	0.254×10^{-3}	1.44×10^{-3}	7.347	44.31	42.13

Finite element analysis

For each intrinsic compressibility modulus of the solid phase (K_s) of the unmineralized cartilage, and for each point in time during the loading cycle, the gradient of fluid pressure in the tissue was small, resulting in relatively small fluid velocities. The fluid pressure in the unmineralized cartilage during loading was between 0.001 and 0.980 kPa higher than the applied hydrostatic pressure of 13 kPa if K_s of the unmineralized cartilage was lower than K_f, i.e. lower than 2200 MPa. This

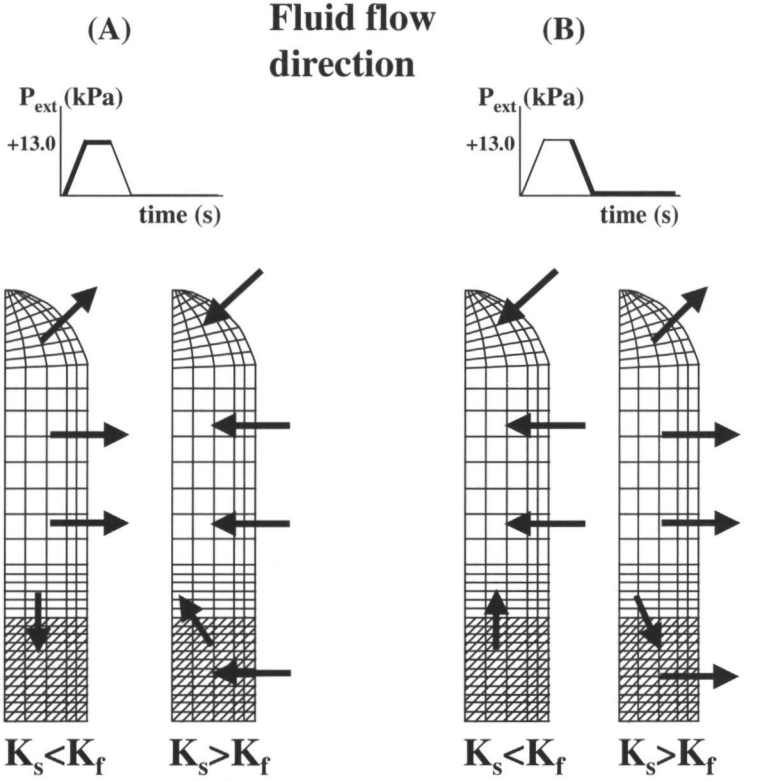

Figure 3: Schematic presentation of the fluid flow direction during loading **(A)** and unloading **(B)**. **(A)** When the K_s value of unmineralized cartilage was lower than K_f then the fluid mainly flowed outwards. Fluid was also transported through the mineralization region. In case that K_s was higher than K_f, the pressure in the unmineralized tissue was lower than the applied pressure. As a consequence, the fluid flowed inwards. **(B)** When the load was released the direction of the fluid flow was reversed.

was caused by the solid phase, which volume was decreased more under the applied hydrostatic pressure than the volume of water. As a consequence, the pressure of the fluid was increased. As fluid always flows from a high pressure towards a lower one, the fluid flowed predominantly outwards (Figure 3A), with maximum velocities between 4.8×10^{-8} and 9.0×10^{-5} mm/s, for K_s values between 1000 and 1 MPa, respectively. When the load was released, the fluid flow reversed its direction (Figure 3B). In the case that K_s of the unmineralized cartilage was higher than K_f, the pressure in the tissue was about 0.0005 kPa lower than the applied pressure during loading. As a consequence, the fluid flowed inwards with a maximum velocity of

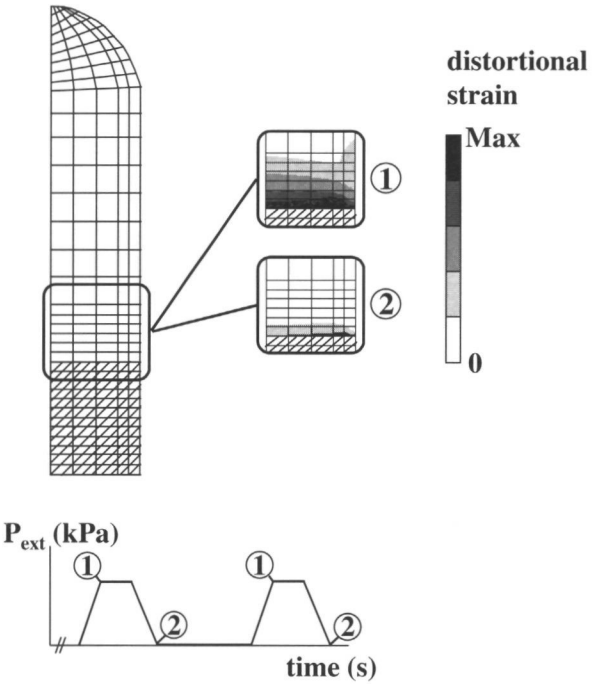

Figure 4: Patterns of the distortional strain when the load is applied (1) and when the load is released (2). The distortional strain was prominent in the hypertrophied area and the pattern of deformation was about the same for every K_s value for the unmineralized cartilage. The value of 'Max' depends on the K_s value (see Figure 5).

about -4.0×10^{-8} mm/s (Figure 3A). When the load was released the direction of the fluid flow was again reversed (Figure 3B).

The pattern of deformation in the unmineralized cartilage was about the same for every K_s value, but its quantitative significance depended on the K_s value (Figure 4, 5). Due to the different material properties of mineralized and unmineralized regions, distortional strains (or octahedral shear strains) occurred in the region of hypertrophied cells (Figure 4), whereas peak shear stress values were prominent in the already mineralized area (data not shown). At the end of the loading phase, the maximum distortional strain in the hypertrophied area was between 0.4 and 4707.0 μstrain for K_s values between 10000 and 1 MPa, respectively (Figure 5). When the load is released, this value was reduced, but not entirely to zero, because of the time inertia effect (Figure 4). Thus, the quantitative value of the distortional strain changed with the

modulus K_s (Figure 5). When the K_s value increased, the total change in volume in the unmineralized cartilage decreased, resulting in decreased shear strain values.

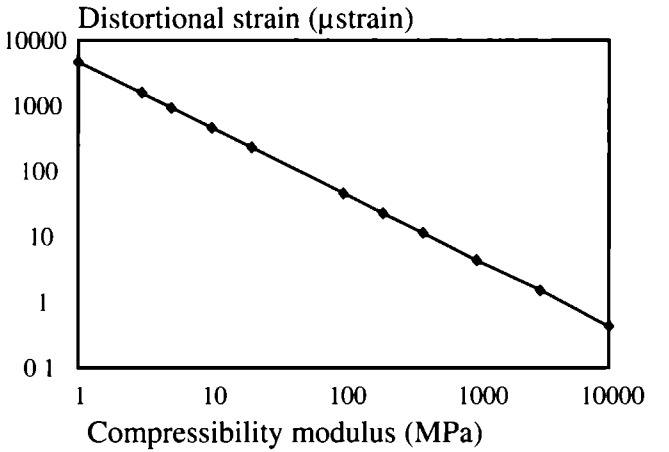

Figure 5: The maximum distortional strain at one point in the tissue during loading as a function of the compressibility modulus (K_s) of the unmineralized cartilage The strain decreases with an increasing K_s value Note that the scaling is logarithmic

DISCUSSION

In the present study the organ culture experiments of Klein-Nulend et al. (1986) were analyzed to determine which factor is the most likely one to have stimulated the mineralization process It has to be appreciated that the hydrostatic pressure of 13 kPa applied to the fetal metatarsals is much less than what is exerted on adult articular cartilage (Afoke, 1987). The value of 13 kPa is estimated to be the stress exerted on the cartilage *in vivo* as a result of the first muscle contractions (Klein-Nulend et al., 1986). Although muscle contractions cause other deformation patterns than pure hydrostatic load does, the experimentally applied pressure may be of the same order of magnitude as the resulting pressures in the tissue due to muscle forces.

We showed that the changes in dissolved gas concentration, pH and temperature in the culture medium were relatively small. Although Lo et al. (1994) showed that small changes in CO_2 concentration may affect cell behavior, we calculated that these changes were only present in the superficial layer (42 μm) of the culture medium

The one-second compression period from 100 kPa to 113 kPa was far too short for CO_2 to reach (and affect) the tissue. Hence, when the height of the culture medium column (1700 μm) and the thickness of the fetal metatarsal (300-400 μm) lying on the bottom of that column are considered, it seems unlikely that the mineralization process was stimulated by fluctuations in dissolved gas concentration, pH or temperature during the experiment. Therefore, we assume that the tissue was stimulated by the intermittent hydrostatic pressure itself. An additional point in favor of this argument is that the calculated change in pH during the experiments would work against mineralization. It should be noted that the effect of serum proteins, amino acids and other medium components are ignored in the calculation of changes in the pH of the culture medium; the medium was treated as a simple bicarbonate buffer. However, the effect of these components is probably negligible as they are likely to minimize pH changes resulting from fluctuation in partial CO_2 pressure.

The first mechanical variable considered in the FE analysis was the fluid flow. It was shown that the influence of the fluid flow on the mineralization process was probably negligible as the fluid pressure gradients in the tissue were very small.

Wong and Carter (1990) simulated the same dynamic culture experiments with a linear-elastic FE model. They suggested that a combination of shear stress and hydrostatic pressure, the so-called osteogenic index, stimulated the mineralization process. We could not confirm this hypothesis in the present study. This is not surprising, since the poroelastic tissue properties differ considerably from linear-elastic ones. In our poroelastic analysis, the intrinsic compressibility of the solid matrix showed to have a major impact on the resulting distributions of the mechanical variables. The distortional strain was prominent in the hypertrophied region, which is precisely the region were the mineralization process proceeds. For this reason, the distortional strain seemed to be a factor likely to have stimulated the mineralization process. The value of the strain, however, is very sensitive to the compressibility K_s. This implies that the value of K_s must be known, before the probability of distortional strain as a mechanical stimulus can be assessed. If the solid phase is assumed to be intrinsically incompressible, i.e. K_s is infinite, then the pressure inside the tissue is exactly the same as the hydrostatic pressure externally applied. Hence, the pressure varies at every point in the tissue between 0 and 13 kPa, depending on the time in the loading cycle. As a consequence, the fluid velocity is zero and no deformation occurs.

Little is known about the intrinsic compressibility modulus of fetal cartilage. Ultrasound measurements showed that adult articular cartilage has a compressibility

modulus of 3400 MPa (Tepic et al., 1983). As this value mostly depends on the collagen content, it is likely that the value for fetal tissue is between the value of adult articular cartilage (3400 MPa) and that of water (2200 MPa). In that case, the maximum distortional strain in the loading cycle is reduced to about 2 μstrain (Figure 5). To the knowledge of the authors it has never been shown that 2 μstrain stimulates cell expressions significantly. However, Wright et al. (1996) showed that chondrocytes might react with cell hyperpolarization to strain values of about 10-15 μstrain. These values are, however, much larger than those found in the FE analysis, for realistic K_s values as mentioned above. It is therefore not likely that the distortional strain enhanced the mineralization process in the culture experiments.

As the material property values might be critical for the validity of the computational model, additional analyses were performed (data not shown) in which extreme values of the other material properties were implemented to determine their significance for the results and conclusion. For the unmineralized cartilage, the permeability was varied between 2×10^{-15} and 2×10^{-14} $m^4/N.s$, a porosity value of 0.80 was used (which would include all the water in the tissue), the Young's modulus was varied between 0.34 MPa and 1.0 MPa, and the Poisson's ratio was varied between 0.10 and 0.4. For the mineralized cartilage, the permeability was varied between 2×10^{-16} and 2×10^{-15} $m^4/N.s$, a porosity value of 0.65 was used, a Young's modulus of 250 MPa was used, and a K_s value of 5000 MPa was used. It was found that these variations had only minor effects on the results, compared to variation of K_s for the unmineralized cartilage (data not shown). Hence, the central conclusion remains unchanged if material properties are varied in the above-mentioned range.

If the distortional strain was not the factor to have stimulated the mineralization process in the experiment, then the only candidate variable that is left is the hydrostatic pressure itself. Other studies have already shown that hydrostatic pressure may change cell activity (Urban, 1994; Urban and Hall, 1994; Lammi et al., 1994; Parkkinen et al., 1994, 1995; Hall, 1997; Klein-Nulend et al., 1995; Takano-Yamamoto et al., 1991). The pressure might create the physical environment, which promotes the mineralization process. A possible explanation for such a mechanism could be the effect of the chemical potential of water (Gu et al., 1993, 1997). This notion is based on the triphasic theory (Lai et al, 1991), according to which the chemical potential of extracellular water has to be equilibrated by the chemical potential of the intracellular water. If the equilibrium across the cell membranes is disturbed, the chemical potential is the driving force to restore the balance. Chemical

potential is a function of, among others, the fluid pressure and the concentration of ions (Lai et al, 1991) This means that if the pressure in the extracellular matrix changes, then the chemical potential of the water in the extracellular matrix changes as well In this way it is possible that the chemical potential of the water in the extracellular matrix is not in equilibrium with the chemical potential of water in the cells, as there is a membrane in between This disturbance can be restored by changing the ion concentration across the cell membrane Hence, when the cyclic hydrostatic pressure is applied to the tissue in the organ culture experiments, the balance across the cell membranes may possibly be disturbed, and restored again by diffusion of ions until equilibrium is reached again As a consequence, the intracellular and extracellular concentrations of various ions may change, which may have an effect on intracellular signal transduction, eventually leading to changes in the speed of mineralization during the dynamic loading experiment Without the externally applied pressure, the mineralization process *in vitro* still takes place, although the production of mineral is less than in the loaded case It can be hypothesized that chondrocytes, during the process of cellular hypertrophy, start to exert pressure on the extracellular matrix (Pauwels, 1980) This cell-derived pressure may, in an as yet unknown manner help to create the natural physical environment to initiate the mineralization process In that case the externally applied hydrostatic pressure of the culture experiments may have enhanced the mineralization process by further enhancing this process

In conclusion, it is not likely that the distortional strain enhanced the mineralization process in the cyclic hydrostatic pressure experiments The only other candidate is the hydrostatic pressure itself, which may have created the right physical environment, enhancing the mineralization process through diffusion of ions However, further studies are required to test this possibility in more detail

REFERENCES

Afoke NYP, Byers PD, Hutton WC Contact pressures in the human hip joint J Bone Joint Surg [Br] 69B 536-541, 1987

Atkins PW Physical chemistry 4th edition, pp 761-773, Oxford University Press, Oxford-Melbourne-Tokyo, 1990

Bachrach NM Growth plate chondrocyte deformation in situ and a biphasic inclusion model for cells within hydrated soft tissues PhD thesis, Columbia University, 1995

Biot MA General theory of three-dimensional consolidation J Appl Physics 12 155-164, 1941

Bowen RM Compressible porous media models by use of the theory of mixtures Int J Eng Sci 20 697-735, 1992

Burger EH, Klein-Nulend J, Veldhuijzen JP Modulation of osteogenesis in fetal bone rudiments by mechanical stress in vitro J Biomech 24, Suppl 1 101-109, 1991

Carew TE, Ramesh NV, Dali JP Compressibility of the arterial wall Circ Res 23 61-68, 1968

Cohen B, Chorney GS, Phillips DP, Dick HM, Mow VC Inhomogeneous and anisotropic mechanical properties of bovine growth plate and chondroepiphysis Trans Orthop Res Soc 17 153, 1992

De Boer R Highlights in the historical development of the porous media theory Toward a consistent macroscopic theory Appl Mech Rev 49 201-262, 1996

Frank EH, Grodzinsky AJ Cartilage mechanics-I Electrokinetic transduction and the effects of electrolyte pH and ionic strength J Biomech 20 615-627, 1987

Gray ML, Pizzanelli AM, Grodzinsky AJ, Lee RC Mechanical and physicochemical determinants of the chondrocyte biosynthetic response J Orthop Res 6 777-792, 1988

Griffiths PJF, Thomas JDR The gaseous state In Calculations in advanced physical chemistry, pp 37-46, Edward Arnold Ltd, London, 1962

Gu WY, Lai WM, Mow VC Transport of fluid and ions through a porous-permeable charged-hydrated tissue, and streaming potential data on normal bovine articular cartilage J Biomech 26 709-723, 1993

Gu WY, Lai WM, Mow VC A triphasic analysis of negative osmotic flows through charged hydrated soft tissues J Biomech 30 71-78, 1997

Hall AC Hydrostatic pressure directly affects the activity of articular chondrocyte membrane transporters Trans Orthop Res Soc 22 177, 1997

Huiskes R, van Donkelaar CC, Jepsen KJ, Weinans H, Goldstein SA, Burger EH The mechanical consequences of mineralization in fetal bone Trans Orthop Res Soc 20 450, 1995

Kim Y-J, Sah RLY, Grodzinsky AJ, Plaas AHK, Sandy JD Mechanical regulation of cartilage biosynthetic behavior Physical stimuli Arch Biochem Biophys 311 1-12, 1994

Kim Y-J, Bonassar, LJ, Grodzinsky AJ The role of cartilage streaming potential, fluid flow and pressure in the stimulation of chondrocyte biosynthesis during dynamic compression J Biomech, 28 1055-1066, 1995

Klein-Nulend J, van der Plas A, Semeins CM, Ajubi NE, Frangos JA, Nijweide PJ, Burger EH Sensitivity of osteocytes to biomechanical stress in vitro FASEB 9 441-445, 1995

Klein-Nulend J, Veldhuijzen JP, Burger EH Increased calcification of growth plate cartilage as a result of compressive force in vitro Arthritis Rheum 29 1002-1009, 1986

Lai WM, Hou JS, Mow VC A triphasic theory for the swelling and deformation behaviors of articular cartilage J Biomech Eng 113 245-258, 1991

Lammi MJ, Inkinen R, Parkkinen JJ, Hakkinen T, Jortikka M, Nelimarkka LO, Jarvelainen HT, Tammi MI Expression of reduced amounts of structurally altered aggrecan in articular cartilage chondrocytes exposed to high hydrostatic pressure J Bioch 304 723-730, 1994

Lo C-M, Keese CR, Giaever I pH changes in pulsed CO_2 incubators cause periodic changes in cell morphology Exp Cell Res 213 391-397, 1994

Marion JB Gas dynamics In General physics with bioscience essays, pp 191-211, John Wiley & Sons,

USA, 1979

Mow VC, Kuei SC, Lai WM, Armstrong CG Biphasic creep and stress relaxation of articular cartilage in compression Theory and experiments J Biomech Eng 102 73-84, 1980

Mow VC, Holmes MH, Lai WM Fluid transport and mechanical properties of articular cartilage a review J Biomech 17 377-394, 1984

Mow VC, Zhu W, Ratcliffe A Structure and function of articular cartilage and meniscus In Basic Orthopaedic Biomechanics Eds VC Mow and WC Hayes, pp 143-198, Raven press, Ltd, New York, 1991

Parkkinen JJ, Lammi MJ, Tammi MI, Helminen HJ Proteoglycan synthesis and cytoskeleton in hydrostatically loaded chondrocytes In Cell mechanics and cellular engineering Eds VC Mow, F Guilak, R Transon-Tay, RM Hochmuth, pp 420-444, Springer-Verlag, New York, 1994

Parkkinen JJ, Lammi MJ, Inkinen R, Jortikka M, Tammi M, Virtanen I, Helminen HJ Influence of short-term hydrostatic pressure on organization of stress fibers in cultured chondrocytes J Orthop Res 13 495-502, 1995

Pauwels F Biomechanics of fracture healing In Biomechanics of the locomotor apparatus, Translated from the 1965 German edition by P Manquet and R Furlong, pp 106-120, Springer, Berlin, 1980

Perry RH Chemical Engineers' Handbook, pp 673-676, McGraw-Hill book company, New York, 1950

Prendergast PJ, van Driel WD, Kuiper JH A comparison of finite element codes for the solution of biphasic poroelastic problems Proc Inst Mech Eng H210 131-136, 1996

Simon BR Multiphase poroelastic finite element models for soft tissue structures App Mech Rev 45 191-218, 1992

Spilker RL, Suh JK, Mow VC A finite element formulation of the nonlinear biphasic model for articular cartilage and hydrated soft tissue including strain-dependent permeability In Computational Methods in Bioengineering Eds RL Spilker and BR Simon, pp 81-92, BED-9, ASME, New York, 1988

Takano-Yamamoto T, Soma S, Nakagawa K, Kobayashi Y, Kawakami M, Sakuda M Comparison of the effects of hydrostatic compressive force on glycosaminoglycan synthesis and proliferation in rabbit chondrocytes from mandibular condylar cartilage, nasal septum, and spheno-occipital synchondrosis in vitro Am J Orthod Dentofac Orthop 99 448-455, 1991

Tamura Y, Suzuki N, Mihashi K Adiabatic compressibility of myosin subfragment-1 and heavy meromyosin with or without nucleotide Biophys J 65 1899-1905, 1993

Tepic S, Macirowski T, Mann RW Mechanical properties of articular cartilage elucidated by osmotic loading and ultrasound Proc Natl Acad Sci USA, 80 3331-3333, 1983

Torzilli PA Water content and equilibrium water partition in immature cartilage J Orthop Res 6 766-769, 1988

Urban JPG The chondrocyte A cell under pressure Br J Rheum 33 901-908, 1994

Urban JPG, Hall AC The effects of hydrostatic and osmotic pressures on chondrocyte metabolism In Cell mechanics and cellular engineering Eds VC Mow, F Guilak, R Transon-Tay, and RM Hochmuth, pp 398-419, Springer-Verlag, New York, 1994

Washburn EW International critical tables of numerical data, physics, chemistry and technology Vol 3, pp 210-212, McGraw-Hill Book Company New York, London, 1928

Weast RC Handbook of chemistry and physics 51th edition, The Chemical Rubber Co Cleveland,

Ohio, 1970-1971

Wong M, Carter DR Theoretical stress analysis of organ culture osteogenesis Bone 11 127-131, 1990

Wright M, Jobanputra P, Bavington C, Salter DM, Nuki G Effects of intermittent pressure-induced strain on the electrophysiology of cultured human chondrocytes Evidence for the presence of stretch-activated membrane ion channels Clin Sci 90 61-71, 1996

LETTER TO THE EDITOR

Linear-elastic and poroelastic models of cartilage can produce comparable stress results: a comment on Tanck et al. (J Biomech 32:153-161, 1999)

We would like to comment on an important issue raised in the recent article by Tanck et al (1999) that focuses on the role of shear and hydrostatic stress in the mineralization of fetal cartilage This issue concerns the type of material model that is appropriate for analyzing cartilage Tanck et al used a poroelastic model consisting of fluid and solid phases, while an earlier examination of the same system by Wong and Carter (1990) used a single-phase elastic model In discussing the earlier work of Wong and Carter, Tanck et al state "it is questionable whether the stress patterns determined (by Wong and Carter) in a linear-elastic FE analysis are realistic" Tanck et al argue in favor of a poroelastic model since two-phase materials, like cartilage, "are known to display strong non-linear, time-dependent deformational behavior when loaded" Unfortunately, Tanck et al do not point out that the relevance of this statement can only be assessed fairly when further details of the analysis to be performed are taken into consideration One must know the type of loading (static vs cyclic, loading rate or frequency) and specifics of the boundary conditions (e g , whether artificial free surfaces exist for fluid flow) before an informed decision can be made about the appropriateness of a specific material model

In order to understand this issue, it is valuable to briefly examine two insightful articles that discuss material models appropriate for studying the response of cartilage to physiological loads Higginson and Snaith (1979) experimentally determined the stiffness of cartilage in confined compression and concluded that "the dynamic response of cartilage to oscillating loads of typical physiological magnitudes and frequencies is almost linear/elastic" They also note that because of the very low value of the permeability of cartilage "fluid flow makes a negligible contribution to the response" Brown and Singerman (1986) studied the mechanical response of the fetal human chondroepiphysis using the bi-phasic KLM model developed by Mow et al (1980) When describing their results Brown and Singerman state that "the behavior of the KLM solution approaches that of a single-phase elastic solid for strain rates greater than 10^{1} s^{1} for the relaxation phase, and above 10^{2} s^{1} for the compression phases" They also note that "strain rates in normal level walking are on

the order of 10^0 s^{-1}" In addition, they note that the transient (inelastic) component of the response in their study "would appear to be of relatively minor importance in whole-joint structural models"

With this as background we return to the analyses of the cartilage explant examined by Wong and Carter (1990) and Tanck et al (1999) and note that this is one example where the single-phase elastic model and the two-phase poroelastic model yield very similar results for certain solution variables A case in point is the distortional strain patterns at the time of peak load In spite of the concern voiced by Tanck et al that the stress or strain patterns predicted by Wong and Carter may be suspect, the strain patterns shown by Tanck et al are not noticeably different from the patterns shown by Wong and Carter Another example of how the poroelastic and linear elastic analyses can give similar results is shown in Figure 1

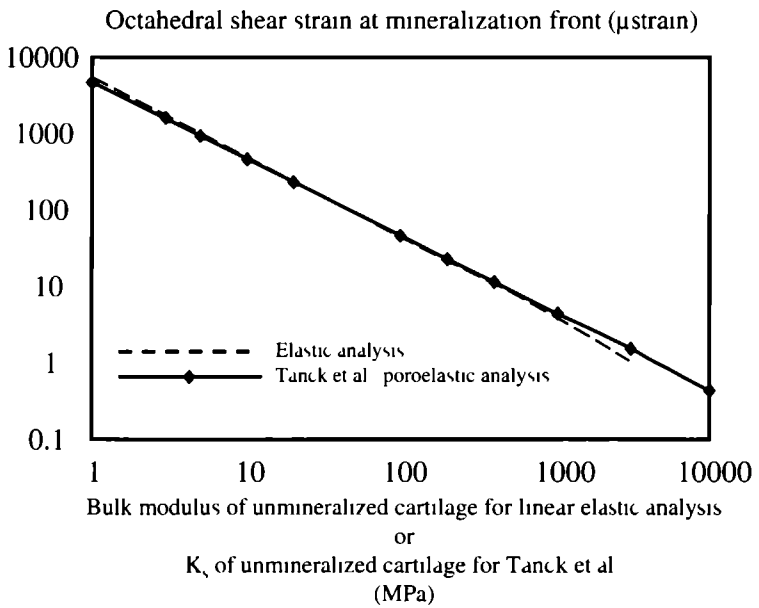

Figure 1: The effect of bulk modulus on the value of the shear strain within the unmineralized cartilage at the mineralization front

In this figure both analyses illustrate the point that as the value of the bulk modulus of the unmineralized tissue increases, the value of the shear strain at the interface

decreases In their discussion Tanck et al suggest that the maximum value of the shear strain at the mineralization front is 2 0 microstrain, while Wong and Carter predict a value in excess of 140 microstrain If these two groups of investigators had used consistent material properties, not only the patterns but also the strain magnitudes would have been similar The reason that the results are so similar is simple to understand, given the low permeability of cartilage, minimal fluid flow occurs for the cyclic loading frequencies considered and the response is therefore very nearly linear elastic

Prendergast et al (1996) have shown that the poroelastic theory is compatible with the bi-phasic theory of Mow et al (1980) Two recent studies (Ateshian et al , 1994, Soltz and Ateshian, 1998) that utilized the bi-phasic theory with simulated *in vivo* conditions show that the low permeability and lack of significant fluid flow within articular cartilage leads to fluid pressurization during loading which "typically lasts longer than the duration of most physiological loading" The authors also state that this pressurization supports up to "90% of the applied load for durations of 400 s or more" (Soltz and Ateshian, 1998) The lack of significant fluid flow and the associated pressurization in the short term are responsible for the near-linear elastic response seen by Higginson and Snaith (1979) and Brown and Singerman (1986)

The studies by Higginson and Snaith (1979), Brown and Singerman (1986), Ateshian et al (1994), and Soltz and Ateshian, (1998) show that there is a 20-year history that supports the applicability of a single-phase, linear-elastic model for cartilage when considering cyclic loads of frequencies greater than, say, 0 01 or 0 1 Hz We feel that this history and its implications are invaluable to those performing analyses of tissues, like cartilage, that have very low permeability and negligible fluid flow for many physiological loading conditions There certainly are situations where a poroelastic model can provide insights that cannot be obtained when using a single-phase elastic model However, depending on the research question a single-phase elastic model for cartilage, when used appropriately, is not only acceptable, but at times may be preferable

DR Carter
GS Beaupré

REFERENCES

Ateshian GA, Lai WM, Zhu WB, Mow VC An asymptotic solution for the contact of two biphasic cartilage layers J Biomech 27 1347-1360, 1994

Brown TD, Singerman RJ Experimental determination of the linear biphasic constitutive coefficients of human fetal proximal femoral chondroepiphysis J Biomech 19 597-605, 1986

Higginson GR, Snaith JE The mechanical stiffness of articular cartilage in confined oscillating compression Eng Med 8 11-14, 1979

Mow VC, Kuei SC, Lai WM, Armstrong CG Biphasic creep and stress relaxation of articular cartilage in compression theory and experiment J Biomech Eng 102 73 84, 1980

Prendergast PJ, van Driel WD, Kuiper JH A comparison of finite element codes for the solution of biphasic poroelastic problems J Mech Eng, Part H 210 131-136, 1996

Soltz MA, Ateshian GA Experimental verification and theoretical prediction of cartilage fluid pressurization at an impermeable contact interface in confined compression J Biomech 31 927-934, 1998

Tanck E, van Driel WD, Hagen JW, Burger EH, Blankevoort L, Huiskes R Why does intermittent hydrostatic pressure enhance the mineralization process in fetal cartilage? J Biomech 32 153-161, 1999

Wong M, Carter DR Theoretical stress analysis of organ culture osteogenesis Bone 11 127-131, 1990

AUTHORS RESPONSE

We thank Drs. Beaupré and Carter for their interest in our article (Tanck et al., 1999). They take issue with our statement relative to the appropriateness of using linear-elastic analyses for poroelastic or biphasic materials. They state, in conclusion, that "...depending on the research question a single-phase elastic model for cartilage, when used appropriately, is not only acceptable, but at times may be preferable." Generally speaking, we couldn't agree more. But their letter is somewhat ambivalent. Both their group (Wong and Carter, 1990) and we (Tanck et al., 1999) analyzed the same experiments concerning mineralization in fetal mouse metatarsals under hydrostatic external loading; they using a single-phase elastic model, we a biphasic time-dependent one. It is at least suggested in their letter that for such an experiment the single-phase linear-elastic approach is equally appropriate, as the strain patterns found in both analyses are similar, be it that the absolute values are more than two orders of magnitude apart. But this, the difference in strain values, is precisely why a single-phase elastic model is not appropriate for this experiment.

So, although we do adhere to their general statement, cited above, the question is then when a single-phase approach is appropriate and when not. It is not appropriate if the permeability of the bi-phasic tissue to be analyzed is large relative to the loading frequency, as Beaupré and Carter suggest themselves. It is not appropriate when information about the second (fluid) phase itself is required, as for instance information about flow patterns (Prendergast et al., 1997; Huiskes et al., 1997). And it is not appropriate when the tissue analyzed is incompressible, while the external load is hydrostatic pressure. These last two issues in particular were relevant in our analyses of the experiments mentioned. We wished to investigate the possible roles of fluid pressure and fluid flow on mineralization, not just the one of strain, as in the paper of Wong and Carter (1990). We concluded that effects of strain on mineralization patterns in these experiments were unlikely, as strain was extremely minute at a maximum of 2 microstrain. Wong and Carter (1990) concluded the opposite, because their maximal strain was sizeable at 140 microstrain. We maintain that this high value is an artefact, due to the negligence of incompressibility. Maybe, if their analyses would be repeated with a Poisson's ratio between 0.499 and 0.500, which is more realistic than the 0.470 they used, the same would be found. But we doubt whether the FE-analysis could handle that.

REFERENCES

Huiskes R, van Driel WD, Prendergast PJ, Søballe K: A biomechanical regulatory model for periprosthetic fibrous-tissue differentiation. J Mat Sci Mat Med 8:785-788, 1997.

Prendergast PJ, Huiskes R, Søballe K: Biophysical stimuli on cells during tissue differentiation at implant interfaces. J Biomech 30:539-548, 1997

Tanck E, van Driel WD, Hagen JW, Burger EH, Blankevoort L, Huiskes R: Why does intermittent hydrostatic pressure enhance the mineralization process in fetal cartilage? J Biomech 32:153-161, 1999.

Wong M, Carter DR: Theoretical stress analysis of organ culture osteogenesis. Bone, 11:127-131, 1990.

5

THE INFLUENCE OF MUSCULAR ACTIVITY ON LOCAL MINERALIZATION PATTERNS IN METATARSALS OF THE EMBRYONIC MOUSE

E Tanck, L Blankevoort, A Haaijman, EH Burger, R Huiskes

Journal of Orthopaedic Research, 18: 613-619, 2000

ABSTRACT

This study addressed the theory that local mechanical loading may influence the development of embryonic long bones. Embryonic mouse metatarsal rudiments were cultured as whole organs, and the geometry of the primary ossification center was compared with rudiments that had developed *in utero*. The mineralization front *in vivo* was found to be nearly straight, whereas *in vitro* it acquired a more convex shape due to a slower mineralization rate at the periphery of the mineralized cylinder. A poroelastic finite element (FE) analysis was performed to calculate the local distributions of distortional strain and fluid pressure at the mineralization front in the metatarsal during loading *in vivo* as a result of muscle contractions in the embryonic hindlimbs. The distribution of fluid pressure from the FE analysis could not explain the difference in mineralization shape. The most likely candidate to explain the difference was the distortional strain, resulting from muscle contraction, which is absent *in vitro*, as its value at the periphery was significantly higher than in the center of the tissue. Without external loads, the mineralization process may be considered as a pre-programmed process, starting at the center of the tissue and resulting in a spherical mineralization front. Strain modulates the rate of the mineralization process *in vivo*, resulting in the straight mineralization front. These results suggest that disturbances in muscle development are likely to produce disturbed mineralization patterns, resulting in a disordered osteogenic process.

INTRODUCTION

Endochondral ossification is an important process in embryonic bone development, statural growth, and fracture healing. The process follows a basic sequence of events involving the proliferation of chondrocytes, chondrocyte hypertrophy, matrix mineralization, resorption of mineralized matrix, and ultimately bone formation.

Matrix mineralization in a long bone is regulated by a combination of genetic, biological, and biomechanical factors (Carter et al., 1991). Several studies have indicated that biomechanical forces influence the endochondral ossification process. Chemical paralysis of muscles in the chick embryo diminished growth of the skeleton (Germiller and Goldstein, 1997; Hosseini and Hogg, 1991). Others showed that intermittent compressive forces reduce *in vitro* growth of mandibular condylar

cartilage of rats (Copray et al, 1995a, 1995b, 1995c) In addition, a small intermittent compression induced an increase in the alkaline phosphatase activity in the entire hypertrophied zone suggesting that the dynamic load can influence the onset of the mineralization process (Copray et al , 1995c) It is therefore likely that cartilage mineralization in the embryo may be influenced by muscular activity In the development of the embryonic mouse metatarsal, for example, the mineralization process starts at about 16 days of gestational age At this same age, the embryo starts to move its hindlimbs, indicating the occurrence of muscle contractions in the leg (Burger et al , 1991, Platzer, 1978) Early movement of the limbs is also affirmed in the human embryo in which limb movements occur as soon as the embryo is about $8^1/_2$ weeks postmenstrual age (De Vries et al , 1982)

If indeed the mineralization process is affected by muscular activity, it follows that ossification during organ culture may develop differently from the development *in vivo* A pilot experiment using embryonic mouse metatarsals suggested that the geometry of the *in vitro* mineralization front was more or less spherical, while in *in vivo* mineralized metatarsals it had a flat appearance Furthermore, in accordance with earlier observations, the mineralization rate of the cultured long bone rudiments was slower than *in vivo* (Burger et al , 1991, Klein-Nulend et al , 1986) Carter et al (1987, 1988) and Wong and Carter (1990a, 1990b) proposed that cyclic shear stresses accelerate the endochondral ossification process and cyclic compressive dilatational stresses inhibit ossification A study of Klein-Nulend et al (1986) showed that small intermittent hydrostatic pressure increased the mineralization rate in cartilaginous metatarsals of embryonic mice In a recent study, these experiments were simulated using an axialsymmetric poroelastic finite element model (Tanck et al , 1999) The results suggested that the increased mineralization could be explained by hydrostatic fluid pressure itself, whereas deformation was insignificant for the applied material parameters (Tanck et al , 1999) The role of deformation on the mineralization process was therefore unclear In the present study, muscular load was applied to a three-dimensional finite element model to analyze the possible roles of deformation and fluid pressure in the mineralization process (Carter et al , 1987, Carter and Wong, 1988, Tanck et al , 1999, Wong and Carter, 1990a, 1990b) Two questions were addressed Is the geometry of the mineralization front different between *in vitro* mineralized mouse metatarsals compared to *in vivo* mineralized ones? and, if so, do local distributions of distortional strain and fluid pressure distinguish the center from the periphery? To answer these questions, the shape of the primary ossification center

of *in vivo* mineralized metatarsals of the mouse was compared with metatarsals ossified during organ culture. In addition, a poroelastic three-dimensional finite element analysis was performed to determine the local distributions of distortional strain and fluid pressure, derived from limb muscle contractions, at the mineralization front.

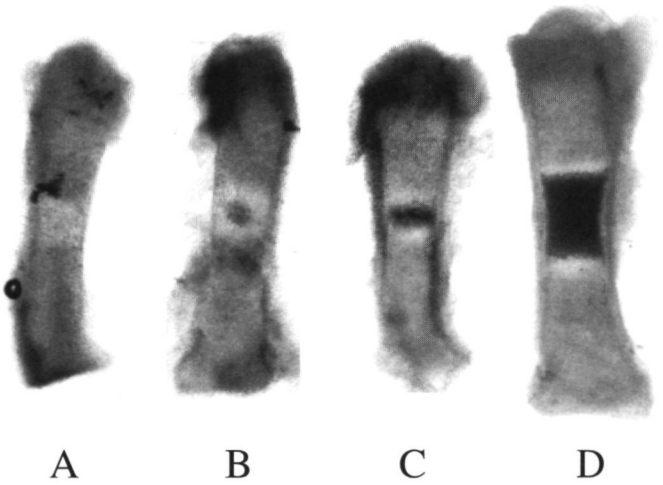

Figure 1: Subsequent stages of the *in vivo* mineralization process in mouse metatarsals at 16 **(A)**, 16^{+} **(B)** and **(C),** and 17 **(D)** days of gestational age. **A)**: Just before mineralization; the center of the rudiment is somewhat lighter because of hypertrophy of the chondrocytes. **B)**: Cartilage mineralization starts as a sphere in the center of the metatarsal. **C)**: Extension of the mineralized zone to the periphery. **D)**: Extension of the mineralized zone towards the epiphyses.

MATERIALS AND METHODS

Metatarsal rudiments from an embryonic mouse were cultured as whole organs, and the geometry of the primary ossification center was compared with rudiments that had developed *in vivo*. Metatarsals were dissected from embryos of pregnant Swiss albino mice (Harlan Inc., Zeist, The Netherlands) at 15, 17, or 18 days of gestational age. The day of vaginal plug discovery equals day zero. Gender was not controlled between the groups. All animal procedures received institutional approval.

Metatarsals at day 15 had not yet started to ossify, and consisted solely of cartilage,

that was beginning to hypertrophy in the center of the rudiment. At 16 days of gestational age, the hypertrophic center was clearly present (Figure 1A). Ossification started in metatarsals at day 16; it began as a sphere in the center (Figure 1B) which rapidly extended towards the periphery, followed by extension towards the epiphyses (Figure 1C). In metatarsals at day 17, ossification was well underway, as shown by a central area of mineralized cartilage (Figure 1D). In metatarsals at day 18, the area of ossification was longer and showed the beginning of a primitive marrow cavity For organ culture, metatarsals at gestational day 15 or 17 were cultured for 5 days or 3 days, respectively, in α-modified essential medium without nucleosides (GIBCO, United Kingdom) supplemented with 0.05 mg/ml ascorbic acid (Merck, Darmstadt, Germany), 0.3 mg/ml L-glutamine (Merck), 0.05 mg/ml gentamycine (GIBCO), 1.25 µg/ml fungizone (GIBCO), 1 mM β-glycerophosphate (Merck), and 0.2% bovine serum albumin fraction V (Sigma Chemical, St. Louis, MO, U.S.A.) (complete medium) The metatarsals were cultured individually in 300 µl complete medium in a 24 wells tissue culture plate (Greiner, Alphen aan de Rijn, The Netherlands) at 37 °C, 98% humidity, and 5% CO_2 in air (Haaijman et al., 1997, Klein-Nulend et al , 1986; Van Loon et al., 1995; Van't Veen et al., 1995).

Measurement of the ossification center

Cultured and non-cultured metatarsals were photographed at x10 magnification. Orientation of the isolated rudiments along the longitudinal axis was impossible. The ossification zone, which appeared dark as a result of matrix mineralization, was measured (Haaijman et al., 1997; Klein-Nulend et al , 1986; Van Loon et al., 1995; Van't Veen et al., 1995) from projected slides at x300 magnification. To analyze the shape of this zone, the difference between the length of the mineral in the center (l_1) and the mean length of the mineral at the periphery ($[l_2+l_3]/2$) was calculated (Figure 2). The mineralization geometry in day-17 metatarsals was compared with that in day 15 metatarsals that were cultured for 5 days; these groups

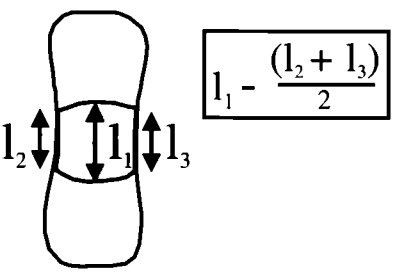

Figure 2: Measurements of the mineralization shape The difference between the length of the mineral in the center, l_1, and the mean length of the mineral at the periphery, $(l_2+l_3)/2$, was measured

can be compared for their developmental stage (Burger et al., 1992; Haaijman et al., 1997). Organ culture slows down the development of the metatarsals. Haaijman et al. (1997) suggested that the developmental stage of the day-15 metatarsals after 6 days of culture resembles that of day-17 metatarsals. Unpublished observations showed that the developmental stage of the day-15 metatarsals that were cultured for 5 days did not differ much from the developmental stage of the day-15 metatarsals that were cultured for 6 days; therefore, the former group could be compared with day-17 metatarsals. The mineralization geometry in the day-17 metatarsals was compared with that in day-17 metatarsals that were cultured for 3 days to study the effects of organ culture in metatarsals in which mineral had formed in the presence of muscle force. The developmental stages of day-17 and day-17 metatarsals that were cultured for 3 days are, however, not directly comparable. Because development after 3 days of culture equals that of about 1 day *in vivo*, the group of day-18 metatarsals was added for comparison with day-17 metatarsals that were cultured for 3 days. Differences between the results for the groups were statistically analyzed using the Student's t-test. In theory, a significant difference between l_2 and l_3 could result in equal lengths of l_1 and $(l_2+l_3)/2$. This could be a disturbing factor for the interpretation of the results. Therefore, differences between l_2 and l_3 were analyzed using a Student's t-test for paired observations.

Finite element analysis

To determine the local mechanical consequences of muscular activity in the hindlimb, a three-dimensional finite element model of an embryonic mouse metatarsal was constructed in which part of the tissue was assumed to be already mineralized (Figure 3). Because of symmetry of the proximal and distal part, only one half of the metatarsal was modeled, with dimensions of 0.6-mm length and 0.3-mm diameter. The analysis was performed using the code DIANA (TNO, Delft, The Netherlands).

As cartilage contains both fluid and solid components, the poroelastic theory was applied (Biot, 1941; Tanck et al., 1999). Each element consisted of both solid and fluid components. Specification for the analysis of biphasic tissues can be found in the literature (Biot, 1941; Bowen, 1982; De Boer, 1996; Mow et al., 1980; Simon, 1992). Collagen and proteoglycans constitute the solid part of the tissue and interstitial water constitutes the fluid part. The solid is assumed to be isotropic, linear elastic, porous and intrinsically incompressible, and the fluid as intrinsically incompressible. The amount of deformation of the tissue is time dependent. The

ossified metatarsal consists of unmineralized and mineralized cartilage, each with its own mechanical properties (0 44 and 117 MPa for Young's modulus [E], $6\ 7\times10^{15}$ and $6\ 7\times10^{16}$ $m^4/N\ s$ for permeability (k), and 0 25 and 0 30 for Poisson's ratio [v], respectively) Although the unmineralized cartilage consists of different zones (resting, proliferation, and hypertrophied parts), it was assumed to have uniform properties in this study For the unmineralized cartilage, Young's modulus and permeability were obtained from average values of literature data on hypertrophied cartilage (Bachrach, 1995, Cohen et al , 1992), whereas the average Poisson's ratio of articular cartilage was used (Mow et al , 1991) In mineralized cartilage, the Young's modulus is increased due to the deposition of calcium phosphate in the matrix (Huiskes et al , 1995) The permeability is decreased and was estimated to be one order of magnitude less than in unmineralized cartilage The Poisson's ratio of bone was used The permeability values of the unmineralized cartilage were varied between 2×10^{15} and 2×10^{14} $m^4/N\ s$

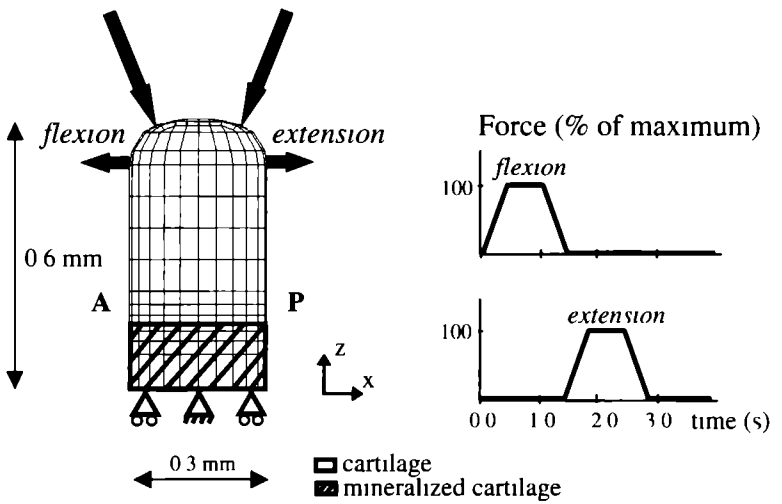

Figure 3: Lateral view of the finite element model of a fetal mouse metatarsal in which part of the metatarsal is mineralized Flexion and extension are successively applied to the model The flexion force is symmetric to the extension force A = anterior, and P = posterior

It was assumed that muscle twitches move the fetal foot in flexion from t=0 to t=1 4 seconds, followed by extension from t=1 4 to t=2 8 seconds, followed by a period of rest (Figure 3) A twitch that was twice as fast was also studied One cycle of flexion

and one cycle of extension were applied in both cases. The tendons of the flexion and extension muscles were assumed to pass through a tendinous sheath with the points of application at the anterior and posterior distal ends of the metatarsal, respectively. The force magnitude was based on estimates reported in the literature, in which physiological cross-sectional areas of flexor and extensor muscles in the hindlimb of fetal mice were measured and related to a maximal force (Klein-Nulend et al., 1986). The muscles produce tensile forces that make the joints contact each other, resulting in compressive forces. From force equilibrium analysis, it was deduced that the compressive force of 8.25×10^{-4} N was about four times larger than the tensile force of 2×10^{-4} N. It should be noted that the compressive forces were distributed over four nodes and that the tensile forces were distributed over two nodes. Because the strain and pressure distributions were evaluated relatively far away from the points of load application, it was of less importance whether the load was applied as a point force or as a distributed force. It was assumed that extension is symmetric to flexion (Figure 3). The local distributions of shear strain and fluid pressure were analyzed in the unmineralized cartilage of the FE model, at the interface with the mineralized cartilage, to analyze the influence of muscle load on the local mineralization pattern.

RESULTS

The mineralization shape of *in vivo* mineralized metatarsals in the group at gestational day 17 was significantly different from that of *in vitro* mineralized metatarsals in the group at gestational day 15 that were cultured for 5 days (Figure 4). The average *in vivo* difference in mineral length between center and periphery was close to zero, indicating that the mineralization front was nearly straight. The mineralization *in vitro* was retarded at the periphery of the tissue, compared to the center, as expressed by the 38 μm average difference in mineral length. If the day-17 metatarsals were cultured for three days, the mineralization was again retarded by about 36 μm at the periphery (Figure 4). This was significantly different from the *in vivo* mineralized metatarsals in the group at day 18, for which the length difference was close to zero (Figure 4). For all groups, l_2 was not statistically different from l_3 ($p<0.05$).

The finite element analysis showed that during maximal flexion the fluid pressure in the unmineralized cartilage at the interface with the mineralized cartilage was highest

at the anterior side, whereas the pressure at the posterior side was the highest during maximal extension (Figure 5). During loading, the pressure at this interface fluctuated between -4 kPa and 11 kPa. The pressure distributions during flexion and extension were virtually symmetric. Furthermore, the fluid pressure in the center of the cross-section was approximately the same as that laterally. The average pressure after one flexion and one extension cycle was very similar for every point in the cross-section, about 4.5 kPa.

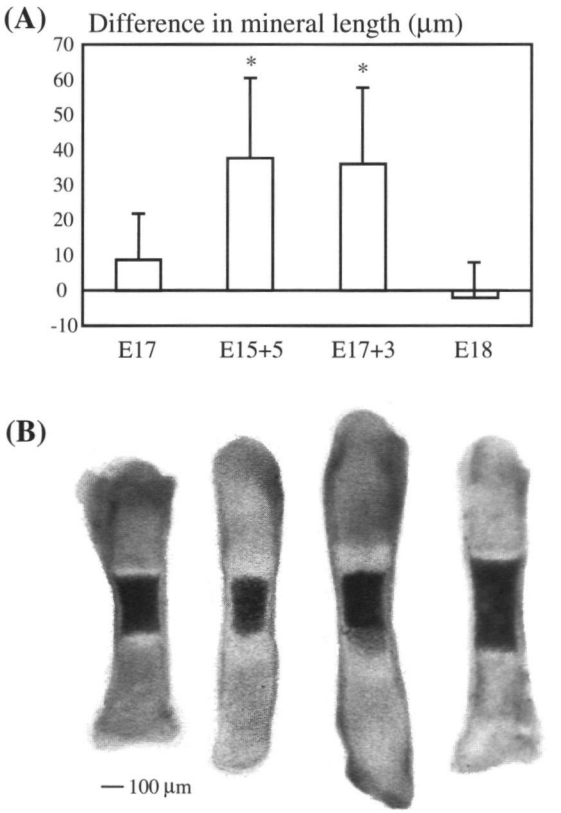

Figure 4: **(A)** Difference between the length of the mineralized zone in the center, l_1, and the periphery, $(l_2+l_3)/2$, of the metatarsal diaphysis (E17 = *in vivo* mineralized metatarsal at 17 days of gestation, E15+5 = *in vitro* mineralized metatarsal at 15 days of gestation with 5 days of culture, E17+3 = *in vivo* mineralized metatarsal at 17 days of gestation with 3 days of culture, and E18 = *in vivo* mineralized metatarsal at 18 days of gestation). *$p<0.05$, compared with E17 and E18. Error bars represent the SD. **(B)** Representative pictures of the metatarsals in the four groups, from left to right: E17, E15+5, E17+3, and E18.

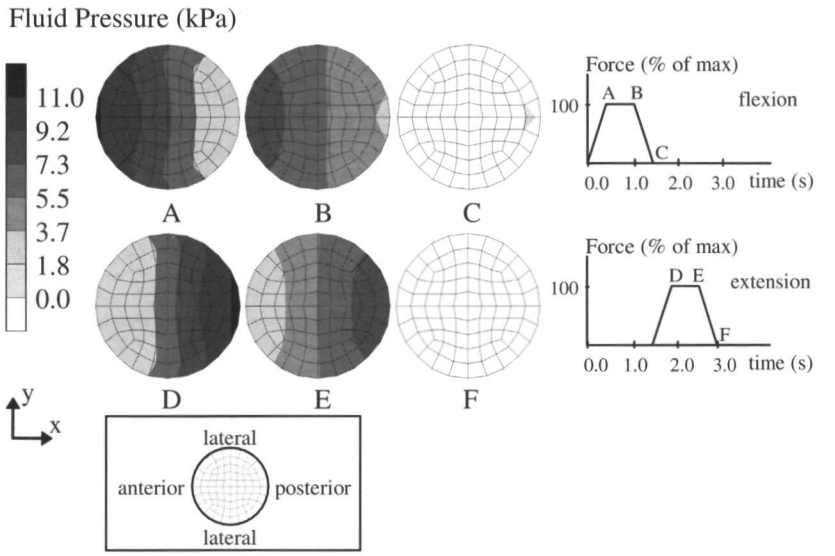

Figure 5: Distributions of fluid pressure in the unmineralized cartilage as calculated by finite element analysis. Cross-sections of the metatarsal at the interface with the mineralized cartilage are shown at different points in time during flexion (**A-C**) and extension (**D-F**).

High distortional strains occurred during one loading cycle in the unmineralized cartilage at the interface with the mineralized cartilage (Figure 6). At the periphery of the cross-section, the distortions during maximal flexion and maximal extension were the highest, at about 3.0%. The distributions of the strain during flexion and extension were again nearly symmetric. Just after load release, i.e. at t=1.4 and 2.8 seconds, the strain reduced to about 0.3%. The average strain after one flexion and one extension cycle at the different cross-sectional points was highest, approximately 1.4%, for all peripheral points, whereas the central point only deformed by about 0.2%.

The maximal values of fluid pressure were 9 and 14 kPa, for $k=2.0\times10^{-14}$ and 2.0×10^{-15} $m^4/N.s$, respectively, and the maximal values of the distortional strain changed by only about 1% in both cases. If the fast twitch was applied, the distribution patterns for fluid pressure and distortional strain remained nearly the same compared to the normal twitch. The maximal value of the fluid pressure increased by 13.8% and the maximal value of the distortional strain decreased by less than 0.5%.

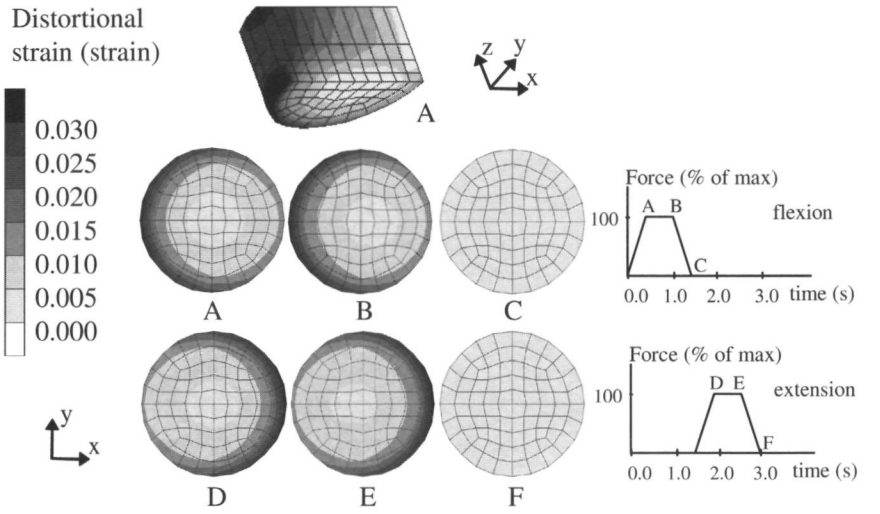

Figure 6: Distributions of distortional strain in the unmineralized cartilage as calculated by finite element analysis. Cross-sections of the metatarsal at the interface with the mineralized cartilage are shown at different points in time during flexion **(A-C)** and extension **(D-F)**. On top, the three-dimensional strain distribution at maximal flexion **(A)** is presented.

DISCUSSION

This study confirmed the qualitative observation that the mineralization front of *in vitro* mineralized metatarsals was more spherical than *in vivo* mineralized ones. The results of the finite element analysis clearly showed that the distributions of the distortional strain at the mineralization front discriminated between the center and periphery of the metatarsal, and hence they were compatible with the difference in mineralization geometry, whereas the fluid pressure distributions were not. Using force and moment equilibrium, it was established that the strain distributions at the level of the mineralization front mainly reflected the compressive force, rather than the bending moment. Many *in vitro* studies have shown that mechanical stimulation influences the chondrocyte metabolism (Gray et al., 1989; Guilak et al., 1994; Lee and Bader, 1997; Sah et al., 1989). Chondrocytes might even react to strain values as low as 15 μstrain (Wright et al., 1996). The mineralization process is a cell-mediated and -controlled process (Hunziker, 1988). In hypertrophied chondrocytes,

intracellular calcium is accumulated, which appears to play an important role in matrix mineralization (Iannotti et al., 1989; Kirsch and Wuthier, 1994; Wu et al., 1995). Guilak et al. (1994) found that the Ca^{2+} concentration in the cytoplasm increased due to cell deformation. In growth plate chondrocytes, an increase in the intracellular calcium induces the formation of matrix vesicles, which are associated with the process of cartilage matrix mineralization (Iannotti et al., 1989). Apart from this mechanism, dynamic strain may increase the chondrocyte proliferation (Lee and Bader, 1997). The largest strains in this study were found at locations where hypertrophied chondrocytes were present: at the periphery of the metatarsal, near the mineralized zone. In conclusion, it is likely that strain has influenced the mineralization process.

The distributions of fluid pressure at the mineralization front could not differentiate between the center and the periphery of the tissue. Hence, the fluid pressure distribution could not explain the differences in mineralization geometry between *in vivo* and *in vitro* mineralized metatarsals. It is, however, possible that it stimulated the mineralization rate of the front as a whole, as Klein-Nulend et al. (1986) showed that an intermittent hydrostatic pressure of 13 kPa at 0.3 Hz increased the mineralization rate in embryonic metatarsals of the mouse compared to unloaded controls. The value of this dynamic pressure is comparable to the fluid pressures found in the present study, which ranged from –4 to 11 kPa at the interface.

Factors other than loading differences might contribute to the differences between *in vivo* and *in vitro* conditions. Even under the best culture conditions some differences still exist with *in vivo* conditions independent of mechanical stress. Suboptimal medium conditions may retard mineralization (Burger et al., 1992; Klein-Nulend et al., 1986). However, adding serum to the medium did not affect the mineralization shape, which was still convex (Klein-Nulend et al., 1986). Therefore, the shape change *in vitro* did not result from a lack of serum growth factors. In addition, nutrient diffusion into the rudiment could in theory create differences between surface and center and could also be altered through mechanical loading. However, for the present loading situation and the low permeabilities used, fluid pressure gradients were small, resulting in insignificant fluid velocities. Nutrient transport through the rudiment will therefore be barely influenced by the load.

The difference in mineralization shape between the *in vivo* and *in vitro* groups probably was actually higher than measured. The measurements of the mineralization shape in the *in vivo* groups sometimes showed negative values. In reality, there could

be more negative values than were actually measured if the periphery of the metatarsal mineralized faster than the center of the tissue. In this case, the mineralization front seemed flat (from all sides) under the microscope, but in fact was concave. This could be one reason why the *in vivo* measurements varied less than the *in vitro* measurements. To verify this possibility, a 3D analysis of the mineralized zone should be performed. If, however, mineralization is faster in the center of the metatarsal than in the periphery (as in the day-15 metatarsals cultured for 5 days and day-17 metatarsals cultured for 3 days), this problem is avoided because the front was really convex (from all sides) under the microscope. A larger difference between *in vivo* and *in vitro* measurements strengthens the suggestion that distortional strain stimulates the mineralization process.

Only the distortional strain and the fluid pressure were evaluated. Distortional strain was selected from the group of solid variables (strains and stresses), and fluid pressure from the group of fluid variables (pressure and fluid velocity). Besides distortional strain, other invariants, like the maximal shear strain, osteogenic index (Wong and Carter, 1990b), and the strain energy density, will be compatible with the difference in mineralization geometries as well. The pressure gradient, as a measure for fluid velocity, was incompatible with the difference in mineralization geometries. Hence, the strain component was apparently the key parameter for compatibility between the mechanical variables and the observed mineralization patterns.

Other studies have examined the process of endochondral ossification. Wong and Carter (1990a) applied intermittent mechanical loading, simulating the active muscular system, to a linear-elastic finite element model of a long bone to simulate the process of endochondral ossification. Cartilage elements were iteratively changed into bone elements. Mineralized cartilage was not modeled in their study. Their results showed that high shear stresses appeared at the bone cartilage interface. The shear stress distributions were similar to the distributions of distortional strain at the mineralized unmineralized cartilage interface in the present study. The experimental data of the present study agree with the theoretical studies of Carter et al. (1987, 1988) and Wong and Carter (1990a, 1990b), which propose that cyclic shear stresses accelerate the endochondral ossification process. Their theory might therefore also be valid for the early mineralization of cartilage before it remodels into bone.

The *in vitro* mineralization process initiates and proceeds without muscular activity. It can be speculated that this may be considered as a pre-programmed process, which occurs without external loads, starting at the center of the cartilaginous tissue,

proceeding in every direction, and finally resulting in a spherical mineralization front. Strain variables through muscle forces might modulate the mineralization process by increasing the mineralization rate at the periphery of the mineralized cylinder, resulting in a straight (or concave) mineralization front.

The finite element model used to determine the influence of muscle force on the mineralization process is only a schematic representation of reality. For example, the unmineralized/mineralized cartilage interface was modeled as completely flat. If a curved interface is used, the conclusion will not change significantly since the highest strains will still be present at the periphery of the metatarsal.

In conclusion, this study showed that the mineralization pattern of *in vivo* calcified metatarsals was different from *in vitro* calcified ones. If this is due to the presence or absence of muscular activity, then distortional strain, rather than hydrostatic pressure, is probably the local mechanical stimulus. This confirms that disturbances in the development of muscles are likely to produce disturbed mineralization patterns resulting in a disordered osteogenic process.

ACKNOWLEDGEMENTS

The authors thank CM Semeins for his contribution.

REFERENCES

Bachrach NM: Chondrocyte contribution to growth plate compressive properties. In: Growth plate chondrocyte deformation in situ and a biphasic inclusion model for cells within hydrated soft tissues, PhD thesis, pp 98-124, Columbia University, 1995.

Biot MA: General theory of three-dimensional consolidation. J Appl Phys, 12:155-164, 1941.

Bowen RM: Compressible porous media models by use of the theory of mixtures. Int J Eng Sci 20:697-735, 1992.

Burger EH, Klein-Nulend J, Veldhuijzen JP: Modulation of osteogenesis in fetal bone rudiments by mechanical stress in vitro. J Biomech 24:101-109, 1991.

Burger EH, Klein-Nulend J, Veldhuijzen JP: Mechanical stress and osteogenesis. J Bone Miner Res 7:S397-S401, 1992.

Carter DR, Orr TE, Fyhrie DP, Schurman DJ: Influences of mechanical stress on prenatal and postnatal skeletal development. Clin Orthop 219:237-250, 1987.

Carter DR, Wong M: The role of mechanical loading histories in the development of diarthrodial

joints J Orthop Res 6 804-816, 1988

Carter DR Wong M, Orr TE Musculoskeletal ontogeny, phylogeny, and functional adaptation J Biomech 24 3-16, 1991

Cohen B, Chorney GS, Phillips DP, Dick HM, Mow VC Inhomogeneous and anisotropic mechanical properties of bovine growth plate and chondroepiphysis Trans Orthop Res Soc 17 153, 1992

Copray JCVM, Jansen HWB, Duterloo HS Effects of compressive forces on proliferation and matrix synthesis in mandibular condylar cartilage of the rat in vitro Arch Oral Biol 30 299-304, 1985a

Copray JCVM, Jansen HWB, Duterloo HS An in-vitro system for studying the effect of variable compressive forces on the mandibular condylar cartilage of the rat Arch Oral Biol 30 305-311, 1985b

Copray JCVM, Jansen HWB, Duterloo HS Effect of compressive forces on phosphatase activity in mandibular condylar cartilage of the rat in vitro J Anat 140 479-489, 1985c

De Boer R Highlights in the historical development of the porous media theory Toward a consistent macroscopic theory Appl Mech Rev 49 201-262, 1996

De Vries JIP Visser GHA, Prechtl HFR The emergence of fetal behavior I Qualitative aspects Early Hum Dev 7 301-322, 1982

Germiller JA, Goldstein SA Structure and function of embryonic growth plate in the absence of functioning skeletal muscle J Orthop Res 15 362-370, 1997

Gray ML, Pizzanelli AM, Lee RC, Grodzinsky AJ, Swann DA Kinetics of the chondrocyte biosynthetic response to compressive load and release Biochim Biophys Acta 991 415-425, 1989

Guilak F, Donahue HJ, Zell RA, Grande D McLeod KJ, Rubin CT Deformation-induced calcium signaling in articular chondrocytes In Cell mechanics and cellular engineering, pp 380-397 Eds VC Mow, F Guilak, R Transon-Tay, and RM Hochmuth, New York, Springer-Verlag, 1994

Haaijman A, D'Souza RN, Bronckers ALJJ, Goei SW, Burger EH OP-1 (BMP-7) affects mRNA expression of type I, II, X collagen, and matrix Gla protein in ossifying long bones in vitro J Bone Miner Res 12 1815-1823, 1997

Hosseini A and Hogg DA The effects of paralysis on skeletal development in the chick embryo I General effects J Anat 177 159 168, 1991

Huiskes R, van Donkelaar CC, Jepsen KJ, Weinans H, Goldstein SA, Burger EH The mechanical consequences of mineralization in fetal bone Trans Orthop Res Soc 20 450, 1995

Hunziker EB Growth plate structure and function Pathol Immunopathol Res 7 9 13, 1988

Iannotti JP, Brighton CT, Stambough JE Subcellular regulation of the ionized calcium pool in isolated growth-plate chondrocytes Clin Orthop 242 285-293, 1989

Iannotti JP, Naidu S, Noguchi Y, Hunt RM, Brighton CT Calcium induced matrix vesicle biogenesis Trans Orthop Res Soc 14 125, 1989

Kirsch T and Wuthier E Stimulation of calcification of growth plate cartilage matrix vesicles by binding to type II and X collagens J Biol Chem 269 11462-11469, 1994

Klein Nulend J, Veldhuijzen JP Burger EH Increased calcification of growth plate cartilage as a result of compressive force in vitro Arth Rheum 29 1002-1009, 1986

Lee DA and Bader DL Compressive strains at physiological frequencies influence the metabolism of chondrocytes seeded in agarose J Orthop Res 15 181 188, 1997

Mow VC, Kuei SC, Lai WM, Armstrong CG Biphasic creep and stress relaxation of articular cartilage

in compression Theory and experiments J Biomech Eng 102 73-84, 1980

Mow VC, Zhu W, Ratcliffe A Structure and function of articular cartilage and meniscus In Basic Orthopaedic Biomechanics, pp 143-198 Eds VC Mow and WC Hayes, New York, Raven press, 1991

Platzer AC The ultrastructure of normal myogenesis in the limb of the mouse Anat Rec 190 639-658, 1978

Sah RLY, Kim YJ, Doong JYH, Grodzinsky AJ, Plaas AHK, Sandy JD Biosynthetic response of cartilage explants to dynamic compression J Orthop Res 7 619-636, 1989

Simon BR Multiphase poroelastic finite element models for soft tissue structures Appl Mech Rev 45 191-218, 1992

Tanck E, van Driel WD, Hagen JW, Burger EH, Blankevoort L, Huiskes R Why does intermittent hydrostatic pressure enhance the mineralization process in fetal cartilage J Biomech 32 153-161, 1999

Van't Veen SJGA, Hagen JW, van Ginkel FC, Prahl-Andersen B, Burger EH Intermittent compression stimulates cartilage mineralization Bone 17 461-465, 1995

Van Loon JWA, Bervoets DJ, Burger EH, Dieudonné SC, Hagen JW, Semeins CM, Zandieh Doulabi B, Veldhuijzen JP Decreased mineralization and increased calcium release in isolated fetal mouse long bones under near weightlessness J Bone Miner Res 10 550-557, 1995

Wong M and Carter DR A theoretical model of endochondral ossification and bone architectural construction in long bone ontogeny Anat Embryol 181 523-532, 1990a

Wong M and Carter DR Theoretical stress analysis of organ culture osteogenesis Bone 11 127-131, 1990b

Wright M, Jobanputra P, Bavington C, Salter DM, Nuki G Effects of intermittent pressure-induced strain on the electrophysiology of cultured human chondrocytes Evidence for the presence of stretch-activated membrane ion channels Clin Sci 90 61-71, 1996

Wu LNY, Ishikawa Y, Sauer GR, Genge BR, Mwale F, Mishima H, Wuthier RE Morphological and biochemical characterization of mineralizing primary cultures of avian growth plate chondrocytes evidence for cellular processing of Ca^{2+} and Pi prior to matrix mineralization J Cell Bioch 57 218-237, 1995

6

INCREASE IN BONE VOLUME FRACTION PRECEDES ARCHITECTURAL ADAPTATION IN GROWING BONE

E Tanck, J Homminga, GH van Lenthe, R Huiskes

Accepted for publication in Bone

ABSTRACT

In mature trabecular bone, both density and trabecular orientation are adapted to external mechanical loads. Little quantitative data is available on the development of architecture and mechanical adaptation in juvenile trabecular bone. We studied the hypothesis that a time lag occurs between the adaptation of trabecular density and the adaptation of trabecular architecture during the development. To investigate this hypothesis we used ten female pigs at 6, 23, 56, 104, and 230 weeks of age. Three-dimensional morphological and mechanical parameters of trabecular bone samples from the vertebra and proximal tibia were studied using micro-computer tomography and micro finite element analysis. Both bone volume fraction and stiffness increased rapidly in the initial growth phase (from 6 weeks on), whereas the morphological anisotropy started increasing only after 23 weeks of age. In addition, the anisotropy reached its highest value much later in the development than bone volume fraction did. Hence, the alignment of trabeculae is still progressing at the time of peak bone mass. Hence, our hypothesis was supported by the time lag between the increase in trabecular density and the adaptation of the trabecular architecture. The rapid increase of bone volume fraction in the initial growth phase can be explained by the enormous weight increase of the pigs. The trabeculae align at later stages when the increase in weight, and thus the loading, has slowed down considerably compared to the early growth stage. Hence, the trabecular architecture is more efficient in later years. We conclude that density is adapted to external load from the early phase of growth, whereas the trabecular architecture is adapted later in the development.

INTRODUCTION

It is generally accepted that mechanical load plays an important role in development, maintenance, and adaptation of the skeleton. Early long bones are developed from mineralized cartilage and gradually transform into their eventual structure, while density and trabecular orientation are adapted to the mechanical load.

Little quantitative data is available about the development of architecture and mechanical adaptation in juvenile trabecular bone. Korstjens et al. (1995) analyzed the two-dimensional trabecular patterns of the distal radius in children, aged 4-14 years, using radiographs and digital imaging. They found that the fine trabecular

patterns of young children had coarsened in the older ones. In a medieval Nubian population, aged 0-60 years, vertebral morphometry was investigated by Kneissel et al. (1997). They showed that the highest bone volume fraction was present during adolescence when the trabeculae were also more plate-like than in the youngest children. The recent development of micro-computer tomography (μCT) has made it possible to analyze the three-dimensional (3D) architecture of trabecular bone accurately (Feldkamp et al., 1989). To date, this technique has been used to study adult cancellous bone and to investigate the effects of aging (Ciarelli et al., 2000; Ding and Hvid, 2000; Hildebrand et al., 1999; Rüegsegger et al., 1996). In the adult stage, the trabeculae are aligned to the principal stress directions, as Wolff described more than a century ago (Wolff, 1986). In this way, trabecular bone is believed to be adapted to the typical external loads of daily living in both density and architecture. During growth, load increases gradually, which implies that density and architecture would change as well. As an increase in density due to increased loading would only have to involve bone formation, but the adaptation of architecture must involve both formation and resorption, we hypothesize that there is a time lag between these processes. In a computer simulation of bone-cell based modeling and remodeling (Huiskes et al., 2000), it was found that adaptation of density (trabecular thickness) due to increased loading would occur much faster than trabecular adaptation due to changes in loading orientation. We investigated this hypothesis by checking whether this time lag occurs in growing bone. For that purpose, pig-bone between 6 and 230 weeks of age was used. Three-dimensional trabecular bone structures in the vertebra and proximal tibia were studied, using μCT and micro finite element analysis.

MATERIALS AND METHODS

Materials

Bone from ten female pigs from a Dutch farm (Central Animal Laboratory, Nijmegen, The Netherlands) was used. The pigs were 6, 23, 56, 104, and 230 weeks of age (two per age group). Total body weight increased from 12 kg at 6 weeks of age, to 212 kg at 104 weeks of age, after which it stabilized (Figure 1). The growth plates in the proximal tibiae of the 104-week-old pigs were nearly closed, whereas they were completely closed in the 230-week-old pigs. From these observations it can be estimated that 104 weeks in pigs is roughly equivalent to late adolescence (about

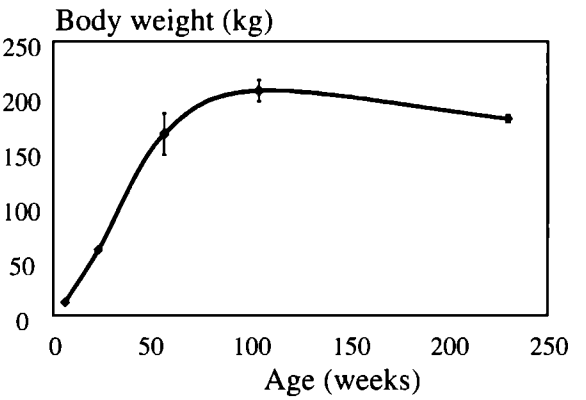

Figure 1: Total body weight of the pigs as a function of age. Error bars represent the SD.

15 years in human), while 230 weeks is adulthood (about 30 years of age in humans). Post-mortem, bone cylinders of 8.5 mm in diameter and about 50 mm in length were drilled out from the weight bearing area of the proximal tibia, i.e. lateral or medial condyle, and the fifth lumbar vertebra (L5) of each animal. These sites were chosen because both are loaded predominantly in axial compression, and they were subject to studies of adult specimens in the literature. The axes of the bone cylinders were parallel to the longitudinal axes of the bones. Institutional approval was obtained for all experiments.

Micro-computed tomography (μCT) scanning

All bone cylinders were scanned in a μCT (μCT 20, Scanco Medical AG., Zürich, Switzerland) with an isotropic spatial resolution of 28 μm (Rüegsegger et al., 1996). From each a 4x4x4 mm^3 volume of interest (VOI) was selected. In the vertebra, the VOI was taken from the center of the vertebral body. In the proximal tibia, one VOI was selected from the epiphysis and one from the metaphysis. In the epiphysis, it was taken approximately midway between the articular cartilage and the growth plate. In the metaphysis it was taken at a distance of about 5 mm from the growth plate. In the pigs with the closed growth plates, the cement line was used to determine the position. The volumes of interest were represented in 22x22x22 μm^3 voxels and segmented using an individually density threshold value. Segmentation was performed visually by comparing slices before and after segmentation for a range of threshold values. The threshold that resulted in the best fit between the two was used. The sensitivity of this method was tested (Hara et al., 2000).

Morphometric and mechanical analysis

The morphological anisotropy was determined from the mean intercept length (Whitehouse, 1974) MIL_{max}/MIL_{min} directly from the segmented scans. The bone volume fraction (BV/TV) was determined from these scans as well. The voxel meshes were subsequently converted to micro finite element (μFE) models with element sizes of 22x22x22 μm^3 for bone cubes of the 6 and 23-week-old pigs, and 44x44x44 μm^3 for bone cubes of the older pigs. The element coarsening of the latter group was done to reduce computer time, without changing the trabecular structure significantly. For one sample we tested the difference in maximal stiffness for the two element sizes and determined that the change was only 0.1%, hence insignificant. Data reduction in the 6 and 23–week-old pigs was performed by reducing the VOI to 2.6×2.6×2.6 mm^3, leaving at least five trabeculae in every direction (Harrigan et al., 1988). The apparent mechanical properties were determined with the μFE models as were the orientations of the three principal mechanical axes. These μFE models have been shown to give accurate estimates of the apparent elastic moduli of cancellous bone (Jacobs et al., 1999; Kabel et al., 1999b; Ladd and Kinney, 1998; Van Rietbergen et al., 1995). A tissue modulus of 5 GPa was assumed for all specimens.

Data analysis was performed between age categories per site, i.e. for the vertebra, tibia epiphysis, and tibia metaphysis separately, using one-way ANOVA with age as grouping variable. If the result was significant, it was followed by an all pairwise multiple comparison procedure using the Tukey test. In addition, an average value of the three sites was determined for each animal. This resulted in a mean plus standard deviation (SD) for the pigs at each age category on which similar statistical data analysis was performed, i.e. one-way ANOVA with age as grouping variable, followed by the Tukey test, if required. Differences were considered statistically significant at $p<0.05$.

RESULTS

The 3-D reconstructions showed clear differences in trabecular structure with age (Figure 2). For the youngest bones, the structure was refined whereas in older bones it had developed into a much coarser trabecular structure.

The bone volume fraction (BV/TV) increased rapidly in the initial growth phase, followed by a slight decrease and then a stabilization (Figure 3). The increase was

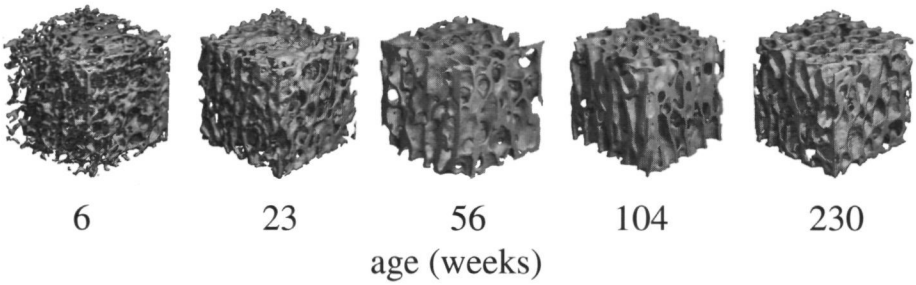

Figure 2: Illustration of the trabecular structure of pig vertebrae versus age.

significant between 6 and 56 weeks (Figure 3). BV/TV and total body weight did not exactly follow the same trend; while total body weight reached a maximum at 104 weeks of age and was stable from there on, BV/TV reached its maximum at 56 weeks, decreased (although not significantly) and stabilized from 104 weeks on (Figure 1 and 3).

On average, the early morphological anisotropy was relatively low (Figure 4); it did not increase from 6 to 23 weeks. After 23 weeks of age, the anisotropy increased significantly until 104 weeks of age, after which it remained about the same.

On average, the maximal (E_{max}) elastic moduli increased with age until 104 weeks, after which they stabilized (Figure 5). For the separate locations, the trends of E_{max} versus age were similar, but only for the vertebrae the increase with age was significant.

The angle between the stiffest direction and the axial loading direction (angle α)

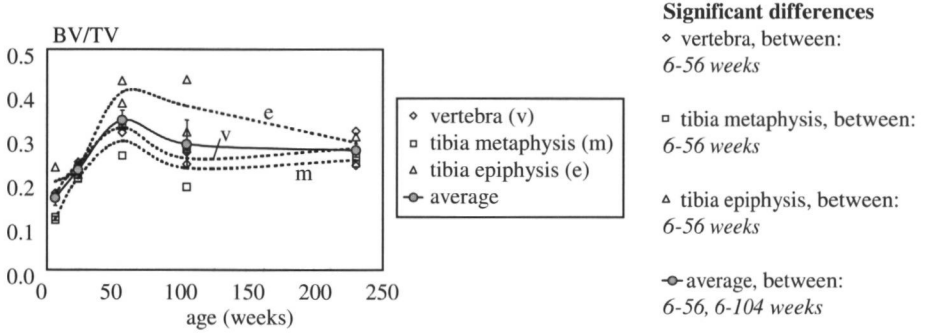

Figure 3: Bone volume fraction (BV/TV) as a function of age. Each dotted line represents the trend for one location, i.e. vertebra, tibia metaphysis, and tibia epiphysis. The continuous line shows the average BV/TV for the pigs. Error bars represent the SD of the average value per pig. At the right side, all significant differences are listed.

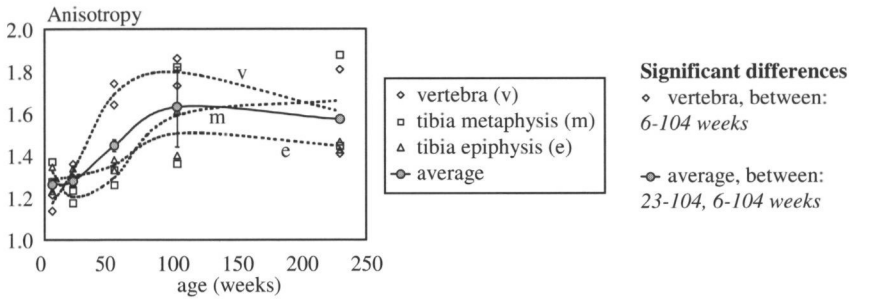

Figure 4: Anisotropy as a function of age. Each dotted line represents the trend for one location. The continuous line shows the average anisotropy for the pigs. Error bars represent the SD of the average value per pig. At the right side, all significant differences are listed.

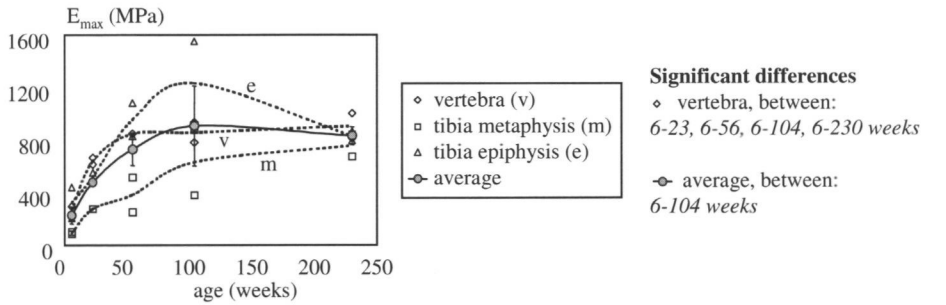

Figure 5: Maximal stiffness (E_{max}) as a function of age. Each dotted line represents the trend for one location. The continuous line shows the average E_{max} for the pigs. Error bars represent the SD of the average value per pig. At the right side, all significant differences are listed.

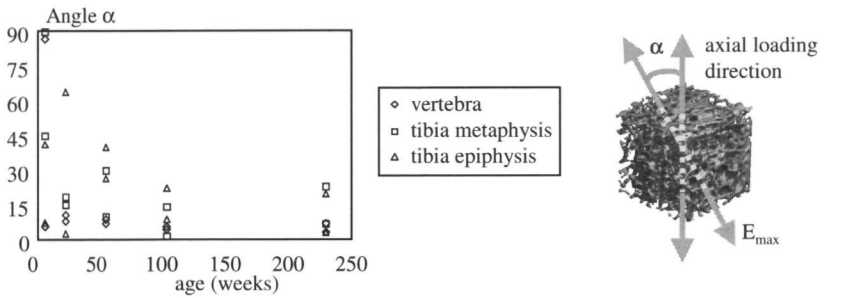

Figure 6: Illustration of the angle between the stiffest direction of the trabeculae and the axial loading direction, as a function of age.

decreased with age (Figure 6). The standard deviation of angle α showed a decrease with age (Figure 6); at 6 weeks of age, the angle varied between 0 and 90 degrees, whereas it remained under 23 degrees from the age of 104 weeks on. After 104 weeks, angle α of the vertebra was constantly below seven degrees, whereas the values for the tibia varied more (Figure 6). This may be explained by the fact that the vertebra is primarily loaded in axial compression, whereas the loads on the tibia are more variable.

DISCUSSION

This study showed that density is adapted to external load from the early phase of growth, whereas the trabecular architecture is adapted later in the development. During initial growth bone becomes denser by trabecular deposition, as was also found from histo-morphometry in rats (Chow et al., 1993). The rapid increase of bone volume fraction (BV/TV) in the initial growth phase might be explained by the explosive weight increase in the early development. It is likely that this results in increased mechanical loads to the bones as, in growing pigs, body weight increases relatively faster than bone mass and bone cross sectional area (Richmont and Berg, 1972). The trabeculae align at a later stage, when the increase in weight, hence in the loads, is slower compared to the early growth stage. This suggests that in the early growth stage, when the trabecular architecture is not optimally adapted to external loads yet, mechanical adaptation is achieved through increased bone mass, and that the trabecular architecture is more efficient in later years.

The thought of a more efficient trabecular structure in later years is confirmed by the development of morphological anisotropy, which, on average only started after 23 weeks of age. At 56 weeks of age bone volume fraction peaks, while the alignment of trabeculae is still progressing until 104 weeks of age. Furthermore, the reducing variation of angle α, between the principal material axis and the load, with age also illustrates the increasing structural organization in later years.

Since the submission of this article, Nafei et al. (2000a, 2000b) published a study of morphological and mechanical properties in the growing bones of sheep. Generally, the results of the present study are in agreement with their observations. They found, amongst others, that the elastic modulus, the bone volume fraction, and the architectural anisotropy positively correlated with increasing age. In addition, the

values of all parameters differed significantly in immature and mature sheep.

The maximal stiffness (E_{max}) is determined by three parameters: the tissue modulus, bone volume fraction (BV/TV), and architecture (Kabel et al., 1999a; Van Rietbergen et al., 1998). In this study, the tissue modulus was assumed to be constant while in reality the modulus increases during growth due to a higher mineral content per tissue volume (Fujita et al., 1999; Mølgaard et al., 1998; Nafei et al., 2000a). Hence, the relationship between real stiffness and age is stronger, and would probably lead to more significant results. The development of stiffness (E_{max}) can be explained by the combined development of volume fraction and anisotropy. The increase of E_{max} from 6 till 56 weeks of age is mainly caused by the increased volume fraction, whereas the increase from 56 till 104 weeks of age is caused by the increased anisotropy. As stiffness and strength are highly correlated (Keaveny et al., 1994), trabecular bone also becomes stronger during growth.

There are some limitations in the present study. First, there may have been slight differences between the drill direction to obtain the bone cylinder and the axial loading direction. Second, the axial loading direction may differ from the principal stress direction. These two possible inaccuracies only affect the value of the angle α. The maximal effect on angle α is estimated to be 23 degrees, based on the result that angle α is not zero but maximal 23 degrees after the equilibrium stage of 104 weeks of age (Figure 6). This does, however, not affect the conclusion that the variation of angle α decreases with age. Another limitation is the small number of pigs per age category. One of the consequences of small numbers per age category is the difficulty to obtain significant results. However, the results showed some important significances for all parameters. Furthermore, the analysis of trends of different parameters improves the insight in trabecular bone adaptation.

In summary, this study supported our hypothesis. The results showed the presence of a time lag between the increase in trabecular density and the adaptation of the trabecular architecture. Bone volume fraction increased rapidly in the initial growth phase, whereas anisotropy started increasing at a later stage. In addition, the anisotropy reached its highest value much later in the development than bone volume fraction did. This was in agreement with computer simulations of bone-cell based modeling and remodeling, in which adaptation of density due to increased loading occurred much faster than trabecular adaptation due to changes in loading direction (Huiskes et al., 2000). In conclusion, density is adapted from the early phase of growth, whereas the trabecular architecture is adapted later in the development, when

the mechanical adaptation produces a more efficient architecture

ACKNOWLEDGEMENTS

The authors thank T Hara for his assistance in obtaining the bone specimens

REFERENCES

Chow JWM, Badve S, Chambers TJ Bone formation is not coupled to bone resorption in a site-specific manner in adult rats Anat Rec 236 366-372, 1993

Ciarelli TE, Fyhrie DP, Schaffler MB, Goldstein SA Variations in three-dimensional cancellous bone architecture of the proximal femur in female hip fractures and in controls J Bone Miner Res 15 32-40, 2000

Ding M, Hvid I Quantification of age-related changes in the structure model type and trabecular thickness of human tibial cancellous bone Bone 26 291-295, 2000

Feldkamp LA, Goldstein SA, Parfitt AM, Jesion G, Kleerekoper M The direct examination of three-dimensional bone architecture in vitro by computed tomography J Bone Miner Res 4 3-11, 1989

Fujita T, Fujii Y, Goto B Measurement of forearm bone in children by peripheral computed tomography Calcif Tissue Int 64 34-39, 1999

Hara T, Tanck E, Homminga J, Huiskes R The influence of micro-CT threshold variations on the assessment of structural and mechanical trabecular bone properties 12th Conf Eur Soc Biomech p63, 2000

Harrigan TP, Jasty M, Mann RW, Harris WH Limitations of the continuum assumption in cancellous bone J Biomech 21 269-275, 1988

Hildebrand T, Laib A, Muller R, Dequeker J, Ruegsegger P Direct three-dimensional morphometric analysis of human cancellous bone microstructural data from spine, femur, iliac crest, and calcaneus J Bone Miner Res 14 1167-1174, 1999

Huiskes R, Ruimerman R, van Lenthe GH, Janssen JD Effects of mechanical forces on maintenance and adaptation of form in trabecular bone Nature 405 704-706, 2000

Jacobs CR, Davis BR, Rieger CJ, Francis JJ, Saad M, Fyhrie DP The impact of boundary conditions and mesh size on the accuracy of cancellous bone tissue modulus determination using large-scale finite-element modeling J Biomech 32 1159-1164, 1999

Kabel J, Odgaard A, Van Rietbergen B, Huiskes R Connectivity and elastic properties of cancellous bone Bone 24 115-120, 1999a

Kabel J, Van Rietbergen B, Dalstra M, Odgaard A, Huiskes R The role of an effective isotropic tissue modulus in the elastic properties of cancellous bone J Biomech 32 673-680, 1999b

Keaveny TM, Wachtel EF, Ford CM, Hayes WC: Differences between the tensile and compressive strengths of bovine tibial trabecular bone depend on modulus. J Biomech 27:1137-1146, 1994.

Kneissel M, Roscher P, Steiner W, Schamall D, Kalchhauser G, Boyde A, Teschler-Nicola M: Cancellous bone structure in the growing and aging lumbar spine in a historic nubian population. Calcif Tissue Int 61:95-100, 1997.

Korstjens CM, Geraets WGM, van Ginkel FC, Prahl-Andersen B, van der Stelt PF, Burger EH: Longitudinal analysis of radiographic trabecular pattern by image processing. Bone 17:527-532, 1995.

Ladd AJC, Kinney JH: Numerical errors and uncertainties in finite-element modeling of trabecular bone. J Biomech 31:941-945, 1998.

Mølgaard C, Thomsen BL, Michaelsen KF: Influence of weight, age and puberty on bone size and bone mineral content in healthy children and adolescents. Acta Paediatr 87:494-494, 1998.

Nafei A, Danielsen CC, Linde F, Hvid I: Properties of growing trabecular ovine bone. Part I: mechanical and physical properties. J Bone Joint Surg [Br] 82B:910-920, 2000a.

Nafei A, Kabel J, Odgaard A, Linde F, Hvid I: Properties of growing trabecular ovine bone. Part II: architectural and mechanical properties. J Bone Joint Surg [Br] 82B:921-927, 2000b.

Richmont RJ, Berg RT: Bone growth and distribution in swine as influenced by liveweight, breed, sex, and ration. Can J Anim Sci 52:47-56, 1972.

Rüegsegger P, Koller B, Müller R: A microtomographic system for the nondestructive evaluation of bone architecture. Calcif Tissue Int 58:24-29, 1996.

Van Rietbergen B, Huiskes R, Weinans H, Odgaard A, Kabel J: The role of trabecular architecture in the anisotropic mechanical properties of bone. In: Bone structure and remodeling. Eds A Odgaard and H Weinans, World Scientific, Singapore, 1995.

Van Rietbergen B, Odgaard A, Kabel J, Huiskes R: Relationships between bone morphology and bone elastic properties can be accurately quantified using high-resolution computer reconstructions. J Orthop Res 16:23-28, 1998.

Whitehouse WJ: The quantitative morphology of anisotropic trabecular bone. J Microsc 101:153-168, 1974.

Wolff J: Das Gesetz der Transformation der Knochen, Hirchwild, Berlin, 1892; translated as The Law of Bone Remodeling by P Maquet, and R Furlong, Berlin: Springer-Verlag, 1986.

7

CHARACTERIZATION OF THE THREE-DIMENSIONAL MORPHOLOGY OF EPIPHYSEAL AND METAPHYSEAL TRABECULAR BONE IN IMMATURE PIGS

E Tanck, T Hara, R Huiskes

Submitted for publication

ABSTRACT

During growth, the trabecular architecture in the metaphysis is gradually renewed due to the development of new trabeculae from the growth plate, whereas trabeculae in the epiphysis are formed from the secondary ossification center earlier in the development. Hence, trabeculae in the epiphysis are relatively older than those in the metaphysis. Previously, we showed that trabeculae align to the orientation of the dominant forces gradually with age, which takes some time. We hypothesize that during growth, the relatively older trabecular architecture in the epiphysis is better adapted to mechanical load than the younger architecture in the metaphysis. As a first step to test this hypothesis, the three-dimensional (3D) morphology of the trabecular structure in the metaphysis and epiphysis of growing pigs was characterized in this study, using micro-computer tomography. The results showed that the trabecular architecture in the epiphysis had higher bone volume fraction, thicker trabeculae, and higher bone surface density compared to the structure in the metaphysis. In addition, its structure was plate-like, whereas the structure in the metaphysis was more rod-like. The anisotropy was somewhat higher in the epiphysis compared to the metaphysis, but not significantly so. However, the standard deviations of anisotropy were very significantly different. The trabecular structure of the epiphysis showed a low variability in anisotropy, which reflects its better structural organization compared to that in the metaphysis, for which the degree of anisotropy was much more variable. In conclusion, the 3D morphology of the trabecular structure in the epiphysis and metaphysis differed considerably. The structure in the epiphysis might reflect a more mature developmental stage in growth and mechanical adaptation as compared to metaphyseal bone.

INTRODUCTION

Young long bones increase their lengths due to the presence of growth plates, in which subsequently chondrocyte proliferation, chondrocyte hypertrophy, matrix mineralization, matrix resorption, and bone formation take place. Trabecular bone in the epiphysis is developed from the secondary ossification center, whereas trabeculae in the metaphysis are formed by the growth plate.

During growth, the 3D-trabecular-bone architecture in the metaphysis is gradually

renewed due to the development of new trabeculae from the growth plate, whereas trabeculae in the epiphysis are formed from the secondary ossification center early in the development. In rats, the highest bone formation rates were found after birth, which decreased continuously with increasing age at both sites (Sontag, 1992). Both formation rates and resorption rates were higher in the metaphysis than in the epiphysis, and during the first 150 days of age, formation rates were higher than resorption rates (Sontag, 1992). In the developmental stage, trabeculae in the epiphysis are relatively older than those in the metaphysis. Hence, its architecture should reflect a more mature state in growth and remodeling. Previously, it was shown that trabeculae align to the orientation of the dominant forces gradually with age (Tanck et al., 2001), which takes some time. We hypothesize that during growth, the relatively older trabecular architecture in the epiphysis is better adapted to the external mechanical load than the younger architecture in the metaphysis. As a first step to test this hypothesis, the 3D morphology of the trabecular structure in the metaphysis and epiphysis of growing pigs was characterized in this study.

MATERIALS AND METHODS

We used tibiae of five female pigs at 23 weeks of age from a Dutch farm (Central Animal Laboratory, Nijmegen, The Netherlands). It can be estimated that 23 weeks in pigs is roughly equivalent to 8 years of age in human. Post-mortem, bone cylinders of 8.5 mm in diameter and about 50 mm in length were drilled from the medial proximal tibiae (epiphysis and metaphysis) of the animals. The axes of the bone cylinders were parallel to the longitudinal axes of the bones. Institutional approval was obtained for all experiments.

All bone cylinders were scanned in a micro-computer tomography (μCT 20, Scanco Medical AG., Zürich, Switzerland) scanner with an isotropic resolution of 22 μm. From the epiphysis and metaphysis, a 4x4x4 mm^3 volume of interest (VOI) was selected. In the epiphysis, it was taken approximately halfway between the articular cartilage and the growth plate. In the metaphysis it was taken in the secondary spongiosa, at a distance of about 7 mm from the growth plate. The volumes of interest were represented in 22x22x22 μm^3 voxels and segmented using an individual density threshold value.

From the 3D reconstructions, we determined the bone volume fraction (BV/TV),

degree of anisotropy (MIL_{max}/MIL_{min}), trabecular number (Tb.N), trabecular thickness (Tb.Th), trabecular spacing (TB.S), bone surface density (BS/TV), connectivity density (Odgaard and Gundersen, 1993), and structure model index (SMI) (Hildebrand and Rüegsegger, 1997). The SMI varies between zero and three, whereby an SMI of zero represents an infinite plate structure and an SMI of three an infinite circular cylinder.

The data was statistically analyzed using Student's t-tests for paired analyses. Standard deviations were compared using the F-test. Differences were considered statistically significant at $p<0.05$.

RESULTS

The trabecular architecture of the epiphysis was different from that of the metaphysis (Figure 1), the latter being more refined than the former.

The bone volume fraction was significantly higher in the epiphysis compared to the metaphysis, 0.25 (± 0.02) and 0.13 (± 0.04), respectively (Figure 2A). The average trabecular thickness was higher in the epiphysis than in the metaphysis; 107 (± 6) μm versus 91 (± 5) μm, respectively ($p<0.05$).

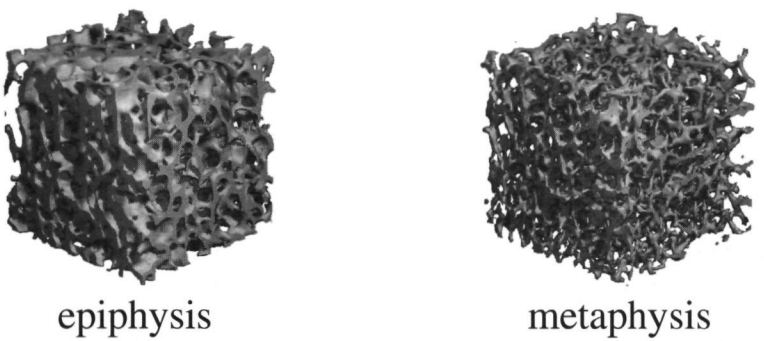

Figure 1: Illustration of the trabecular structure in the proximal epiphysis and metaphysis of tibiae in 23-week old pigs.

Although the degree of anisotropy was not significantly different between epiphysis and metaphysis (1.46 versus 1.40) their standard deviations (SD) were very

significantly different (Figure 2B). The SD of anisotropy was four times higher in the metaphysis than in the epiphysis, 0.19 versus 0.05, respectively (Figure 2B).
The bone surface density was significantly higher in the epiphysis than in the metaphysis, i.e 5 6 (± 0.5) /mm versus 4.2 (± 0.9) /mm (Figure 2C). In addition, the structure model index was much lower for the epiphysis as compared to the metaphysis, i.e. 0.47 (± 0.19) versus 2.23 (± 0.21) ($p<0.05$, Figure 2D). No significant differences were found between epiphysis and metaphysis in trabecular number, trabecular spacing and connectivity density, which values were approximately 2.5/mm, 380 µm, and 22/mm^3, respectively.

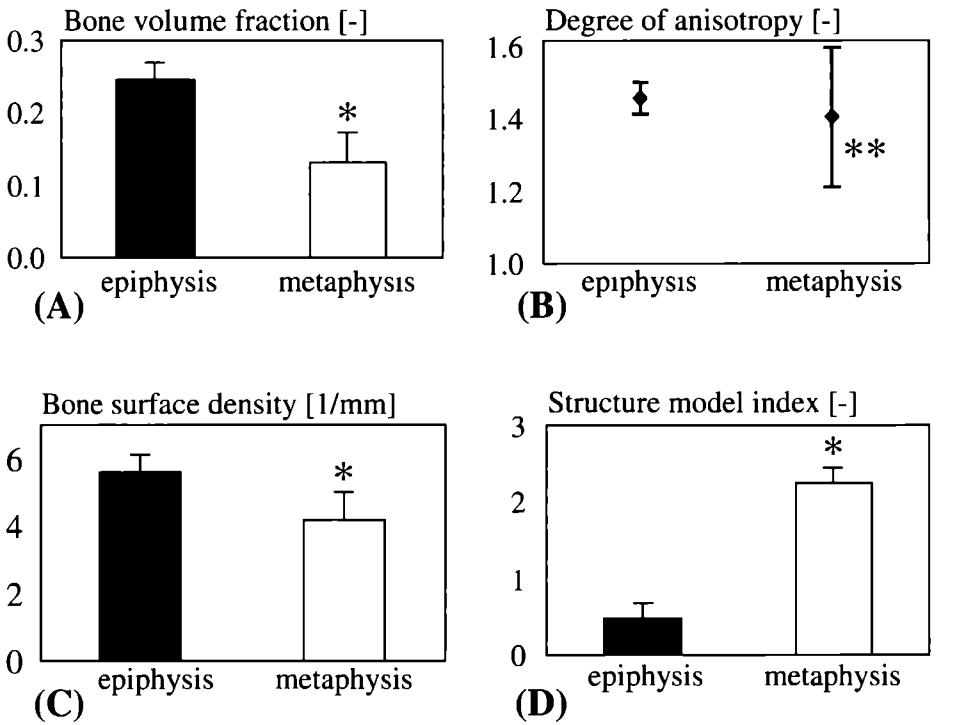

Figure 2: Bone volume fraction (BV/TV) **(A)**, degree of anisotropy **(B)**, bone surface density (BS/TV) **(C)**, and structure model index **(D)** for the bone specimens from the epiphysis and metaphysis Error bars represent the SD * p<0 05 versus *mean value* of epiphysis, ** p<0 05 versus *SD* of epiphysis

DISCUSSION

This study showed substantial differences in the 3D morphological parameters of epiphyseal and metaphyseal trabecular bone. The structure model index for the trabecular architecture in the epiphysis implies that its structure is plate-like, whereas the structure in the metaphysis is more rod-like. The low variety in the anisotropy of the epiphysis suggests that the structure is better organized compared to the structure in the metaphysis, for which the degree of anisotropy was much more variable. This corresponds with our hypothesis that the relatively older trabeculae in the epiphysis are better adapted to the external mechanical load than the trabeculae in the metaphysis during growth.

There are some limitations in the present study. We assume that the principal load direction is similar in the epiphysis and metaphysis. However, there may be differences between epiphyseal and metaphyseal loads, which should be investigated in future research. In addition, the nature of the biological adaptation may be different in the two sites. For example, spaceflight of normal 38-day-old rats for two weeks resulted in decreased mRNA levels for bone matrix proteins (osteonectin and collagen) in the distal femoral metaphysis but not in the distal femoral epiphysis (Evans et al., 1998). Another limitation is that we only analyzed the differences between epiphysis and metaphysis at 23 weeks of age. In a previous study, morphological parameters were also determined in bones of older pigs, but the number of pigs was only two per age category (Tanck et al., 2001). General information about trends could be obtained from this study. It was shown that structural organization and anisotropy increases in later years. However, it is not possible to retrieve detailed information from this study. For this purpose, further research would be required.

The higher bone volume fraction in the epiphysis, compared to the metaphysis, was also found in rats from 3 months of age and older (Bagi et al., 1994; Baldock et al., 1999; Martin and Zissimos, 1991; Westerlind et al., 1997) and suggests that the trabeculae in the epiphysis bear higher loads than those in the metaphysis, as higher loads result in increased bone mass. Besides increased bone mass, the tissue properties may also differ between epiphysis and metaphysis as Lee et al. (1998) showed by nanoindentation in rats; trabeculae in the epiphysis were about 30% stiffer than in the metaphysis.

Recently, many studies have been performed to analyze the behavior of trabecular

bone structure in the epiphysis and metaphysis (Baldock et al , 1998a, 1998b, 1999a, 1999b, Bay et al , 2000, Sontag, 1992, Turner, 1999, Westerlind et al., 1997) Ovariectomy in adult rats resulted in significant reduction in bone density in the metaphysis whereas bone mass in the epiphysis remained the same (Baldock et al , 1999b, Turner, 1999, Westerlind et al , 1997) Others showed decreased bone density in the epiphysis after ovariectomizing the rats during growth, although the reduction of bone mass in the metaphysis was generally much higher (Bagi et al , 1994, Baldock et al , 1998a, Martin and Zissimos, 1991) Ovariectomy resulted in increased osteoblast cell activity and increased osteoclast surface at both sites (Baldock et al , 1999b), but resorption seemed to be more pronounced in the metaphysis (Baldock et al , 1999a) In addition, after training these rats on treadmills, bone mass increased at both sites, while reducing the load through space flight decreased bone mass, also in the epiphysis (Turner, 1999, Westerlind et al , 1997)

In a previous study, using 3D strain-mapping techniques in rat tibiae, higher shear strains were measured in the metaphysis than in the epiphysis (Bay et al , 2000) This suggests that the metaphysis is less adapted to shear strains than the epiphysis These results seem to contradict the prevailing theory that after ovariectomy in rats, bone in the epiphysis is saved due to high strain energy density (SED) levels, whereas bone in the metaphysis will lose mass due to low SED levels (Turner, 1999, Westerlind et al , 1997) This theory is based on a study of Westerlind et al , (1997) but it is not necessarily true Using finite element analysis to calculate the stress patterns in the epiphysis and metaphysis of the distal femora in rats, they found higher SED levels in the epiphysis than in the metaphysis (Westerlind et al , 1997) After ovariectomy, increased bone loss in the metaphysis was found, whereas no bone loss was found in the epiphysis They attributed these results to their finding that the metaphysis experiences less load than the epiphysis and therefore bone loss is more likely However, the stiffness value that they used for cancellous bone was independent of bone density, meaning that densely packed trabecular areas were given similar material properties as areas with less trabeculae Hence, the SED levels in bone tissue itself are still unknown, which makes it difficult to draw conclusions about mechanical stimulation in both regions, and about the reason why the bone balance after ovariectomy is more stable in the epiphysis than in the metaphysis A solution may be found by calculating the SED levels at tissue level using micromechanical finite element models (Van Rietbergen et al , 1995)

In conclusion, the 3D morphology of the trabecular structure in the epiphysis and

metaphysis differed considerably The hypothesis that the trabecular structure in the epiphysis reflects a more mature stage in growth and mechanical adaptation as compared to metaphyseal bone is sustained At later stages of development the metaphysis will then probably catch up with the epiphysis as a structure adapted to mechanical loads is expected at maturity, after the growth plate is closed

REFERENCES

Bagi CM, Brommage R, Deleon L, Adams S, Rosen D, Sommer A Benefit of systemically administered rhIGF-I and rhIGF-I/IGFBP-3 on cancellous bone in ovariectomized rats J Bone Miner Res 9 1301-1312, 1994

Baldock PAJ, Moore RJ, Durbridge TC, Morris HA Comparison of three methods for estimation of bone resorption following ovariectomy in the distal femur and the proximal tibia of the rat Bone 24 597-602, 1999

Baldock PAJ, Morris HA, Moore RJ, Need AG, Durbridge TC Prepuberal oophorectomy limits the accumulation of cancellous bone in the femur of growing rats with long-term effects on metaphyseal bone architecture Calcif Tissue Int 62 244 249, 1998

Baldock PAJ, Morris HA, Need AG, Moore RJ, Durbridge TC Variation in the short-term changes in bone cell activity in three regions of the distal femur immediately following ovariectomy J Bone Miner Res 13 1451-1457, 1998

Baldock PAJ, Need AG, Moore RJ, Durbridge TC, Morris HA Discordance between bone turnover and bone loss effects of aging and ovariectomy in the rat J Bone Miner Res 14 1442-1448 1999

Bay BK, Smith T, Fyhrie D, Yeni Y Mechanical strain stimulus does not explain postovariectomy maintenance of bone balance in the rat proximal tibial epiphysis 12th Conf Eur Soc Biomech, p34, 2000

Evans GL, Morey-Holton E, Turner RT Spaceflight has compartment- and gene specific effects on mRNA levels for bone matrix proteins in rat femur J Appl Physiol 84 2132-2137, 1998

Hildebrand T, Ruegsegger P Quantification of bone microarchitecture with the structure model index Comp Meth Biomech Biomed Eng 1 15-23, 1997

Lee FYI, Rho JY, Harten R, Parsons JR, Behrens FF Micromechanical properties of epiphyseal trabecular bone and primary spongiosa around the physis an in situ nanoindentation study J Ped Orthop 18 582-585, 1998

Martin RB, Zissimos SL Relationships between marrow fat and bone turnover in ovariectomized and intact rats Bone 12 123-131, 1991

Odgaard A, Gundersen HJG Quantification of connectivity in cancellous bone, with special emphasis on 3 D reconstructions Bone 14 173-182, 1993

Sontag W Age-dependent morphometric alterations in the distal femora of male and female rats Bone 13 297-310, 1992

Tanck E, Homminga J, van Lenthe GH, Huiskes R Increase in bone volume fraction precedes architectural adaptation in growing bone Bone (accepted), 2001

Turner RT Mechanical signaling in the development of postmenopausal osteoporosis Lupus 8 388-392, 1999

Van Rietbergen B, Weinans H, Huiskes R, Odgaard A A new method to determine trabecular bone elastic properties and loading using micromechanical finite–element models J Biomech 28·69-81, 1995

Westerlind KC, Wronski TJ, Ritman EL, Luo ZP, An KN, Bell NH, Turner RT Estrogen regulates the rate of bone turnover but bone balance in ovariectomized rats is modulated by prevailing mechanical strain Proc Natl Acad Sci 94 4199-4204, 1997

8

GENERAL DISCUSSION

In this thesis, the influence of mechanical loading on different stages in the development from embryonic to adult bone was described. Mechanical loading plays an important role in development, maintenance, and adaptation of the skeleton. Disturbed loading may lead to congenital deformities, disturbed fracture healing, osteoporosis, and osteoarthritis. The processes during embryonic bone development are largely similar to the processes in growth plates and during fracture healing. Hence, proper understanding of normal bone development is important for prevention and treatment of musculoskeletal congenital deformities, deformities during growth, osteoporosis and osteoarthritis, but also for fracture healing.

Animals were used to study several aspects of mechanical loading effects on bone development. Embryonic mice were used to study cartilage mineralization, as this process is well defined in these species (Burger et al., 1992). This means that the gestational age at which mineralization first occurs is known precisely for various skeletal elements. Because resorption starts about two days later, at least in metatarsal bones, the process of cartilage mineralization could also be studied in isolation, before blood vessels penetrate the tissue, and before bone formation occurs. Pigs were used to study the development of the three-dimensional architecture of trabecular bone. They were chosen because even in young pigs the bones are big enough for analysis of the trabecular architecture. In addition, the bones of most pigs could be obtained from slaughter material, which prevented unnecessary animal death.

The first stage of bone development we studied was chondrocyte hypertrophy (chapter three). It was shown that during cell hypertrophy cell volume increases relative to matrix volume, which is a precondition to support the hypothesis that cell hypertrophy pressurizes the matrix. In addition, increase of chondrocyte volume was accompanied by increase in mineralization rate, which is a precondition for the hypothesis that larger cell volumes result in increased mineralization rates through the increased pressures. However, we only showed that our hypothesis, that hypertrophic cells pressurize the matrix and subsequently increase the mineralization process, is feasible. The amount of pressure to the extracellular matrix, and the stresses in the collagen network, are unknown. These will depend on the material properties of matrix and cells, matrix production, cell growth, and transport of fluid and matrix components between cells and matrix. For this purpose, embryonic mouse metatarsals can be exposed to different osmotic environments, so that cells inside the tissue will shrink or swell. The change in cell volume can potentially be determined

using confocal laser scanning microscopy (Errington et al., 1997). Similar experiments could be performed on isolated cells from embryonic metatarsals. By analyzing differences in cell swelling between isolated cells and cells surrounded by matrix, the role of the matrix could be elucidated. The pressure in the extracellular matrix and the stresses in the collagen network might be calculated using finite element analysis. Whether increased pressure increases the mineralization rate may be tested using culture experiments of embryonic mouse metatarsals. Although it would be difficult, one could, for example, investigate whether different osmotic environments lead to different mineralization rates, provided that this treatment does not interfere with chondrocyte basal metabolism.

Cartilage mineralization was the next stage of bone development we studied. There are indications that the mineralization process is stimulated by mechanical loads. For instance, the initiation of the mineralization process in embryonic mice coincides with the start of the first muscle contractions (Burger et al., 1991). In addition, in embryonic metatarsals of the mouse the mineralization geometry in the presence of muscular forces differed from that *in vitro*, in the absence of muscular forces (chapter five of this thesis). The conclusion of our study was that distortional strain was the most likely candidate to explain this difference. This is in agreement with the theory of Carter et al. (1987, 1988). In contrast, the role of hydrostatic pressure on the mineralization process remained unclear; we could not prove nor exclude the possibility that hydrostatic pressure increased the mineralization process. Carter et al. (1987, 1988) suggested that hydrostatic pressure inhibits the endochondral ossification process. It is worthwhile to elucidate this issue in future research.

Although we found indications that mechanical load affects the mineralization process, there was no hard evidence. It can be questioned whether any experiment can prove if, or how, mechanical load stimulates the tissue, since each experiment has its own limitations. Many experiments are performed on cells or organs *in vitro* (Klein-Nulend et al., 1986, 1995; Van Loon et al., 1995). The weakness of culture experiments is that even under the best culture conditions, differences still exist with the *in vivo* situation. Animal experiments, on the other hand, are difficult to control. It is hard to quantitatively determine the mechanical stress and strain situation *in vivo*. In addition, many factors besides mechanical load may affect the process, like hormones or other biological stimuli. For example, Germiller et al. (1997) performed experiments on chick embryos, which showed that chemical paralysis reduced proliferation of chondrocytes and reduced the maximal size of hypertrophic cells. In

such experiments, other factors besides muscle paralysis may have influenced bone development as well, so that direct evidence is difficult to obtain.

Indications that mechanical load stimulates tissue development can also be found in studies on tissue differentiation. If fibrous tissue changes into cartilaginous tissue, and subsequently into bone tissue, different cell types are involved. It can be hypothesized that a specific cell type develops in the mechanical environment it feels comfortable in. In a study on fracture healing, Park et al. (1998) suggested that shear motion promoted greater cartilage differentiation between the fragments than did axial motion or locked external fixation. In contrast, lack of consistency in the direction of movement between the two fragments may delay the process, possibly resulting in non-union of the fracture (Park et al, 1998). Søballe et al. (1992a, 1992b, 1993) showed that the rate of tissue differentiation around implants was affected by the amount of micromotion between bone and implant. Micromotions of 150 μm resulted in faster development from fibrous tissue to bone tissue compared to micromotions of 500 μm (Søballe 1992a, 1992b, 1993; Prendergast et al., 1997). Hence, for both fracture healing and tissue differentiation, it seems likely that mechanical load at least partly determines whether ossification starts and bone develops or that the tissue remains fibrous or cartilaginous.

Pauwels (1980) introduced phase diagrams for tissue differentiation, which predict what type of tissue would develop if the mechanical loading condition is known, with strain and hydrostatic pressure as mechanical determinants. Based on these diagrams, Carter et al. (1987, 1988) combined cyclic shear stress and cyclic hydrostatic stress in an osteogenic index. Using computer simulations they showed that bone development and fracture healing could be predicted, assuming the osteogenic index as a stimulus. One of the limitations of their model is that an unknown empirical constant is present in the mathematical formula, which is varied for each separate case. In addition, to simulate bone development based on the osteogenic index, they included a maturation index for the age of the tissue. Prendergast et al. (1997) introduced an alternative phase diagram based on strain and fluid flow, and were able to explain tissue differentiation patterns around implants. Subsequently, a biomechanical regulatory model was developed, which was able to predict the sequence of tissue differentiation (Huiskes et al., 1997). One of the shortcomings of these phase diagrams is that they predict tissue not only to develop into another tissue, but also to return to the original tissue. This is not realistic for endochondral ossification, as this process occurs only in one direction; if the tissue is mineralized there is no way back. Bone can be

resorbed by osteoclasts, of course, but that does not bring back cartilage. The same is true for fracture healing. Once the soft tissue between the fractured bone parts ossifies, the ossification process continues and does not reverse. In addition, the diagrams may suggest that mature cell types differentiate from other mature cell types. It is, however, unlikely that cartilage cells develop into bone cells (Szuwart et al., 1998; Gerstenfeld and Shapiro, 1996). These examples show that the process is far more complicated than the diagrams suggest. Nonetheless, the studies are important to gain deeper insight in the mechanical consequence of the endochondral ossification process.

Researching the effects of reduced load to the skeleton can also improve insight in bone development. It has been found that bone density decreases significantly under microgravity conditions (Collet et al., 1997). This was attributed to decreased bone formation, while resorption seemed to be less affected (Collet et al., 1997). Consequently, the astronauts have an increased fracture risk when they return to earth. After a six-months-flight and a six-month-recovery period, the trabecular bone density in the tibia of an adult astronaut was not yet recovered to normal values (Collet et al., 1997). This shows that it takes more time to recover bone density than to reduce it during space flight. The effects of microgravity on bone growth have also been studied. Chicken embryos, which were carried in a space shuttle for seven days under microgravity, showed no significant differences in bone development compared to controls, from a histological point of view (Suda, 1998). All normal processes took place and the bones developed well. Length measurements were, however, not reported in this study (Suda, 1998). In growing rats, longitudinal bone growth was not affected by eleven days of space flight (Westerlind and Turner, 1995). In contrast, Duke et al. (1990) found significant changes in growth plates of rats that had been in space for 12.5 days: the proliferative zone was increased whereas the hypertrophic and calcified zones were significantly reduced. *In vitro* cultures of embryonic mouse metatarsals also showed that the mineralization was reduced compared to controls (Van Loon et al., 1995). Klement and Spooner (1999) showed that the mineralized area in embryonic mouse metatarsals exposed to microgravity was about similar in size compared to ground controls, but the mineral composition or density was compromized. Thus, additional research is required to clarify the role of reduced load on bone growth. It would also be interesting to study the long-term effects of microgravity on *in vivo* bone development.

Trabecular bone architecture was the last stage in bone development we studied. We

suggested that trabecular bone density is adapted to external mechanical load from the early phase of growth, whereas the orientation of trabeculae is adapted to the main loading direction only gradually. In the adult stage, the trabeculae are aligned to the principal stress directions (Wolff, 1986). Trabecular bone is believed to be adapted to the external loads of daily living in both density and architecture. If the external loads change, bone density will change as well, which was shown several times (Nichols et al., 1994; Rubin and Lanyon, 1994; Zhang et al., 1992). It was also shown that bone architecture around implants or during fracture healing adapt to the new loading situations (Guldberg et al., 1996; Richards et al., 1998). In these cases bone is regenerating, i.e. modeling, whereas in the adult stage bone is remodeling. We believe, however, that similar cell processes are concerned in both modeling and remodeling (Huiskes et al., 2000). It has, however, never been proven that mature trabeculae reorient to alternative loading directions (Bertram and Swartz, 1991). We suggest that this lack of evidence may be explained by the duration of the experiments, which were probably too short to prove that mature bone really adapts to a changed loading direction. This theory is based on our study of trabecular bone development in pigs (chapter six), but also on results of computer simulations (Huiskes et al., 2000). Both studies indicated that it takes a long time, i.e. in the order of years, before trabeculae are re-oriented to the principal stress directions. The feasibility of this hypothesis could be tested by long-term experiments, in which mature bones are subjected to alternative loading directions.

We showed that morphological anisotropy increased gradually during bone development; the trabeculae gradually aligned to the main loading direction (chapter six). In a later stage of life, many humans develop osteoporotic bones. Bone density is decreased, trabecular architecture is changed, and bone fractures occur, mainly in the hip, vertebrae, and wrist. In osteoporotic bones, the adaptation process seems to be exaggerated. The anisotropy increases (Ciarelli et al., 2000), probably due to resorption of trabeculae perpendicular to the main loading direction. Hence, when bone mass decreases, the remaining mass seems to be even better adapted to the primary loading direction. But if an osteoporotic person makes an odd movement or falls, bone fracture may subsequently occur since the load direction then differs from the main loading direction. It is important to understand the mechanisms of osteoporosis development for prevention and treatment of the problem. A high peak bone mass in the twenties would be a good prevention for osteoporosis. However, if this goal is reached by high body weight, other health problems may arise, like heart

attacks and osteoarthritis

The principal question for this thesis was how different stages in bone development are influenced by mechanical loading The research was particularly focused on cartilage mineralization and development of trabecular bone Processes like cartilage resorption, tissue vascularisation, the first bone formation, and the development of cortical bone were not investigated We realize that bone development is regulated by a combination of mechanical, biological and genetic factors, and that their interactions are very complex The research described here was most of all fundamental, meant to gain deeper insight in the process We have shown that it is likely that bone development is affected by mechanical load Even at the embryonic stage, bone development appeared to be affected by mechanical stimuli Whether chondrocyte swelling contributes to mechanical pressure and subsequently stimulates mineralization is unsure and should be investigated in future research We found indications that cartilage mineralization is stimulated by mechanical force, as is the development of trabecular architecture For most of the developmental stages we proposed research directions to further study the process This could eventually lead to complete understanding of bone development so that focused efforts can be made to prevent and treat congenital deformities, osteoporosis, and osteoarthritis, and make fracture healing more effective

REFERENCES

Bertram JEA, Swartz SM The 'law of bone transformation' a case of crying Wolff? Biol Rev 66 245-273, 1991

Burger EH, Klein-Nulend J, Veldhuijzen JP Modulation of osteogenesis in fetal bone rudiments by mechanical stress in vitro J Biomech 24 101-109, 1991

Burger EH, Klein-Nulend J, Veldhuijzen JP Mechanical stress and osteogenesis in vitro J Bone Miner Res 7 S397-S401, 1992

Carter DR, Orr TE, Fyhrie DP, Schurman DJ Influences of mechanical stress on prenatal and postnatal skeletal development Clin Orthop 219 237-250, 1987

Carter DR, Wong M The role of mechanical loading histories in the development of diarthrodial joints J Orthop Res 6 804-816, 1988

Ciarelli TE, Fyhrie DP, Schaffler MB, Goldstein SA Variations in three-dimensional cancellous bone architecture of the proximal femur in female hip fractures and in controls J Bone Miner Res 15 32-40, 2000

Collet P, Uebelhart D, Vico L, Moro L, Hartmann D, Roth M, Alexandre C Effects of 1- and 6-

month spaceflight on bone mass and biochemistry in two humans Bone 20 547-551, 1997

Duke PJ, Durnova G, Montufar-Solis D Histomorphometric and electron microscopic analyses of tibial epiphyseal plates from Cosmos 1887 rats FASEB J 4 41-46, 1990

Errington RJ, Fricker MD, Wood JL, Hall AC, White NS Four-dimensional imaging of living chondrocytes in cartilage using confocal microscopy a pragmatic approach Am J Physiol Cell Physiol 41 C1040-C1051, 1997

Germiller JA, Goldstein SA Structure and function of embryonic growth plate in the absence of functioning skeletal muscle J Orthop Res 15 362-370, 1997

Gerstenfeld LC, Shapiro FD Expression of bone-specific genes by hypertrophic chondrocytes implications of the complex functions of the hypertrophic chondrocyte during endochondral bone development J Cell Biochem 62 1-9, 1996

Guldberg RE, Richards M, Caldwell NJ, Kuelske CL, Goldstein SA Trabecular bone adaptation to variations in porous-coated implant topology J Biomech 30 147-153, 1997

Huiskes R, van Driel WD, Prendergast PJ, Søballe K A biomechanical regulatory model for periprosthetic fibrous-tissue differentiation J Mat Sci Mat Med 8 785-788, 1997

Huiskes R, Ruimerman R, van Lenthe GH, Janssen JD Effects of mechanical forces on maintenance and adaptation of form in trabecular bone Nature 405 704-706, 2000

Klein-Nulend J, Veldhuijzen JP, Burger EH Increased calcification of growth plate cartilage as a result of compressive force in vitro Arth Rheum 29 1002-1009, 1986

Klein-Nulend J, van der Plas A, Semeins CM, Ajubi NE, Frangos JA, Nijweide PJ, Burger EH Sensitivity of osteocytes to biomechanical stress in vitro FASEB J 9 441-445, 1995

Klement BJ, Spooner BS Mineralization and growth of cultured embryonic skeletal tissue in microgravity Bone 24 349-359, 1999

Nichols DL, Sanborn CF, Bonnick SL, Ben-Ezra V, Gench B, DiMarco NM The effects of gymnastics training on bone mineral density Med Sci Sports Exerc 26 1220-1225, 1994

Park SH, O'Connor K, Mckellop H, Sarmiento A The influence of active shear or compressive motion on fracture-healing J Bone Joint Surg [Am] 6 868-878, 1998

Pauwels F Biomechanics of fracture healing In Biomechanics of the locomotor apparatus Translated from the 1965 German edition by P Manquet and R Furlong, pp 106-120, Springer, Berlin, 1980

Prendergast PJ, Huiskes R, Søballe K Biophysical stimuli on cells during tissue differentiation at implant interfaces J Biomech, 30 539-548, 1997

Richards M, Goulet JA, Weiss JA, Waanders NA, Schaffler MB, Goldstein SA Bone regeneration and fracture healing Experience with distraction osteogenesis model Clin Orthop 355 S191-S204, 1998

Rubin CT, Lanyon LE Regulation of bone formation by applied dynamic loads J Bone Joint Surg [Am] 66 397-402, 1984

Søballe K, Hansen ES, Rasmussen HB, Jørgensen PH, Bunger C Tissue ingrowth into titanium and hydroxyapatite coated implants during stable and unstable mechanical conditions J Orthop Res 10 285-299, 1992a

Søballe K, Rasmussen HB, Hansen ES, Bunger C Hydroxyapatite coating modifies implant membrane formation Controlled micromotion studied in dogs Acta Orthop Scand 63 128-140, 1992b

Søballe K, Hansen ES, Rasmussen HB, Bunger C Hydroxyapatite coating converts fibrous tissue to bone around loaded implants J Bone Joint Surg [Br] 75B 270-278, 1993

Suda T Lessons from the space experiment SL-J/FMPT/L7 the effect of microgravity on chicken embryogenesis and bone formation Bone 22 73S-78S, 1998

Szuwart T, Kierdorf H, Kierdorf U, Clemen G Ultrastructural aspects of cartilage formation, mineralization, and degeneration during primary antler growth in fallow deer (dama dama) Ann Anat 180 501-510, 1998

Van Loon JWA, Bervoets DJ, Burger EH, Dieudonné SC, Hagen JW, Semeins CM, Zandieh Doulabi B, Veldhuijzen JP Decreased mineralization and increased calcium release in isolated fetal mouse long bones under near weightlessness J Bone Miner Res 10 550-557, 1995

Westerlind KC, Turner RT The skeletal effects of spaceflight in growing rats tissue-specific alterations in mRNA levels for TGF-beta J Bone Miner Res 10 843-848, 1995

Wolff J Das Gesetz der Transformation der Knochen, Hirchwild, Berlin, 1892, translated as The Law of Bone Remodeling by P Maquet and R Furlong, Springer-Verlag, Berlin, 1986

Zhang J, Feldblum PJ, Fortney JA Moderate physical activity and bone density among perimenopausal women Am J Public Health 82 736-738, 1992

SUMMARY

In embryonic development of long bones, a cartilaginous anlage develops into bone tissue The development from embryonic cartilage to mature bone passes many stages like chondrocyte proliferation, chondrocyte hypertrophy, mineralization of the cartilage matrix, penetration of blood vessels in the tissue, resorption of mineralized cartilage, and bone formation These processes continue in the growth plates, where longitudinal growth takes place At maturity, the longitudinal growth stops and the growth plates close Mechanically, two types of bone are present in adult long bones, cortical bone, which is dense and compact, and trabecular bone, which is porous, owing to its structure of rods and plates

The purpose of this thesis was to study the influence of mechanical loading on different processes in the development from embryonic to mature bone If for any reason one of these processes is disturbed, a compromised bone development and function may result Proper understanding of the regulatory mechanisms in bone development is important for prevention and treatment of musculoskeletal developmental deformities and osteoporosis, and also for bone regeneration during fracture healing and implant fixation, and for tissue engineering

The first stage in bone development that was studied was chondrocyte hypertrophy In chapter three the hypothesis that hypertrophic chondrocytes pressurize the extracellular matrix and subsequently initiate or stimulate the mineralization process was discussed It was shown that during cell hypertrophy cell volume increased relatively to matrix volume, which is a precondition to support the theory that cell hypertrophy pressurizes the matrix In addition, increase of chondrocyte volume was accompanied by increase in mineralization rate, which is a precondition for the theory that larger cell volumes result in increased mineralization rates through the increased pressures However, we only showed that the hypothesis is feasible Additional research is required to test whether the hypothesis can be confirmed

Cartilage mineralization was the next stage in bone development that was studied In chapter two, we showed that the stiffness for embryonic rudiments during mineralization increases by two orders of magnitude within one day Hence, within a period of hours, the chondrocytes in the calcifying cartilage experience a significant change in mechanical environment that will lead to decreased cell deformation and stress shielding Since the transition is so sudden and gigantic, it can be seen as a process of 'catastrophic' proportion for the cells

Indications were found that mechanical loads stimulate the mineralization process In chapter four, the mineralization process in the *in vitro* experiments, in which

embryonic mouse metatarsals were externally loaded with an intermittent hydrostatic pressure, were evaluated. A poroelastic finite element analysis (FEA) was performed to calculate the local distributions of distortional strain and fluid pressure at the mineralization front in the metatarsal during intermittent hydrostatic loading. Distortional strains appeared to be insignificant under these loading conditions. Hydrostatic pressure was the only candidate left to have stimulated the mineralization process. We then hypothesized that the pressure may have created the physical environment enhancing the mineralization process, in which diffusion of ions may have contributed. In chapter five the influence of muscular forces on the local mineralization process in embryonic metatarsals of the mouse was studied. The mineralization front *in vivo*, in the presence of muscular forces, was found to be nearly straight, whereas *in vitro* it acquired a more convex shape. Using poroelastic FEA, local distributions of distortional strain and fluid pressure at the mineralization front during muscular loading showed that the role of hydrostatic pressure was unclear. It might have stimulated the mineralization front as a whole, but we could not prove nor exclude this possibility. The most likely candidate to explain the difference between *in vivo* and *in vitro* mineralization geometry was distortional strain, resulting from muscle contractions.

The last stage during development that was studied was trabecular bone. In chapter six, we questioned how trabecular bone density and architecture would change during growth. Morphological and mechanical parameters of three-dimensional (3D) trabecular bone samples from the vertebra and proximal tibia of pigs were studied using micro-computer tomography (μCT) and micro FEA. The results showed that both bone volume fraction and stiffness increased rapidly in the initial growth phase, whereas the morphological anisotropy started to increase at a later stage. In addition, the anisotropy reached its highest value much later in the development than bone volume fraction did. We concluded that density is adapted to external load from the early phase of growth, whereas the trabecular architecture is adapted later in the development.

The results of chapter six let us hypothesize that during growth, the relatively older trabecular architecture in the epiphysis is better adapted to mechanical load than the younger architecture in the metaphysis, in which the trabeculae are gradually renewed due to the presence of a growth plate. As a first step to test this hypothesis, the 3D morphology of the trabecular structure in the metaphysis and epiphysis of growing pigs was characterized in chapter seven, using μCT. The results showed that the trabecular architecture in the epiphysis had higher bone volume fraction, thicker

trabeculae, and higher bone surface density compared to the structure in the metaphysis. In addition, its structure was plate-like, whereas the structure in the metaphysis was more rod-like. The anisotropy was somewhat higher in the epiphysis compared to the metaphysis, but not significantly so. However, the standard deviations of anisotropy were very significantly different. The trabecular structure of the epiphysis showed a low variety in anisotropy, which reflects its better structural organization compared to that in the metaphysis, for which the degree of anisotropy was much more variable. This sustains the hypothesis that the trabecular structure in the epiphysis reflects a more mature stage in growth and mechanical adaptation as compared to metaphyseal bone.

In chapter eight, we discussed the study in general and concluded that it is realistic that bone development is influenced by mechanical load. The research described in this thesis combined cell biological and biomechanical techniques, meant to gain more insight in the process of bone development and its relation to mechanical forces. For most of the developmental stages we suggested research directions to further study the process. Eventually, this could lead to a complete understanding of bone development, so that attempts could be made to better prevent and treat congenital deformities, osteoporosis, and osteoarthritis, and to make fracture healing more efficient.

SAMENVATTING

Tijdens de embryonale ontwikkeling van lange pijpbeenderen wordt kraakbeen vervangen door botweefsel. De ontwikkeling doorloopt opeenvolgende stadia zoals het delen (proliferatie) en opzwellen (hypertrofie) van chondrocyten, mineralisatie van de kraakbeenmatrix, binnenkomst van bloedvaten, resorptie van gemineraliseerd kraakbeen en botformatie. Deze processen gaan door in de groeischijven waar lengtegroei plaatsvindt. Bij volwassenen is de lengtegroei gestopt en zijn de groeischijven gesloten. Lange pijpbeenderen bestaan uit twee typen bot, te weten corticaal bot - dicht en compact - en trabeculair bot dat door de structuur van staafjes en plaatjes poreus is.

Het doel van dit proefschrift is het onderzoek naar de invloed van mechanische belasting op de verschillende processen in de ontwikkeling van embryonaal tot volwassen bot. Als een van deze processen verstoord wordt kan dit leiden tot een verstoorde botontwikkeling c.q. botfunctie. Goed begrip van het regelmechanisme van botontwikkeling is dan ook van belang voor preventie en behandeling van aangeboren afwijkingen aan het spier-skeletstelsel en osteoporose, voor botregeneratie tijdens fractuurheling en fixatie van implantaten en voor tissue engineering.

Hypertrofie van chondrocyten is het eerste stadium van de botontwikkeling dat onderzocht is. In hoofdstuk drie wordt de hypothese bediscussieerd dat hypertrofe chondrocyten de extracellulaire matrix onder druk zetten en vervolgens het mineralisatieproces initiëren of stimuleren. Aangetoond is dat het celvolume tijdens celzwelling relatief toenam ten opzichte van het matrixvolume. Dit is een voorwaarde voor de theorie dat celzwelling tot verhoogde druk in de matrix leidt. Voorts bleek dat een groter celvolume gepaard gaat met een toegenomen mineralisatiesnelheid. Hiermee wordt voldaan aan de voorwaarde voor de theorie dat grotere celvolumes door verhoogde druk resulteren in toegenomen mineralisatiesnelheid. Hiermee is derhalve aangetoond dat de genoemde hypothese mogelijk is. Aanvullend onderzoek is nodig om te onderzoeken of de hypothese inderdaad bevestigd kan worden.

Het volgende stadium in de ontwikkeling van bot dat bestudeerd is, is de mineralisatie van kraakbeen. In hoofdstuk twee hebben we laten zien dat tijdens mineralisatie de stijfheid van embryonaal bot binnen een dag met factor 100 toeneemt. Gevolg is dat de chondrocyten die in het verkalkende kraakbeen zitten in korte tijd een significante verandering in hun mechanische omgeving voelen. Dit leidt tot afgenomen celvervorming en stress shielding. Omdat dit proces zo snel gaat en gigantisch is kan het beschouwd worden als een catastrofaal proces voor de cellen.

Er zijn indicaties gevonden dat mechanische belasting het mineralisatieproces stimuleert. In hoofdstuk vier werd het mineralisatieproces geëvalueerd van *in vitro* experimenten. Tijdens deze experimenten werden embryonale middenvoetsbeentjes van de muis extern belast met een dynamische hydrostatische druk. Een poroelastisch eindige elementen analyse (EEA) werd uitgevoerd om de lokale verdeling van deviatorische rek en hydrostatische druk te berekenen aan het mineralisatiefront tijdens de intermitterende belasting. De deviatorische rek bleek verwaarloosbaar klein te zijn onder deze belastingscondities. De hydrostatische druk was hierdoor de enige overgebleven kandidaat om het mineralisatieproces te stimuleren. We hebben als hypothese aangenomen dat hydrostatische druk de juiste fysische omgeving creëert om het mineralisatieproces te bevorderen. Diffusie van ionen kan hierbij een rol spelen.

In hoofdstuk vijf is de invloed van spierkracht op het lokale mineralisatieproces in embryonale middenvoetsbeentjes van de muis bestudeerd. Het mineralisatiefront *in vivo* - in de aanwezigheid van spierkrachten - was recht terwijl het front *in vitro* convex was. Met behulp van een poroelastische EEA werd de lokale verdeling van deviatorische rek en hydrostatische druk aan het mineralisatiefront tijdens spierbelasting berekend. De rol van hydrostatische druk was onduidelijk. De druk kon het gehele mineralisatiefront gestimuleerd hebben. Dit kon echter niet bewezen noch uitgesloten worden. De meest waarschijnlijke parameter om het verschil tussen *in vivo* en *in vitro* mineralisatie te verklaren was de door spiercontracties veroorzaakte deviatorische rek.

Trabeculair bot is het laatste stadium tijdens de botontwikkeling dat onderzocht is. In hoofdstuk zes is de vraag gesteld op welke wijze trabeculaire botdichtheid en architectuur veranderen tijdens groei. Van trabeculaire botstukjes uit wervels en proximale tibiae van varkens werden met behulp van micro-computer tomografie (μCT) en micro EEA drie-dimensionale (3D) morfologische en mechanische parameters bestudeerd. De resultaten toonden aan dat de botvolumefractie en de stijfheid snel toenemen in de initiële groeifase. De toename van morfologische anisotropie vindt echter pas op een later tijdstip plaats. Voorts bereikte de anisotropie zijn hoogste waarde in een veel later stadium dan de botvolumefractie. We concluderen dat dichtheid vanaf de vroege ontwikkelingsfase geadapteerd is aan de externe belasting terwijl de trabeculaire architectuur zich pas later aanpast.

De resultaten van hoofdstuk zes hebben tot de hypothese geleid dat tijdens de groei de relatief oudere trabeculaire structuur in de epifyse beter is aanpast aan de

mechanische belasting dan de jonge architectuur in de metafyse waar de trabekels telkens vernieuwd worden door de aanwezigheid van de groeiplaat Als een eerste stap om deze hypothese te testen is in hoofdstuk zeven de 3D-morfologie van de trabeculaire structuur in de metafyse en epifyse in groeiende varkens onderzocht met behulp van µCT De resultaten laten zien dat de trabeculaire architectuur in de epifyse een hogere botdichtheid, dikkere trabekels en een hogere botoppervlaktedichtheid had in vergelijking tot de structuur in de metafyse Voorts was de structuur meer plaatvormig terwijl de structuur in de metafyse meer staafvormig was De anisotropie in de epifyse was iets hoger dan in de metafyse Dit was echter niet significant De standaarddeviaties van de anisotropie waren echter sterk significant verschillend De variatie in de anisotropie van de trabeculaire structuur in de epifyse was klein hetgeen duidt op een betere structurele organisatie dan in de metafyse (waar de variatie in de anisotropie veel groter was) Dit ondersteunt de hypothese dat de trabeculaire structuur in de epifyse tijdens groei en mechanische adaptatie een volwassener stadium reflecteert dan bot in de metafyse

In hoofdstuk acht wordt tenslotte de gehele studie bediscussieerd We concluderen dat het realistisch is om te veronderstellen dat botontwikkeling beinvloed wordt door mechanische belasting Het onderzoek in dit proefschrift is fundamenteel en derhalve bedoeld om een dieper inzicht te krijgen in het botontwikkelingsproces en de relatie met mechanische belasting Voor de meeste ontwikkelingsstadia hebben we richtingen voor nader onderzoek aangegeven Uiteindelijk kan dit leiden tot een compleet begrip van botontwikkeling waardoor pogingen gedaan kunnen worden ter preventie en behandeling van aangeboren afwijkingen, osteoporose en osteoarthrose en om fractuurheling efficienter te kunnen maken

TANCKWOORD

Toen ik tijdens mijn afstuderen bij de sectie biomechanica in 1995 de kans kreeg om te solliciteren naar een baan als 'onderzoeker in opleiding' op dezelfde afdeling wilde ik dat zo graag dat ik er tijdens de tweede sollicitatieronde niet veel van bakte. Gedesillusioneerd keerde ik naar huis. Daar aangekomen was er telefoon voor mij: Professor Huiskes met het nieuws dat ik toch was gekozen. Ik kreeg felicitaties én de opdracht om in het vervolg niet meer zo zenuwachtig te zijn.

Na ruim vijf jaar is mijn boekje af. Ik schrijf 'mijn boekje', maar dat is eigenlijk niet terecht; alleen had ik het nooit voor elkaar gekregen. Velen hebben mij –al dan niet bewust- geholpen met de totstandkoming ervan. En al die mensen wil ik bij deze heel erg bedanken. Enkelen wil ik speciaal noemen:

Mijn (co-)promotores, Rik Huiskes, Els Burger en Leendert Blankevoort. Rik, bedankt dat ik de kans heb gekregen om de wetenschappelijke wereld te leren kennen. Het is een mooie wereld waar ik nog lang in hoop te werken. Ik heb enorm veel van je geleerd en doe dat trouwens nog steeds. Ik ben blij dat je me de ruimte hebt gegeven om het onderzoek op eigen wijze uit te voeren en dat je bijstuurde waar dat nodig was. Els, jouw deskundigheid op het biologische gebied is enorm. Bedankt voor de enthousiaste discussies en je relativerende woorden als er eens een experiment mislukte. Leendert, bedankt voor je betrokkenheid, je kritische blik en je goede adviezen. Mijn enthousiasme voor het onderwijs komt deels bij jou vandaan.

Mijn (oud) kamergenoten Margriet Mullender, Dorethé Mommersteeg, Sanne van der Donk, Jan Stolk, Jasper Homminga en Harry van Lenthe hebben ervoor gezorgd dat het onderzoekswerk een aangename bezigheid was, en nog steeds is. Discussies over het schrijven van artikelen, geven van presentaties, wetenschappelijke problemen, onderwijs, maar ook over de toekomst, sport, vakantie, vriendschap en muziek waren onmisbaar voor mij. Sanne, heel erg bedankt voor het nalezen en corrigeren van mijn proefschrift. Harry, Jan, Sanne en Jasper, veel succes met de afronding van jullie promotieonderzoek!

De overige (ex-)collega's van het Orthopaedic Research Lab bedank ik voor de goede sfeer die er heerst. Nico, jouw enthousiaste begeleiding tijdens mijn afstuderen heeft er mede toe geleid dat ik interesse voor het onderzoek heb gekregen. Willem, dankjewel voor je handigheid en je gezelligheid. Rene, bedankt voor je geduld en je

snelheid om me te helpen bij de (vele) problemen op computergebied. Marlies, Jellien en Ineke jullie positieve instelling en jullie rol in het reilen en zeilen van de afdeling waren onmisbaar. Huub, Marco, Stefan, Marieke, Erwin, Joan, Chris, Pieter, Dinie, Tony, Natascha, Harrie en Bert bedankt voor jullie bijdragen aan de goede sfeer van vroeger en nu.

Ik ben altijd hartelijk ontvangen op de afdeling orale celbiologie aan de Vrije Universiteit in Amsterdam en voelde me daardoor snel thuis. Speciaal wil ik Cor Semeins, Dirk-Jan Bervoets, en Jolanda de Blieck noemen omdat jullie altijd klaar stonden en veel werk voor me hebben gedaan op het biologische en experimentele gebied. Dank jullie wel! Ton van Maarsseveen (VU) wil ik bedanken voor zijn goede hulp bij het uitvoeren van een pilot-studie. Het mineralisatieproces op celniveau filmen bleek uiteindelijk toch iets moeilijker dan verwacht.

Willem van Driel, Jan-Willem Hagen en Anne Haaijman bedankt voor jullie belangrijke bijdragen aan mijn onderzoek. Rachel Errington, thank you for your support at the confocal microscope. Toshi, thank you for your nice work and your enthousiasm. I enjoyed the stories about Japan. Hans Smits en Huib Croes wil ik bedanken voor hun hulp op gebied van microscopie en laboratoriumvaardigheden. Ton de Haan, bedankt voor je deskundige adviezen op het gebied van de statistiek. Marion van Gellekom en Marije van Dijk, jullie hebben als studentes goed werk voor mijn onderzoek gedaan. Dank jullie wel.

De mensen van het centraal dierenlaboratorium in Nijmegen wil ik bedanken voor de prettige samenwerking. Ik wil met name Fred Philipsen, Ton Peters, en Frans van Munsteren bedanken voor hun hulp bij het 'wassen van mijn varkentjes'.

Naast mijn werk heb ik stoom af kunnen blazen door tegen tafeltennisballetjes te slaan, te zwemmen, te fietsen en hard te lopen. Ik wil speciaal Piet Geurts bedanken voor de onvergetelijke tijd en goede sfeer bij ttv Hoonhorst. Ik bewonder je geduld, begrip, enthousiasme en het luisterend oor en dat je altijd hebt gehad. Piet, Mariëtte, Heleen en Cora, bedankt voor jullie gezelligheid, ga zo door! Bij Ciko'66 en TVA kan ik mijn hersens weer resetten, wat soms hard nodig is. Alle energie die ik daar kwijt raak krijg ik dubbel en dwars weer terug. Daarbij is de sfeer ook nog eens geweldig!

Mijn ouders wil ik bedanken voor hun grote steun. Jullie staan altijd klaar en hebben ervoor gezorgd dat ik onbezorgd kon studeren. Bedankt!

Albert, ik wil jou het meest bedanken van iedereen. Als iemand mij er doorheen kan helpen ben jij het wel. Ik vind het geweldig dat we zoveel samen kunnen doen, al is dat er wel wat bij ingeschoten de laatste tijd. Maar nu is het boekje af en kunnen we er weer volop tegenaan!

CURRICULUM VITAE

Ik ben geboren op 18 november 1971 in Zevenaar. Mijn carrière is begonnen op de Fioretti kleuterschool te Babberich, waarna ik 6 jaar basisonderwijs heb gevolgd op de St. Franciscusschool te Babberich. In 1990 behaalde ik het VWO diploma op het Liemers College te Zevenaar. Vervolgens studeerde ik Biomedische Gezondheidswetenschappen aan de Katholieke Universiteit Nijmegen (KUN) met als afstudeerrichting bewegingswetenschappen. Om me verder te verdiepen in de biomechanica heb ik een jaar Werktuigbouwkunde gestudeerd aan de Universiteit Twente (1993-1994). Vervolgens liep ik twee stages bij -toen nog- de afdeling Orthopaedie, sectie biomechanica in Nijmegen, onder leiding van dr. ir. N. Verdonschot. Daarbij stond onderzoek op het gebied van heupprothesen centraal. In 1995 studeerde ik af en begon op dezelfde afdeling te werken als onderzoeker in opleiding in dienst van de Nederlandse organisatie voor Wetenschappelijk Onderzoek (NWO). Het project was een samenwerking tussen het Orthopaedic Research Lab - onder leiding van prof. dr. ir. R. Huiskes- en de vakgroep Orale Celbiologie van de Vrije Universiteit in Amsterdam, onder leiding van prof. dr. E.H. Burger. Het onderzoek heeft uiteindelijk geresulteerd in dit proefschrift. Sinds 1999 ben ik als junior onderzoeker werkzaam in het NWO- project 'bone cell mechanosensitivity, estrogen deficiency, and osteoporosis'. De komende jaren zal ik dit onderzoek voortzetten. Daarnaast ben ik sinds 1 januari 2001 werkzaam als Universitair Docent aan de KUN voor de studierichting Biomedische Gezondheidswetenschappen. Ik ben getrouwd met Albert.